

RE-REDUCING THE SOUTHERN POLAR ZONE  
OF THE YALE PHOTOGRAPHIC STAR CATALOGUE

By

JANE E. MORRISON

A DISSERTATION PRESENTED TO THE GRADUATE SCHOOL  
OF THE UNIVERSITY OF FLORIDA IN PARTIAL FULFILLMENT  
OF THE REQUIREMENTS FOR THE DEGREE OF  
DOCTOR OF PHILOSOPHY

UNIVERSITY OF FLORIDA

1995

To Abby, Ben, Taylor and Atticus.

## ACKNOWLEDGMENTS

This project would never have been possible with the support and advice from many members of the astronomical community, my family and friends. First of all I would like to thank my thesis advisor, Dr. Eichhorn for his patience, advice, insight and colorful conversations. By his own example I have developed a passion for scientific research.

I would like to thank the members of my committee, Haywood Smith, John Oliver, Ralph Selfridge, and Kwan-Yu Chen for their counsel and support.

I would like to thank my parents for their moral support and encouragement. I would especially like to thank them for instilling in me the desire to always find the best in every situation and for sharing with me their belief that I can achieve any goal I set my mind to. Both of these qualities have enabled me to finish this project while enjoying nearly every moment.

An extra special thanks goes to my friend and colleague, Ricky Smart, for his enduring patience and unending support, without which this project may not have been possible. I would also like to thank him for never a dull moment.

For fun, food and frolicking I would like to send hugs and kisses to Jaydeep Mukherjee, Sumita Jayaraman, Caroline Simpson, Ron Drimmel, Chuck Higgins, Leonard Garcia, Stephen Kortenkamp, Elaine Mahon and cast of thousands.

Thanks to Lenny and Croaker for ghostwriting my biographic sketch.

For providing the raw measurement of the Southern Polar Zone of the Yale Photographic Star catalog and an early release of the International Reference Star catalog, I would like to thank Tom Corbin and Sean Urban from the United States Naval Observatory.

For providing background information concerning this project I would like to thanks Dorrit Hoffleit, Fred Fallon, and Bill Van Altena.

The bulk of the computing has been carried out on the Northeast Regional Data Centers IBM computer under their Research Computing Initiative program. This computing time has saved me many hours.

## TABLE OF CONTENTS

ACKNOWLEDGMENTS . . . . .	iii
LIST OF TABLES . . . . .	vii
LIST OF FIGURES . . . . .	viii
ABSTRACT . . . . .	xi
CHAPTERS	
1. INTRODUCTION . . . . .	1
Original Reduction . . . . .	7
Why Do a Re-Reduction? . . . . .	8
2. PHOTOGRAPHIC ASTROMETRY . . . . .	14
Standard Coordinates and their Relationship to the Equatorial Coordinates . . . . .	15
Determining the Equatorial Coordinates from the Measured Coordinates . . . . .	17
The Relationship Between the Standard and Measured Coordinates .	20
Some Commonly Used Models . . . . .	28
4-Constant Model . . . . .	29
6-Constant Model . . . . .	31
12-Constant Model . . . . .	32
Spherical Correction . . . . .	34
3. LEAST SQUARES . . . . .	45
Theory of Least Squares . . . . .	45
Traditional (Linear Least Squares) . . . . .	47
Nonlinear Least Squares . . . . .	49
4. METHOD OF PLATE REDUCTIONS . . . . .	56
Single Plate Reduction: Using Least Squares to Determine the Plate Parameters. . . . .	57
Final Positions from a Single Plate Reduction, . . . . .	68
Overlap Plate Reduction . . . . .	69
Example of Overlap Reduction. . . . .	83
Set up the equations of condition . . . . .	86
Determine $J'$ . . . . .	90
Determine $a$ . . . . .	93

Determine $\beta$ . . . . .	94
5. OBSERVATIONS . . . . .	96
Observations for the Southern Polar Zone . . . . .	96
Measurement of Stars . . . . .	97
Magnitude System . . . . .	101
6. PLATE REDUCTIONS . . . . .	102
Reference Catalog . . . . .	102
External Catalog . . . . .	104
Determining the Plate Model . . . . .	107
Single Plate Reduction . . . . .	108
Final Positions from the Single Plate Solution . . . . .	114
Overlapping Plate Reduction . . . . .	119
Conclusions . . . . .	126
Future Work . . . . .	129
BIBLIOGRAPHY . . . . .	168
BIOGRAPHICAL SKETCH . . . . .	172

## LIST OF TABLES

Table 1: Yale Zones . . . . .	6
Table 2: Refraction Information for plates 1–32 . . . . .	43
Table 3: Refraction Information for plates 33–64 . . . . .	44
Table 4: The Yale Plates . . . . .	98
Table 5: Single Plate RMS Results . . . . .	110
Table 6: Overlap Plate RMS Results . . . . .	125
Table 7: RMS Single Plate Comparisons: 15–constant model . . . . .	127
Table 8: RMS Overlap Plate Comparisons: 18–constant model . . . . .	128

## LIST OF FIGURES

Figure 1: The plates for the Southern Polar Zone of the Yale Catalogue . .	12
Figure 2: The Stars of the Southern Polar Yale Zone of the Yale Photographic Star Catalogue . . . . .	13
Figure 3: Gnomonic Projection . . . . .	15
Figure 4: Origin Shift . . . . .	22
Figure 5: Rotation of x-y axis with respect to the $\xi$ - $\eta$ axis . . . . .	23
Figure 6: Nonperpendicularity of axes . . . . .	26
Figure 7: 4-Constant Model: origin shift and rotation of axes . . . . .	29
Figure 8: The effects of refraction on plate 1 . . . . .	39
Figure 9: Example of two overlapping plates . . . . .	84
Figure 10: Distribution of Magnitudes . . . . .	105
Figure 11: The different in positions found from the single plate adjustment for plates 1 and 24 and plates 1 and 25. . . . .	115
Figure 12: The different in positions found from the single plate adjustment for plates 61 and 64 and plates 62 and 63. . . . .	116
Figure 13: Magnitude Dependent Measuring Error, the units of the variances are arcseconds squared. . . . .	123
Figure 14: 6-Constant Single Plate Residuals . . . . .	131
Figure 15: 6-Constant Single Plate Residuals . . . . .	132



Figure 16: 6–Constant Single Plate Residuals . . . . .	133
Figure 17: 6–Constant Single Plate Residuals . . . . .	134
Figure 18: 6–Constant Single Plate Residuals . . . . .	135
Figure 19: 8–Constant Single Plate Residuals . . . . .	136
Figure 20: 8–Constant Single Plate Residuals . . . . .	137
Figure 21: 8–Constant Single Plate Residuals . . . . .	138
Figure 22: 8–Constant Single Plate Residuals . . . . .	139
Figure 23: 8–Constant Single Plate Residuals . . . . .	140
Figure 24: 13–Constant Single Plate Residuals . . . . .	141
Figure 25: 13–Constant Single Plate Residuals . . . . .	142
Figure 26: 13–Constant Single Plate Residuals . . . . .	143
Figure 27: 13–Constant Single Plate Residuals . . . . .	144
Figure 28: 13–Constant Single Plate Residuals . . . . .	145
Figure 29: 15–Constant Single Plate Residuals . . . . .	146
Figure 30: 15–Constant Single Plate Residuals . . . . .	147
Figure 31: 15–Constant Single Plate Residuals . . . . .	148
Figure 32: 15–Constant Single Plate Residuals . . . . .	149
Figure 33: 15–Constant Single Plate Residuals . . . . .	150

Figure 34: 20–Constant Single Plate Residuals . . . . .	151
Figure 35: 20–Constant Single Plate Residuals . . . . .	152
Figure 36: 20–Constant Single Plate Residuals . . . . .	153
Figure 37: 20–Constant Single Plate Residuals . . . . .	154
Figure 38: 20–Constant Single Plate Residuals . . . . .	155
Figure 39: 13–Constant Overlap Residuals . . . . .	156
Figure 40: 13–Constant Overlap Residuals . . . . .	157
Figure 41: 13–Constant Overlap Residuals . . . . .	158
Figure 42: 13–Constant Overlap Residuals . . . . .	159
Figure 43: 15–Constant Overlap Residuals . . . . .	160
Figure 44: 15–Constant Overlap Residuals . . . . .	161
Figure 45: 15–Constant Overlap Residuals . . . . .	162
Figure 46: 15–Constant Overlap Residuals . . . . .	163
Figure 47: 18–Constant Overlap Residuals . . . . .	164
Figure 48: 18–Constant Overlap Residuals . . . . .	165
Figure 49: 18–Constant Overlap Plate Residuals . . . . .	166
Figure 50: 18–Constant Overlap Residuals . . . . .	167

Abstract of Dissertation Presented to the Graduate School  
of the University of Florida in Partial Fulfillment of the  
Requirements for the Degree of Doctor of Philosophy

RE-REDUCING THE SOUTHERN POLAR ZONE OF  
THE YALE PHOTOGRAPHIC STAR CATALOGUE

By

Jane E. Morrison

August, 1995

Chairman: Heinrich Eichhorn  
Major Department: Astronomy

We have re-reduced the Southern Polar Zone of the Yale Photographic Star Catalogue ( $-70^\circ$  to  $-90^\circ$  declination) using an overlapping plate technique. This region was photographed in 1955–56 with 64 overlapping plates and the reduction of these plates (i.e. the determination of the equatorial coordinates of the star images on the plates) was completed in 1971. Because of the scarcity of observations from the Southern Hemisphere prior to the 1970's, this data set is particularly valuable.

The plates were photographed so that they overlapped 50% in right ascension and 50% in declination. Thus every region of the sky was covered by at least 2 plates and sometimes as many as 20 different plates. Originally these plates

were individually reduced. Thus after the reduction, some of the stars had many as 20 different position estimates (i.e. right ascension and declination). Clearly a star occupies one position at one time, but this can not be obtained without mathematically enforcing this constraint on a multiple plate reduction process. Instead, the separately computed values were averaged to give the "best" (in the mathematical statistics sense) estimate for the stellar position.

Taking advantage of the high degree of overlap of these plates, we used a more powerful reduction method for overlapping plates called the overlapping plate technique. This method enforces the simple fact that, at a given instant of time, a star is at only one position. When this constraint is enforced, all the reduction parameters on all plates are obtained simultaneously by solving one large system of equations. The application of these improved reduction procedures and resources to the original measurements have yielded star positions which are a 20% improvement over those originally published. These new estimates of star positions are capable of yielding improved proper motions, which are invaluable data for many aspects of astronomy.

## CHAPTER 1 INTRODUCTION

Astrometry, one of the oldest branches of astronomy, deals with the determination of locations and the positional changes of celestial bodies. The compilation of star catalogs is the domain of astrometry devoted to the determination of accurate and precise positions of celestial bodies. One of the most important tasks of astrometry is to establish a reference frame and maintain it by determining the motions of the reference stars which it represents. Usually these reference frames are defined by a star catalog (i.e. FK4 (Fricke et al., 1963), FK5 (Fricke et al. 1988) and soon the HIPPARCOS catalog). The compilation of star catalogs has been a continuing processes over the centuries. One of the first recorded star catalogs was compiled by Hipparchus (128 B.C.) and contained 850 stars (Abell et al., 1987). Throughout the centuries astronomers have devised and improved upon the methods to compute accurate and precise positions for as many stars as possible. Today the largest star catalog is the Guide Star Catalog (GSC, Lasker et al., 1990) containing roughly 20 million objects with a limiting magnitude of 15<sup>m</sup> and positional standard errors from the plate centers to the edges which vary from 0".5 to 1".1 in the northern celestial hemisphere and from 1".0 to 1".6 in the southern celestial hemisphere (Taff et al., 1990). Containing fewer stars, but with a much higher expected positional accuracy, the HIPPARCOS catalog is the first

star catalog to contain observations solely made in space. This catalog is being produced by the European Space Agency from observations taken by the satellite HIPPARCOS and will contain roughly 120,000 star positions with limiting visual magnitudes between  $7.7^m$  and  $8.7^m$  depending upon the galactic latitude. The individual rms-errors (root mean square-errors) are expected to be 1.3 milliarcseconds (mas) per coordinate in position (Kovalevsky, 1995).

Star positions at only one epoch are of limited use, but they become of enormous value when combined with several epochs and changes in the positions are observed. From studying stellar positional changes several important astronomical parameters can be determined; probably the most important of these are stellar parallaxes and proper motions. Trigonometric parallaxes are the only method for determining stellar distances based only on geometry. Once the distances of stars are known, then a host of other quantities can be found, for example, absolute magnitudes and in double star systems, actual orbit semi-major axes and the sum of the masses of the stars can be determined. Proper motions in combination with radial velocities allow one to study the motion of stars in clusters, to identify stellar associations, to determine the orbital motion of double and multiple star systems and to study the motions within the Galaxy which leads to an understanding of the evolution, structure and rotational curve of the Galaxy.

The considerable distances to stars reduce their proper motion to very small amounts; for most stars these are considered negligible within the current proce-

dures of measuring precision. It is almost always an angle too small to measure with precision in a single year. The majority of stellar proper motions can only be determined after a cumulative effect (as a rule) over many decades produces a measurable change in the stars' position. Most of the detectable proper motions are for nearby stars. Though there are several hundred stars with proper motions greater than  $1.''0$  per year (the largest motion being that of Barnard's Star,  $10.''25$  per year), the mean proper motion of all naked-eye stars is less than  $0.''1$  (Abell et al., 1987). Therefore, in order to detect accurately proper motions we must have extremely accurate and precise positions for the stars with preferably decades having elapsed between observations. Star catalogs, in particular old star catalogs, are extremely useful for the determination of proper motions for a large number of stars. For example, stellar proper motions can be detected by comparing catalogs containing the same stars with epochs several decades apart or by combining the positions found in a single catalog with new observations of the same stars. Thus, one way to improve upon the current proper motion estimates is to improve upon the accuracy of the star positions found in the old star catalogs by using improved reduction techniques and better reference material than was originally available. This is one of the justifications for the work reported on in this paper.

For this project we have re-reduced (re-determined) the star positions found in the Southern Polar Zone of the Yale Photographic Star Catalogue ( $-70^\circ$  to  $-90^\circ$  declination, Lü 1971). Because of the scarcity of southern hemisphere

observatories in the first half of this century, there are few accurate old (by this we mean 50 years or more) star catalogs containing southern declination star positions. Thus, this region of the Yale Zone Catalogues is particularly interesting for it contains some of the oldest accurate observations (epoch 1955–1956) taken with photographic plates of the southern polar zone. In addition, the photographic plates that were used to create this catalog were photographed so that they heavily overlapped (50% in right ascension and 50% in declination); thus, many of the same stars are on several plates. This heavily overlapped pattern is particularly well suited to our reduction technique which has improved the accuracy of the stellar positions and will lead to more accurate and precise proper motions when calculated from the positions found in the improved catalog.

The Southern Polar Zone of the Yale Photographic Star Catalogue is one of many zones which make up the Yale Zone Catalogues. In 1913 the director of the Yale Observatory, Frank Schlesinger (“father of modern astrometry”) initiated a project to photograph the entire sky. He planned to re-observe by photography the positions of the Astronomische Gesellschaft Catalogue (AGK series) stars and then by comparing the older AGK positions with the new Yale determinations to detect the proper motions of stars to the ninth magnitude. Ida Barney collaborated with Schlesinger on this project and after Schlesinger’s death in 1942, continued on her own until 1959. Between 1925 and 1959 they (with very few other colleagues) published some 20 volumes of accurate positions and attainable proper motions



for nearly 146,000 stars in the zone from  $-30^\circ$  to  $+30^\circ$ ,  $+50^\circ$  to  $+60^\circ$  and  $+85^\circ$  to  $+90^\circ$  (Hoffleit, 1962).

Dirk Brouwer, director of the Yale Observatory from 1941 to until his death in January 1966, continued Schlesinger's project and extended it to more southern declinations:  $-30^\circ$  to  $-90^\circ$ . Early in 1960, Brouwer obtained a 2-year contract from the U.S. Army Map Service to re-observe all the stars in the Cape Zone Catalogues for the zones  $-30^\circ$  to  $-50^\circ$  and  $-60^\circ$  to  $-90^\circ$ , involving some 70,000 stars, in order to improve the positions and particularly the proper motions in those zones. Dorrit Hoffleit was appointed to supervise the project, starting at  $-30^\circ$  and working southward (Hoffleit, 1983).

The southern catalogs, like the northern ones, were divided into zones (extended regions of the sky bounded by parallels of declination). Except for the polar caps, each zone was covered by photographic plates centered at the same declination, with the right ascensions of the centers spaced such that the vertical center line of a plate almost coincided with the vertical edges of one of its neighbors (i.e. overlap 50% in right ascension). This produced a double coverage of the sky. The overlap in declination was at most only a few degrees and often none. The Southern Polar Zone has a much stronger overlap pattern than the other zones. This region consists of 4 belts of zones with a declination overlap of 50% between the zones and an overlap of 50% in right ascension within the zones. The Southern Polar zone was photographed according the scheme given in Table 1.

Table 1: Yale Zones

<u>Number of Plates</u>	<u>Center Declination</u>	<u>Separation in R.A.</u>
24	-75	1 <sup>h</sup> 00 <sup>m</sup>
20	-80	1 12
16	-85	1 30
4	-90	6 00

The strong overlap pattern is shown the polar plots in Figure 1. The first plot shows the different declination zones the center representing the Southern Celestial Pole ( $-90^\circ$ ) and the other zones are represented by concentric circles, moving outward from the pole:  $-85^\circ$ ,  $-80^\circ$ ,  $-75^\circ$ ,  $-70^\circ$  and  $-65^\circ$ . The first plot is also only 3 plates, the next 4 plots are graphs for the plates in each zone and the last plot shows all the plates for the region. The number of plates contained is each zone given in Table 1.

The Yale Zone Catalogues have been of enormous importance to positional astronomy and in particular the determination of stellar proper motions. Together they contain hundreds of thousands of stars. Schlesinger had planned to eventually cover the whole sky; however, this aim was not quite achieved, the zones  $+60^\circ$  to  $+85^\circ$ ,  $+30^\circ$  to  $+50^\circ$  and  $-50^\circ$  to  $-60^\circ$  are still lacking. The region we are concerned with is the  $-70^\circ$  to  $-90^\circ$  zone. This was the last Yale zone to be photographed (1955–1956) and has the largest star density and magnitude range of all the Yale zones.

## Original Reduction

The plate material for the Yale Southern Polar Zone Catalogue consists of 64 photographic plates with a sky coverage of  $11^\circ \times 11^\circ$  each. These plates were exposed between September 15, 1955 to August 7, 1956 at Sydney, Australia, measured at the Yale Observatory between 1963 and 1968 and the reduction was completed in 1971. The reduction of the plates (i.e. the determination of the equatorial positions of the images on the plates) was completed in 1971 (Hoffleit, 1971). Figure 2 (top) shows the stars for this catalog on a polar plot. The bottom graph in Figure 2 shows the references used to re-reduce the catalog.

In order to explain the reasoning behind our desire to reduce this catalog, we will briefly outline the procedure for reducing plates. The details of this are given in Chapter 4. The reduction of photographic plates requires the use of a set of reference stars, whose stellar images are on the plate and whose equatorial coordinates are known by previous investigation. In the traditional method of reducing plates, estimates of certain plate parameters, which are numerically different and characteristic for each plate, are determined from least squares reductions of the reference stars' equatorial coordinates with respect to the rectangular coordinate on the plate. These plate parameters are then used to convert field stars images (i.e., nonreference stars) to equatorial coordinates. This method of reducing each plate separately has become known as the "single

plate method.”

The original reduction of the Southern Polar Zone was performed using a single plate method by Phillip Lü and Dorrit Hoffleit. The reference catalog used was the Second Cape Catalog for 1950. The Yale plates were taken between 1955 and 1956, so the reference star positions taken from the Cape were corrected to the epochs of the Yale plates by applying proper motions for intervals of three to nine years. On the average there are 150 to 200 reference stars per plate.

After the reduction, the resulting positions of stars that had been recorded on more than one plate were averaged together. The resulting catalog consists of 18,702 stars with their positions and proper motions on the FK3 system (Third Fundamental Katalog, Astronomisches Rechen-Institut, 1957). “The tabulated probable errors of the positions represent simply the internal consistency between different Yale plates used for each star. They imply that the average probable error of each coordinate determined from a single plate amounts to  $\pm 0.''33$ . This is consistent with the average formal probable error of a plate solution, namely  $\pm 0.''35$ ” (Lü, 1971, p. 29). Note that the (usually quoted) standard errors are about 1.5 times this amount or  $\pm 0.''53$ .

### Why Do a Re-Reduction?

A major drawback of the single plate method is that it produces a different position estimate (right ascension, declination) for each star on each plate, even if

that star also appears on more than one plate. Clearly the star can occupy only one position at one time, but this cannot be obtained without mathematically enforcing this constraint on a multiple plate process. Instead, the separately computed values are averaged to give the “best” (in the mathematical statistics sense) estimate for the stellar position.

As just mentioned, the most important constraint, which was never enforced, is the simple fact that any one star, at a given instant of time, occupies only one position. In the case of the Yale Southern Polar Zone, the plates were so strongly overlapped that most stars occurred on 2 plates, some even on 20 plates. Thus after performing the single plate reduction there were as many as 20 different position estimates for some of these stars. Taking advantage of the rich overlap we have re-reduced the plates using a more powerful reduction technique, the overlapping plate technique (Eichhorn, 1960; for review Eichhorn, 1985). In this method the critical constraint that a star can only have one position at one time is enforced. Then all the reduction parameters on all plates are obtained simultaneously by solving one large system of equations (i.e., by a block adjustment). Whereas the single plate is limited to individual least square reductions of just the reference stars on each plate, the overlapping plate method reduces all the plates at the same time using all the stars (not just the reference stars). More accurate (because the systematic errors on individual plates are diminished as a consequence of the forced plate-to-plate agreement which must now occur) and thus also more precise

positions than those obtained from the single plate reduction are generated by the overlap method. This method also has many capabilities that are not possible with a single plate reduction, such as reducing systematic errors between neighboring plates and the estimation of parameters common to certain data sets at varying levels.

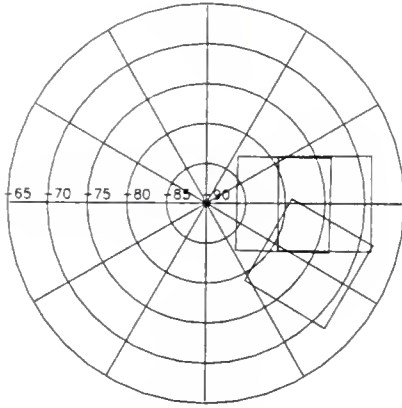
Though the theoretical formation of the overlap method was known when the original reduction was done, it was not used. Originally it had been planned to use an overlap reduction, but as Hoffleit explained in the preface of this catalog, “the planned more elaborate reductions may be a long time forthcoming because of a present shortage of both funds and personnel” (Hoffleit, 1971, p. 3). In fact, when the computations for the Yale Catalogue were carried out, it would have been very difficult to take advantage of the huge number of existing constraints, because enforcing them requires a computing effort that, while almost modest by contemporary standards, was totally prohibitive at the time. Many of the existing geometric and physical constraints could not be enforced and were therefore wasted. The solution using all the available information has become possible only through the emergence of fast computers with large memory capacities.

In addition, we were able to use a more precise and accurate reference star catalog, the International Reference Stars (IRS, Corbin, 1991) which was made available to us by the US Naval Observatory (see Figure 2, bottom). Thus by adjusting the originally measured position of the stars’ images on the plates on

the basis of better reference star position estimates (which were not available when the original reductions were carried out) and using a superior adjustment algorithm, the early positions of these stars have been improved by roughly 20%.

The improvement in the positions found in this old star catalog will improve the proper motion estimates calculated with them. For example the ARCS (Astrographic Catalogue Reference Stars, Corbin and Urban, 1991) and PPM (Positions and Proper Motion Catalog, Bastian et al., 1993) catalogs (both key reference catalogs) used the Yale Southern Polar Zone Catalogue for their determination of proper motions. Thus by improving the positions in the Yale Catalogue we can improve other catalogs that use the positions from the Yale Catalogue. This is especially important in the Southern Celestial Hemisphere, where there are few old reference catalogs. The wholesale improvement of the precision and accuracy of proper motion estimates is one of the keys to improving the precision and accuracy of a large variety of astronomical data. This is one of the reasons why the measurements in the Yale Catalogue, which is based on plates taken several decades ago, are so important.





Plates 1, 3 and 25

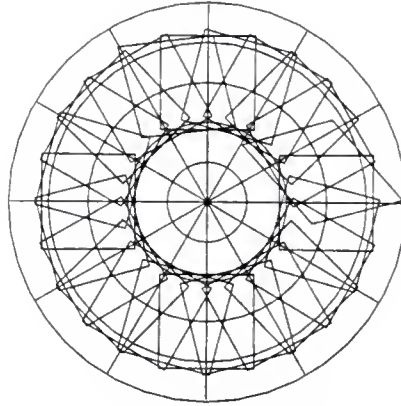
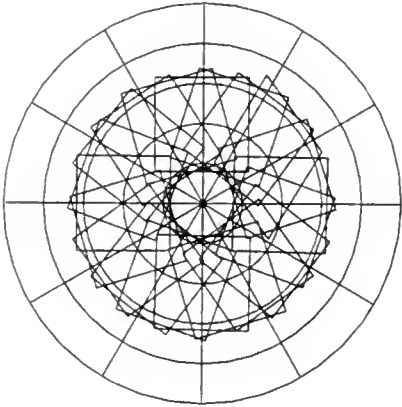
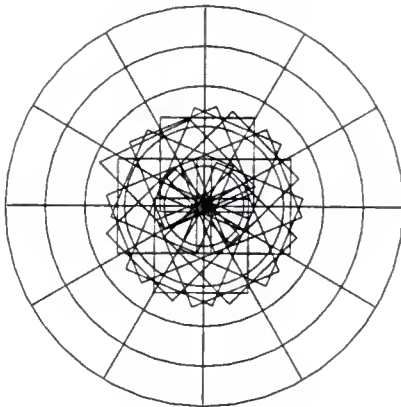
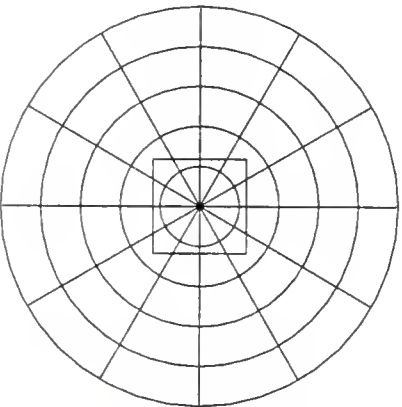
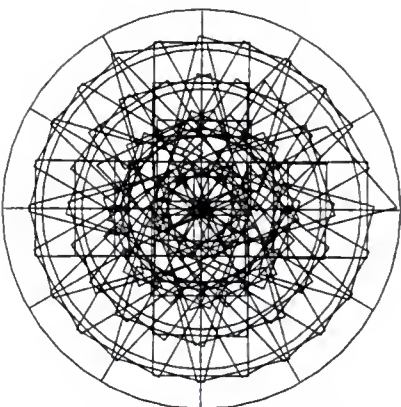
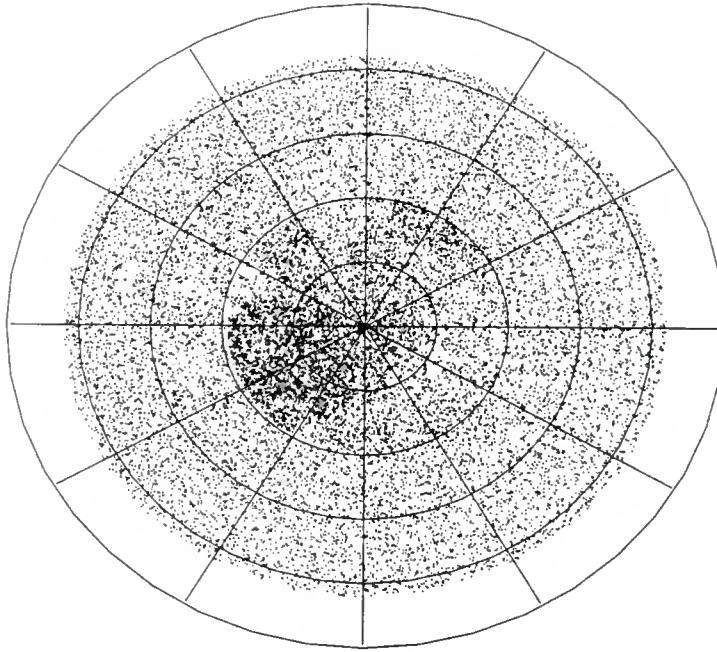
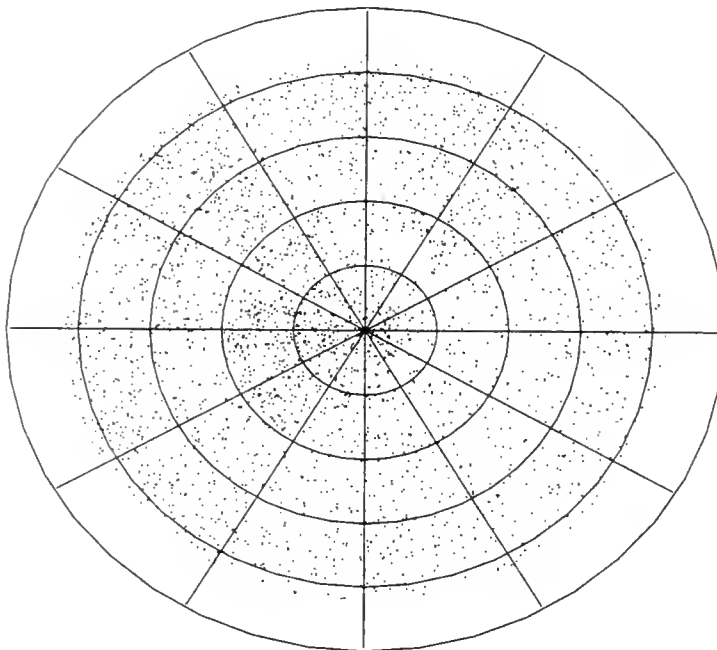
 $-75^\circ$  Zone $-80^\circ$  Zone $-85^\circ$  Zone $-90^\circ$  Zone $-70^\circ$  to  $-90^\circ$  Zone

Figure 1: The plates for the Southern Polar Zone of the Yale Catalogue





Star Images for the Yale Southern Zone



IRS Reference Stars

Figure 2: The Stars of the Southern Polar Yale Zone of the Yale Photographic Star Catalogue

## CHAPTER 2

### PHOTOGRAPHIC ASTROMETRY

One method of creating a star catalog (a list of right ascension and declination of a group of stars) is to photograph a region of the sky with photographic plates. Once the plates are developed, the positions of the star images on the plate in a certain rectangular coordinate system  $(x,y)$  are determined with a measuring machine. The positions of the measurements on the photographic plate can be derived only with the use of a set of known positions of stars whose images are among those recorded on the plate. Their equatorial coordinates are usually found from existing star catalogs. We call such stars *reference stars* and all other stars for which we do not have equatorial coordinates, *field stars*. The goal of catalog compilation is to determine accurately the spherical coordinates (for our purposes, equatorial coordinates) of all the stars imaged on the plate (field stars as well as reference stars).

In the ideal case, one assumes that the optical system (telescope + plate holder) is equivalent to a pinhole camera, in which is governed by the laws of the gnomonic projection. A gnomonic projection is the projection of a spherical surface onto a plane through a point. For descriptive purposes we will assume the existence of the fictitious “celestial sphere” and we will further assume that the center of the celestial sphere lies at the optical center of the objective system.

In this perfect case the portion of the “celestial sphere” where the telescope is pointing is projected onto a plane through the focal point of the telescope. The resulting rectangular coordinates projected onto the plane are known as the standard coordinates  $(\xi, \eta)$ . The usefulness of photography for astrometric positional work is connected with the fact that there exists a simple, rigorous and parameter-free geometrical relationship between positions of objects on the sky and their standard coordinates projected onto the plate.

### Standard Coordinates and their Relationship to the Equatorial Coordinates

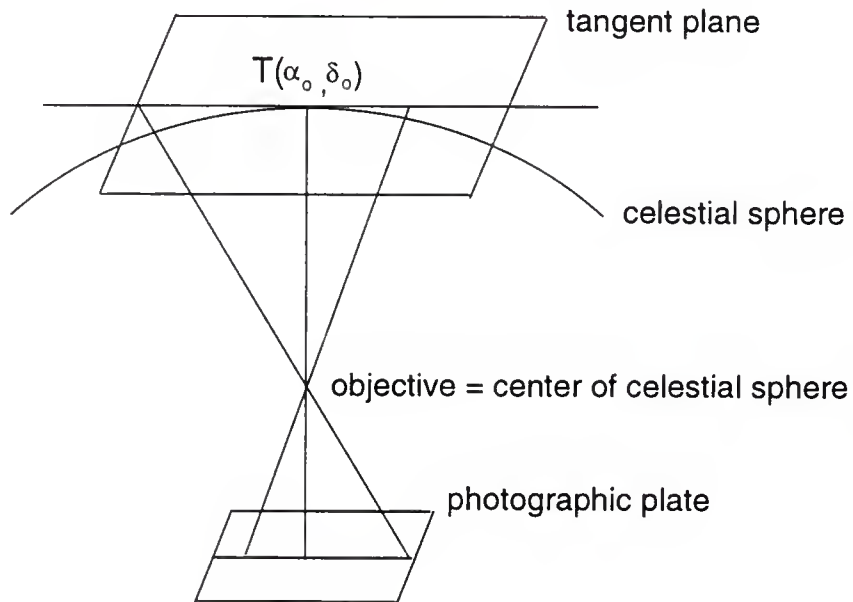


Figure 3: Gnomonic Projection

Imagine a plane which is tangential to the celestial sphere at the point  $\alpha_0, \delta_0$ . In the plane define a left handed coordinate system  $(\xi, \eta)$  (as seen from the center of the sphere), such that its origin is at the tangential point. The positive  $\eta$  axis is tangential to the hour circle through  $\alpha_0$  and points northward. The  $\xi$  axis is tangential to the parallel of declination at  $\delta_0$  and points east (in the direction of increasing right ascension). This plane coordinate system is thus, by definition, parallel to the focal plane of the telescope and therefore parallel to the plane of the photographic plate being used to record the images. The tangential point can also be described as the point in which a line normal to the plate coincides with the optical axis of the telescope and penetrates the plate close to its geometrical center. Thus star positions on the celestial sphere are projected in straight lines through the center of the sphere (which is also the focal point of the telescope) and onto the tangent plate. This geometrical situation is illustrated in figure 3.

If we further assume that the radius of the sphere is equal to 1, the well known relationships between a point on the celestial sphere  $(\alpha, \delta)$  and the gnomonic projection  $(\xi, \eta)$  of this point onto a plane which is tangent to the unit sphere at  $(\alpha_0, \delta_0)$  is given by

$$\begin{aligned}\xi &= \frac{\cos \delta \sin (\alpha - \alpha_0)}{\sin \delta \sin \delta_0 + \cos \delta \cos \delta_0 \cos (\alpha - \alpha_0)} \\ \eta &= \frac{\sin \delta \cos \delta_0 - \cos \delta \sin \delta_0 \cos (\alpha - \alpha_0)}{\sin \delta \sin \delta_0 + \cos \delta \cos \delta_0 \cos (\alpha - \alpha_0)}.\end{aligned}\tag{1}$$

These equations are rigorous and free of estimated parameters, and can be inverted so that  $\alpha$  and  $\delta$  can be found from  $\xi$  and  $\eta$ . Note that  $\xi$  and  $\eta$  are in units of

the telescope's focal length.

However, in practice no real optical device produces images in the same way as a pinhole camera. One needs to take into account such effects as coma, radial distortion, rotation and tilt of the plate when photographed or measured. The measured coordinates  $(x,y)$  are actually approximations to the standard coordinates  $(\xi,\eta)$ .

### Determining the Equatorial Coordinates from the Measured Coordinates

The goal of a plate reduction is the derivation of the spherical equatorial coordinates from the objects' measured positions on the plate. Usually this process is achieved in two steps. First the measured coordinates are transformed to the standard coordinates, then these are converted to equatorial coordinates. The second step has already been dealt with (i.e., equation 1), so only the first remains.

The establishment of the relationship between the standard coordinates  $(\xi,\eta)$  and the measured plate coordinates  $(x,y)$  of the star's images is the fundamental problem of determining the equatorial coordinates. In the ideal case (assuming a pinhole camera), even though the precise position of the image of the tangential point  $(\alpha_0, \delta_0)$  on the plate is not known, it is reasonable to assume that it is near the geometric center of the plate. Plates are usually exposed in such a manner that it is also reasonable to assume that the edges of the plate (i.e. the  $x$  and  $y$  axes) are closely parallel to the  $\xi$  and  $\eta$  axes, respectively. If the origin of the

measured coordinates is chosen to lie at the geometric center of the plate and the axes are properly oriented, to first approximation the standard coordinates are related to the measured coordinates by a factor of the telescope's focal length,  $s$ :

$$\begin{pmatrix} x \\ y \end{pmatrix} = s \begin{pmatrix} \xi \\ \eta \end{pmatrix} + O(1). \quad (2)$$

The unit of length on the plate in the  $\xi$ - $\eta$  system is such that the standard coordinates are equal to 1 at a distance of 1 focal length from the tangential point. Each departure from the ideal imaging process, a gnomonic projection, results in deviations from the perfect relationship in the equation

$$\begin{pmatrix} x - c \\ y - d \end{pmatrix} = s \begin{pmatrix} \cos \phi & \sin \phi \\ -\sin \phi & \cos \phi \end{pmatrix} \begin{pmatrix} \xi \\ \eta \end{pmatrix} \quad (3)$$

where  $c$ ,  $d$  and  $\phi$  are all small quantities of the first order. The end result is a mapping between the standard coordinates and the measured coordinates. Traditionally, this mapping is called a plate model. The plate parameters have traditionally been called plate constants. We prefer the terminology "plate parameters" which indicates that these are adjustment parameters to be estimated by some statistical process.

In the traditional method of reducing plates one assumes there exists for each plate the following relationships

$$\begin{aligned} f(x_i, y_i; m_i, c_i; \alpha_i, \delta_i; a_1, a_2, \dots, a_n) &= 0 \\ g(x_i, y_i; m_i, c_i; \alpha_i, \delta_i; a_1, a_2, \dots, a_n) &= 0 \end{aligned} \quad (4)$$

between the measured coordinates  $x_i, y_i$  of the image of the  $i$ th star, its magnitude  $m_i$  and color index  $c_i$ , and its coordinates  $\alpha_i, \delta_i$ , on the one hand and a set of plate parameters  $\{a_k\}$  on the other hand. If all the plates had been taken with the same telescope, the plate parameters will belong to groups such that some elements vary from plate to plate, others vary from plate to plate but are constrained, and finally some are the same for all plates obtained on the same telescope. (Eichhorn, 1974).

After the functional form of the plate model is established, the plate constants (or estimates thereof) are determined from a statistical adjustment (usually a least squares adjustment), by fitting the measured coordinates to the corresponding spherical coordinates of the reference stars ( $\alpha, \delta$ ). In this case, equations (4) then become the equations of condition for a least squares adjustment in which the  $x_i, y_i, \alpha_i$  and  $\delta_i$  are regarded as observations and the  $a_1, a_2, \dots, a_n$  as the unknown parameters. The  $m_i$  and  $c_i$  are assumed to be known for every star. Of course, there must be enough reference stars to make the system over-determined (i.e., the number of reference stars must be greater than the number of parameters). A good rule of thumb is that there should be at least 3 times as many reference stars as plate parameters. Once the plate parameters are determined the best estimates of the standard coordinates for all the stars (field stars as well as reference stars) can be obtained. Then, after routinely inverting the gnomonic projection (equation 1) the equatorial coordinates for all the stars are computed.



### The Relationship Between the Standard and Measured Coordinates

Even under the most favorable conditions the assumption of a perfect gnomonic projection can only approximate the actual circumstances. It is clear that neither telescope nor measuring machine can be constructed with perfect accuracy. First of all, there is no optical system in practical use which unites in a single point all light rays that enter the front component of the objective from the same direction. In reality there are many deviations from the ideal situation which require small corrections to be added to equation (2). These departures from the perfect gnomonic projection are “instrumental.” Others, which rotate and distort the coordinate system with respect to which the position estimates of the reference stars are catalogued, may be termed astronomical effects and include refraction, aberration, precession and nutation. We will deal separately with these two types of “corrections.” The “instrumental” corrections will be characterized by the plate model and the “spherical” corrections will be discussed in the next section.

Below is a list of some of the more common departures from the ideal gnomonic projection; this list is by no means exhaustive:

1. Shift in the origin of the  $x$ - $y$  coordinate system with respect to the  $\xi$ - $\eta$  coordinate system ( $c$  and  $d$  in equation 3)
2. Rotation of the  $\xi$ - $\eta$  axis with respect to the  $x$ - $y$  axis.



3. The  $\xi$ - $\eta$  scale may be different from the x-y scale, due to a poorly known focal length.
4. Tilt of the x-y focal plane with respect to the  $\xi$ - $\eta$  focal plane, this will cause an incorrect tangential point.
5. Different scales on each axis, due to different measuring screws or otherwise introduced by the measuring device.
6. Lens aberrations (distortion, spherical aberration, coma, astigmatism, chromatic aberration) affect the position of the stellar centroids either by enlarging them (thus making it more difficult to determine the center) or by an actual shift in positions, both of which vary depending on the location on the plate. These effects plus peculiarities of the process of photographic image formation render the positions of the star's images on the plate dependent on their magnitudes and spectra expressed in terms of color indices. These conditions lead to the inclusion of the  $m_i$  and  $c_i$  terms in the mapping between x-y and  $\xi$ - $\eta$  coordinate systems.
7. Besides lens aberration "smeared out" or "blow up " images can be produced by guiding errors, developing errors (e.g. emulsion shifts), and bad seeing. These can and do affect the position of the stellar centroids.

Each departure from the ideal imaging process results in deviations from the relationship  $x=s\xi$ ;  $y=s\eta$ . Given below are the relationships between the standard

coordinates and the measured coordinates to correct for many of the commonly experienced errors.

1. Translation error: If the photographic plate is not centered correctly on the measuring machine, there will be a systematic difference between the measured coordinates and ideal coordinates.

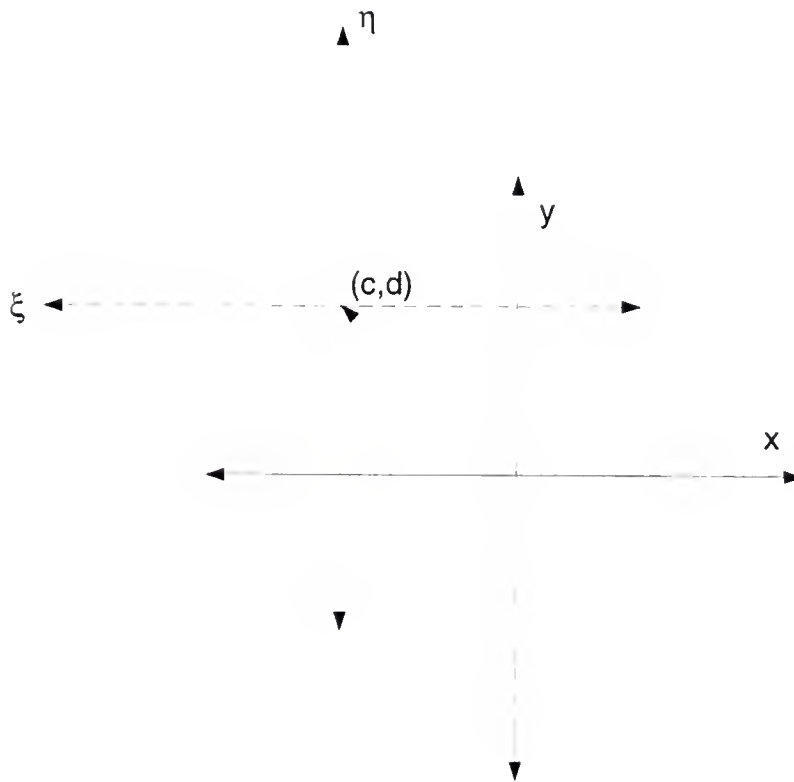


Figure 4: Origin Shift

$$x - s\xi = c$$

$$y - s\eta = d$$

(5)

2. Rotation: If the photographic plate is correctly centered, but rotated relative to the measuring machine axes by an angle  $\phi$  ( $\phi > 0$  for counterclockwise).

$$\begin{aligned} x &= s(\xi \cos \phi + \eta \sin \phi) \\ y &= s(\eta \cos \phi - \xi \sin \phi). \end{aligned} \quad (6)$$

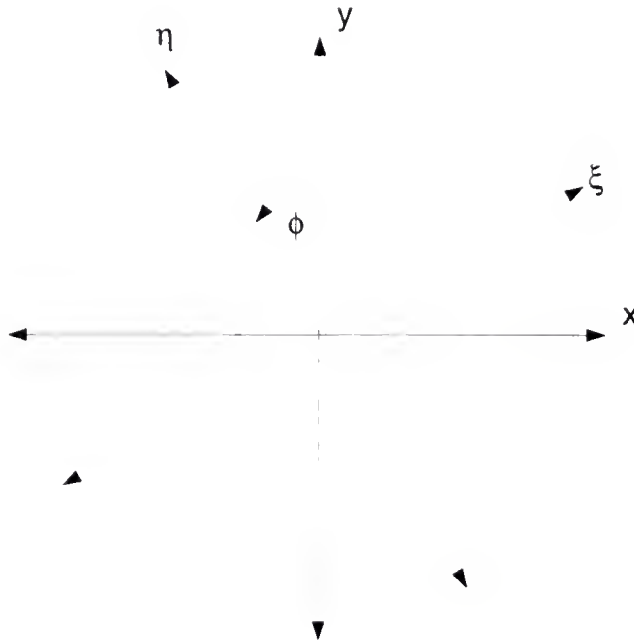


Figure 5: Rotation of x-y axis with respect to the  $\xi$ - $\eta$  axis

3. Imprecise focal length: An incorrect focal length can cause differences in the scales between the  $\xi, \eta$  system and x,y system. This can be corrected by making small changes in  $\xi$  and  $\eta$ :

$$\begin{aligned} x - s\xi &= a\xi \\ y - s\eta &= e\eta. \end{aligned} \quad (7)$$

4. Center error (tangent point error): For wide fields ( say over  $5^\circ \times 5^\circ$ ) the extraneous methods for the determination of  $\alpha_0$  and  $\delta_0$  yield approximate values of these equations and thus they must be corrected differentially. If the actual position of the tangential point is  $(\alpha_0+d\alpha_0)$ ,  $(\delta_0+d\delta_0)$  instead of  $\alpha_0, \delta_0$ , values of  $\xi, \eta$  will be incorrect if calculated only from  $\alpha_0, \delta_0$ . It can be shown to first order in  $d\alpha_0$  and  $d\delta_0$  (Eichhorn, 1971) that the centering error can be corrected (to first order) by

$$x - s\xi = (\cos \delta_0 d\alpha_0) \xi^2 + d\delta_0 \xi \eta \quad (8)$$

$$y - s\eta = (\cos \delta_0 d\alpha_0) \xi \eta + d\delta_0 \eta^2$$

provided that the plate was oriented during measurement so that the  $x$  and  $\xi$  axis as well as the  $y$  and  $\eta$  axes are nearly parallel and  $(\xi, \eta)$  are in radians

If  $d\alpha_0$  and  $d\delta_0$  turn out to be large, it is recommended that the calculation be repeated with the newly calculated  $\xi, \eta$  now referred to the tangential point  $\alpha_0+d\alpha_0$  and  $\delta_0+d\delta_0$ . This may be repeated until further repetitions result in no change in the assumed  $\alpha_0, \delta_0$  (Eichhorn, 1974).

5. Tilt: If the photographic plate is not perpendicular to the optical axis of the telescope but titled by an angle  $\omega$  relative to the focal plane, the errors introduced will be

$$x - s\xi = (p\xi^2 + q\xi\eta) \tan \omega \quad (9)$$

$$y - s\eta = (p\xi\eta + q\eta^2) \tan \omega$$

where  $p$  and  $q$  are constants (Taff 1981). One can see the terms for the corrections for zero point error and tilt have the same form. This is because if

we have a situation where there is a tangential point error this is the equivalent of having an imaginary plate whose true tangent point coincides with our assumed one, but is inclined to the actual plate. Since these two effects can be modeled in a similar manner, they are sometimes combined under that same name. If construction and proper alignment of the telescope has been carefully executed such second order errors may be neglected. However, in the case of large plates (over  $5^\circ \times 5^\circ$ ), it is important that these higher order terms be included (König, 1962).

6. Radial distortion: If the image process produces a net radial distortion, it can be modeled. Radial distortion originates at the intersection point of the optical axis with the focal plane and its origin will, therefore, also be very close to the tangential point. This aberration is radially symmetric and usually modeled in the form

$$\begin{aligned} x - s\xi &= \xi \sum_{k=1}^n R_k (\xi^2 + \eta^2)^k \\ y - s\eta &= \eta \sum_{k=1}^n R_k (\xi^2 + \eta^2)^k \end{aligned} \quad (10)$$

where  $R$  is a constant (Eichhorn 1974). Unless the radial distortion is very strong, and for the field sizes used on photographic catalog astrometry, only the first terms of equations (9) are necessary for appropriate modeling of radial distortion. Thus with  $n = 1$ ,

$$\begin{aligned} x - s\xi &= R\xi(\xi^2 + \eta^2) \\ y - s\eta &= R\eta(\xi^2 + \eta^2). \end{aligned} \quad (11)$$

7. Nonperpendicularity of axes: If the axes of the measuring machine are not perpendicular to each other (in other words  $x$  is not perpendicular to  $y$ ), let  $\psi$  be the angle between the  $\eta$  and  $y$  axes (McNally, 1975)

$$\begin{aligned}x - s\xi &= \eta \tan \psi \\ y - s\eta &= (1 - \sec \psi)\eta.\end{aligned}\tag{12}$$

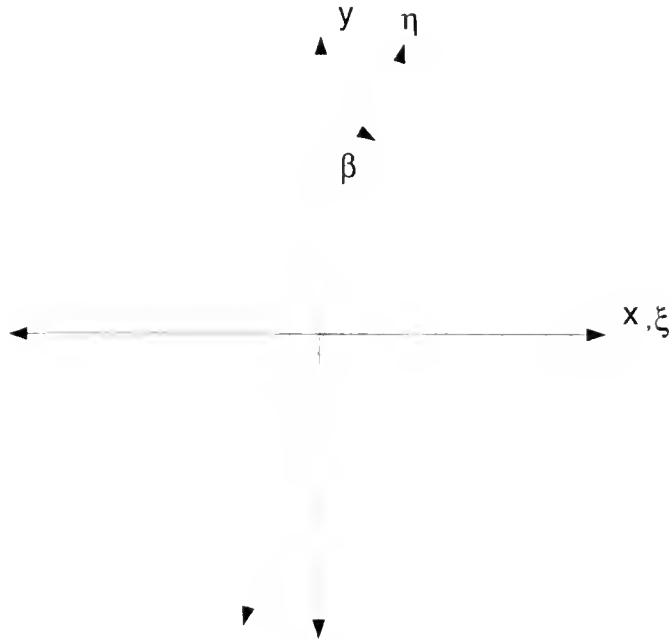


Figure 6: Nonperpendicularity of axes

8. Coma: The effective focal length of the instrument may depend on the apparent magnitude  $m$  of the object that is being imaged. This is coma; it is radial and accounted for by

$$\begin{aligned}x - s\xi &= tmx \\ y - s\eta &= tmy.\end{aligned}\tag{13}$$

Experience shows that the coefficient  $s$  is rather sensitive to the rate of change of the ambient temperature during the exposure. Thus it can not be regarded as a constant for any one objective, although the values obtained in practice will have a tendency to cluster around a certain value (see Eichhorn & Gatewood, 1967).

9. Decentering distortion: If all the components of the objective are not properly aligned, the resulting imperfection is known as decentering distortion. Brown (1966) found that the appropriate corrections to the measured  $x$  and  $y$  coordinates are

$$\begin{aligned} x - s\xi &= \{2[P_1\xi^2 + P_2\xi\eta] + P_1(\xi^2 + \eta^2)\} \left[ 1 + \sum_{k=1}^n P_{k+2}(\xi^2 + \eta^2)^k \right] \\ y - s\eta &= \{2[P_1\xi\eta + P_2\eta^2] + P_2(\xi^2 + \eta^2)\} \left[ 1 + \sum_{k=1}^n P_{k+2}(\xi^2 + \eta^2)^k \right]; \end{aligned} \quad (14)$$

again, under the conditions imposed by catalog photographic astrometry, the terms with  $P_{k+2}$  may usually all be assumed to equal zero, this results in a second order effect

$$\begin{aligned} x - s\xi &= 2[P_1\xi^2 + P_2\xi\eta] + P_1(\xi^2 + \eta^2) \\ y - s\eta &= 2[P_1\xi\eta + P_2\eta^2] + P_2(\xi^2 + \eta^2). \end{aligned} \quad (15)$$

One can see by comparison, the first brackets are exactly the same structure as those that model the correction to the tangential point error (number 4) and tilt (number 5). If the model includes the provisions for correcting the tangential point (or tilt) anyway, the above decentering terms in the brackets can be may "lumped" with them. Then by just adding the  $P_1(\xi^2 + \eta^2)$ ;  $P_2(\xi^2 + \eta^2)$  terms one can account for the corrections due to decentering distortion.

As just indicated the sources of errors are not independent of each other and there is much crossover in effects but they can be modeled in a first order (sometimes second order) approximation that will more than suffice considering their magnitude and the magnitude of the measuring errors. It is worth noting that the coefficients which describe the distortions are very insensitive to changes in the ambient temperature and may thus be regarded as more or less constant for any one objective. This statement is not true for coma, which is, in effect, a dependence of the effective focal length (scale) on magnitude.

### Some Commonly Used Models

The difficulty in establishing the relationship between the standard and measured coordinate system is in determining which terms to include in the model. Eichhorn (1985) writes the relationship (2) in the form

$$\begin{pmatrix} x \\ y \end{pmatrix} = s \begin{pmatrix} \xi \\ \eta \end{pmatrix} + \Xi \mathbf{a} \quad (16)$$

where  $\Xi$ , the model matrix, is a function of  $\xi$ ,  $\eta$ ,  $m$  and  $c$ , and  $\mathbf{a}$  is the vector of plate parameters. The form of the model matrix is determined by probing possible deviations from the gnomonic projection, first adding appropriate terms to a very basic model, and then investigating the adjustment residuals produced by additional terms. When significant terms are found they are added to the model. This trial and error process continues until one is satisfied that one has found the



“best” possible model which approximates the “true” system. We will now look at some of the models which have been employed in the past.

#### 4-Constant Model

The first model we will look at is the simplest and therefore the most basic model; it corrects for errors in the measurements. We will assume the tangential ( $\alpha_0 \delta_0$ ) to be known or determinable by extraneous methods and thus not subject to the adjustment. The scale and orientation of the standard coordinates are fixed by their definition. However, the system of the measured coordinates is dependent on the measuring machine and the accidental orientation of the photographic plate on it. Consequently, the two systems may not agree because the origins of each system might be different and the axes of one system may be rotated with respect to the ones of the other. This situation is demonstrated in figure 7.

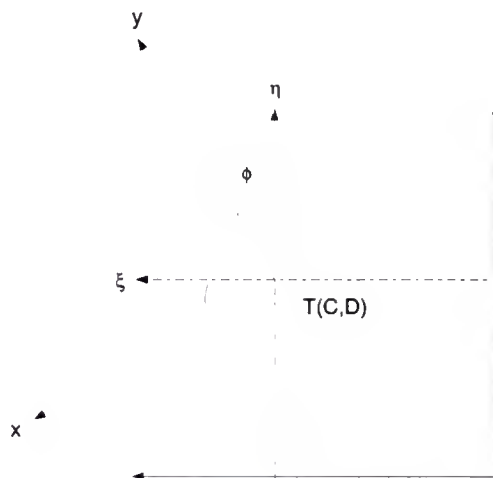


Figure 7: 4-Constant Model: origin shift and rotation of axes

$$x = s(\xi \cos \phi + \eta \sin \phi) + c \quad (17)$$

$$y = s(\eta \cos \phi - \xi \sin \phi) + d.$$

where  $\phi$  is the angle of rotation,  $s$  the focal length and  $c$  and  $d$  the difference in the origins. Combining these effects results in the following model. If we let  $a = s \cos \phi$  and  $b = s \sin \phi$ , then the equation becomes,

$$x = a\xi + b\eta + c \quad (18)$$

$$y = a\eta - b\xi + d.$$

Frequently, equation (18) is written in the form

$$\begin{pmatrix} x \\ y \end{pmatrix} = s \begin{pmatrix} \xi \\ \eta \end{pmatrix} + \begin{pmatrix} \xi & \eta & 1 & 0 \\ \eta & -\xi & 0 & 1 \end{pmatrix} \begin{pmatrix} a \\ b \\ c \\ d \end{pmatrix}. \quad (19)$$

In this case plate model,  $\Xi$ , is the  $2 \times 4$  matrix and the vector of plate constants  $\mathbf{a}$  is  $(a, b, c, \text{ and } d)$ . There are four plate constants, so this model is called the *4- constant model*.

Usually, the plates are measured in such a way that the x-axis is almost parallel to the  $\xi$ -axis which will (if  $x$  and  $y$  are strictly rectangular) render the y-axis almost parallel to the  $\eta$ -axis. This will make  $b$  very small compared to  $a$ . So, when  $\phi \approx 0$ ,

$$a = \rho \cos \phi \quad \cos \phi \approx 1, \quad (20)$$

$$\text{thus, } a \approx \rho$$

and

$$b = \rho \sin \phi \quad \sin \phi \approx 0, \quad (21)$$

$$\text{therefore, } b \approx 0.$$

Thus the term  $a$  is the correction to the assumed focal length. If the  $x$ - $y$  and  $\xi$ - $\eta$  axes are tilted with respect to each other, this term may have a small effect due to this rotation, but the dominant effect is the correction to the focal length.

The inversion of the above equation is

$$\begin{pmatrix} \xi \\ \eta \end{pmatrix} = \frac{1}{a^2 + b^2} \begin{pmatrix} a & -b \\ b & a \end{pmatrix} \left[ \begin{pmatrix} x \\ y \end{pmatrix} - \begin{pmatrix} c \\ d \end{pmatrix} \right] \quad (22)$$

or after introducing certain quantities

$$\begin{pmatrix} \xi \\ \eta \end{pmatrix} = \begin{pmatrix} A & B \\ -B & A \end{pmatrix} \begin{pmatrix} x \\ y \end{pmatrix} + \begin{pmatrix} C \\ D \end{pmatrix} \quad (23)$$

where  $A$ ,  $B$ ,  $C$ ,  $D$  make up the matrix of plate constants. Thus for the 4-constant model a rigorous equation exists for  $\xi$  and  $\eta$  to be solved in terms of the plate constants and  $x$  and  $y$ .

### 6-Constant Model

The 4-constant model does not correct for different scales in the  $x$  and  $y$  measurements. Correcting for this effect, equation (17) becomes

$$\begin{pmatrix} x \\ y \end{pmatrix} = s \begin{pmatrix} \cos \phi & \sin \phi \\ -\sin \phi & \cos \phi \end{pmatrix} \begin{pmatrix} \xi \\ \eta \end{pmatrix} + \begin{pmatrix} c \\ d \end{pmatrix} - \begin{pmatrix} a \\ e \end{pmatrix} \begin{pmatrix} \xi \\ \eta \end{pmatrix} \quad (24)$$

or after multiplying out

$$\begin{aligned} x &= s \cos \phi \xi + s \sin \phi \eta + c - a\xi \\ y &= -s \sin \phi \xi + s \cos \phi \eta + d - e\eta. \end{aligned} \quad (25)$$

After substituting the following values,  $a = \cos \phi - \frac{a}{s}$ ,  $e = \cos \phi - \frac{e}{s}$ ,  $b = \sin \phi$ ,  $f = -\sin \phi$ ,  $c = \frac{c}{s}$ , and  $d = \frac{d}{s}$

$$\begin{pmatrix} x \\ y \end{pmatrix} = s \begin{pmatrix} \xi \\ \eta \end{pmatrix} + \begin{pmatrix} \xi & \eta & 1 & 0 & 0 & 0 \\ 0 & 0 & 0 & \xi & \eta & 1 \end{pmatrix} \begin{pmatrix} a \\ b \\ c \\ e \\ f \\ d \end{pmatrix}. \quad (26)$$

1.  $a$  &  $e$ : correction to assumed focal length.
2.  $b$  &  $f$ : correction for rotation of  $x$ - $y$  system with respect to  $\xi$ - $\eta$  system. This also corrects for nonperpendicularity of the  $x$  and  $y$  axes. These should be approximately equal and opposite in sign.
3.  $c$  &  $d$ : differences in origin of the  $x$ - $y$  system and  $\xi$ - $\eta$  system.

For the 6-constant model there exists an equation analogous to equation (23) for the 4-constant model. In other words  $\xi$  and  $\eta$  can be rigorously solved for from the plate constants and  $x$  and  $y$ . This is not true for the other models we will be using. In those cases, an initial approximation is used and the solution then iterated until a set tolerance is met.

### 12-Constant Model

So far our models have only dealt with terms linear in the standard coordinates  $\xi$  and  $\eta$ . However, there are many “second order” effects that need to be considered, especially when dealing with large plates like the Yale plates ( $11^\circ \times 11^\circ$ ). A standard model for the conversion of the measured coordinates to the

standard coordinates considers corrections for 1) rotation, 2) translational error, 3) tangential point correction, 4) radial distortion, 5) tilt and 6) coma ; it is the *12-constant* model:

$$\begin{pmatrix} x \\ y \end{pmatrix} = s \begin{pmatrix} \xi \\ \eta \end{pmatrix} + \begin{pmatrix} a \\ b \\ c \\ e \\ f \\ e \\ p \\ q \\ i \\ j \\ g \\ h \end{pmatrix} \quad (27)$$

$$\begin{pmatrix} \xi & \eta & 1 & 0 & 0 & 0 & \xi^2 & \xi\eta & m - m_0 & 0 & \xi m & \xi(\xi^2 + \eta^2) \\ 0 & 0 & 0 & \xi & \eta & 1 & \xi\eta & \eta^2 & 0 & m - m_0 & \eta m & \eta(\xi^2 + \eta^2) \end{pmatrix}$$

1.  $a$  &  $e$ : correction to assumed focal length (different in  $x$  and  $y$ ).
2.  $b$  &  $f$ : correction for rotation of  $x$ - $y$  system with  $\xi$ - $\eta$  system. This also corrects for nonperpendicularity of the  $x$  and  $y$  axes
3.  $c$  &  $d$ : differences in origin of the  $x$ - $y$  system and  $\xi$ - $\eta$  system
4.  $p$  &  $q$ : Tangential point correction and tilt
5.  $i$  &  $j$ : magnitude "equations"
6.  $g$ : coma
7.  $h$ : radial distortion

All terms of  $\Xi \mathbf{a}$  are at least one order of magnitude smaller than  $x$ ,  $y$  or  $\xi$ ,  $\eta$  and  $s$  is, of course, an approximation for the focal length. This clearly shows that the rigorous formulas give  $\xi$ ,  $\eta$  not in radians, but rather in units of the focal length; they are indeed dimensionless quantities.

This model is very similar to one we chose to best represent the spherical coordinate system. The actual model and method of determining the model for the Yale plates is given in Chapter 6.

### Spherical Correction

We stated earlier that we split the deviations from the perfect gnomonic projection into instrumental and astronomical effects. The instrumental effects are corrected by the plate model. The astronomical deviations arise because the image formed on the photographic plate represents the refracted apparent topocentric positions of the objects. The standard coordinates are computed from the coordinates listed in star catalogs (e.g. mean positions). To account for the difference between the refracted topocentric apparent positions ( $x$ ,  $y$ ) and the mean positions ( $\xi$ ,  $\eta$ ), corrections for refraction, precession, and for extreme accuracy, diurnal aberration, should be applied. We will not consider diurnal aberration, since its effect is smaller than our measuring error. The effects of precession are accounted for by correcting the reference catalog and influence the results only slightly through refraction.

Atmospheric refraction causes light from a celestial body to be bent as it passes through the Earth's atmosphere. Assuming a simple model for the atmosphere as a plane atmosphere and for small zenith distances, total refraction in the zenith distance can be calculated by

$$z - z_0 = \Delta z = \beta \tan z \quad (28)$$

where  $z$  and  $z_0$  are the topocentric apparent (i.e., unaffected by refraction) and observed refracted zenith (i.e., effected by refraction) distance of the object, respectively.  $\beta$  is the constant of refraction and depends weakly on the temperature and pressure at the observing station (usually this value is about 1 minute of arc). Since  $\Delta z > 0$ , astronomical refraction raises celestial objects toward the zenith. Astronomical refraction ideally does not affect the azimuth.

For large zenith distances, allowance has to be made for the variation of  $\beta$  within the field of the plate; in practice, it suffices to put  $\beta = \beta_0 + \beta' \tan^2 z$ , where  $\beta'$  and  $\beta_0$  are refraction constants and can be found in refraction tables (König, 1933). Thus equation (28) becomes

$$\Delta z = \beta_0 \tan z + \beta' \tan^3 z. \quad (29)$$

We have neglected higher order terms for zenith distance less than  $70^\circ$ .

We will split the effects of atmospheric refraction into those of “absolute” and “differential.” By “absolute” we mean the amount of refraction affecting the

center of plate or more precisely the tangential point. We can think of refraction as shifting all the positions on the plate by this constant amount plus a differential amount which varies across the plate. For example in Figure 8 (top) we have plotted the effects of refraction for plate 1. As one can see the positions are shifted mostly in the  $y$  direction (an average of about  $49''$ ). In Figure 8 (bottom) we have shown the effect across the plate by subtracting the tangential point refraction. Note that the scales for the two graphs are not the same; in the bottom left hand corner of each graph we have plotted the scale:  $50''$  for the top graph and  $5''$  for the bottom one. We will apply a correction for differential refraction, and since our plate model already has a linear term in it we will allow the linear effect of absolute refraction to be taken care of by our plate model.

It has been a frequent practice to account for differential refraction by adding higher order terms to the model. This is usually achieved by adopting a full second and third order polynomial expansion in the coordinates. There are two major disadvantages to using this approach.

Firstly, if the number of parameters is large an unfavorable error propagation of the resulting star positions in the plate field due to the random errors in the  $x$ - $y$  measurements and the reference star positions is introduced (Eichhorn and Williams, 1963); in particular when the number of reference stars per plate is small. Secondly, all effects are mixed up in the model and therefore it is impossible to separate different contributions and evaluate the physical meaning



of the plate parameters in detail.

As we mentioned above we will pre-correct the  $x, y$  measurements for the differential atmospheric refraction. These values are used as observations in the plate reduction. In this way, the number of parameters in the model can be kept to a minimum which will give us a better chance to disentangle the complicated origins of many of the plate parameters (Zacharias et al., 1992).

The usual approach in plate reduction calculations is to transform the equatorial system to the horizon system and make refraction corrections in a simple way in the horizon system. In this manner the effect of refraction is added to the reference positions. However, this leads to the situation where the same star imaged on different plates has different positions due to refraction. From Chapter 1 we stated that the power of the reduction technique that we use, the overlapping plate method (Chapter 4), is that it enforces the constraint that a single star photographed on many plates must have only one position in the sky. Therefore correcting the stars' equatorial coordinates for refraction leads to a different position depending on what plate it was imaged, thereby invalidating our constraint. We have chosen, instead, to pre-correct the measured star images so that they represent the position on a plate if the plate had been observed outside of the atmosphere. We have used the equations developed by König (1933) for calculating the corrections for refraction,  $\Delta x$  and  $\Delta y$ , which are to be applied to the apparent topocentric coordinates,  $x$  and  $y$ . After calculating the zenith distance of

the plates at the time of exposure and then allowing for temperature and pressure we can determine  $\beta_0$  from the refraction Tables 7–13 in König (1933) and let  $\beta' = -0.082''$ . Table 2 and Table 3 contain all the necessary information to determine refraction with the aid of König's refraction tables. In addition, the latitude at the Sydney observatory is  $-33^\circ 51' 41.''1$ , the longitude is  $-10^h 4^m 49.^s06$ , and we have assumed an altitude at sea level and a barometer reading of 750 millibars.

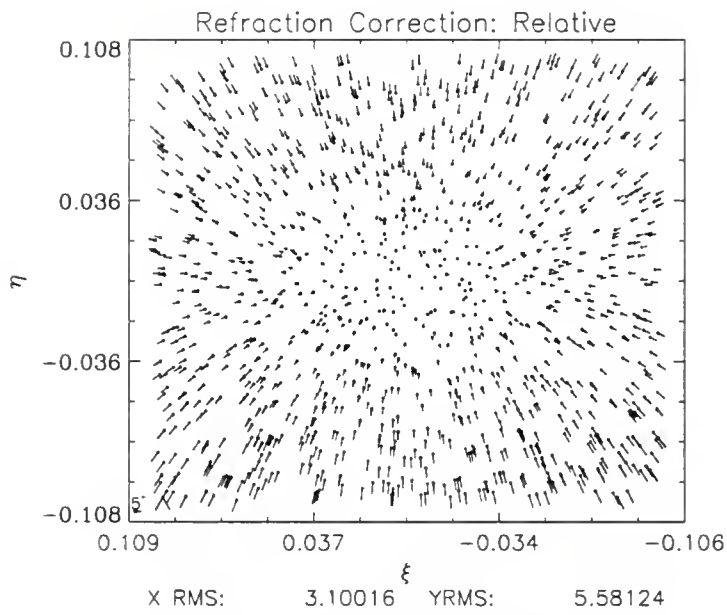
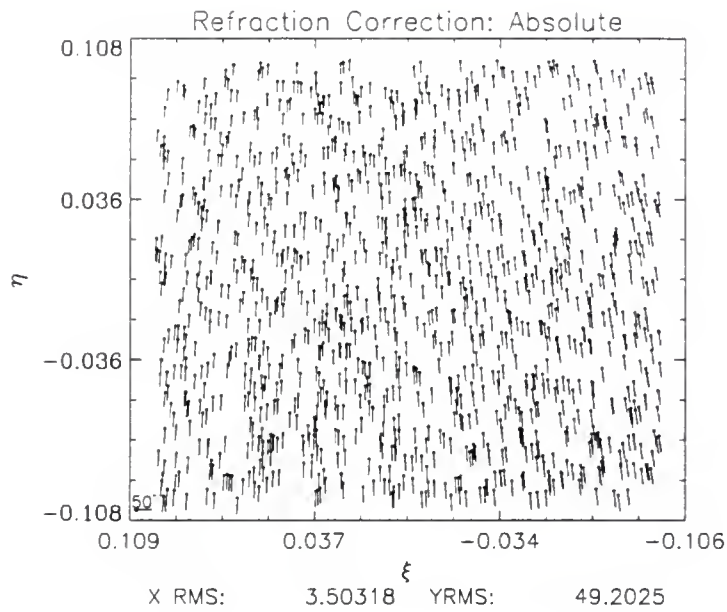


Figure 8: The effects of refraction on plate 1

The tangential point is taken to be the refracted  $\alpha_0, \delta_0$ . The rigorous mathematical relations between the refracted positions and the topocentric positions are somewhat complicated. For practical application, only development into series can be considered; it is therefore necessary to state which terms must be retained and which can be neglected.

In order to obtain the simple expressions for the coefficients of the series, König introduces the following auxiliary quantities

$$\begin{aligned} k_1 &= \tan z \sin \chi \\ k_2 &= \tan z \cos \chi \\ k_3 &= 1 + k_1^2 \\ k_4 &= 1 + k_2^2 \end{aligned} \tag{30}$$

where  $\chi$  is the (refracted) parallactic angle at the tangent point (taken to be the refracted tangential point) and  $k_1$  and  $k_2$  have a simple geometrical meaning; they are the tangential coordinates of the zenith in the plane of the plate. The corrections for the measured values are (to the third order):

$$\begin{aligned} \Delta x &= [\beta k_3 + 2\beta'(1 + k_1^2 + k_2^2)k_1^2]x \\ &\quad - [\beta k_1(k_2 + \tan \delta_0) + 2\beta'(1 + k_1^2 + k_2^2)k_1 k_2]y \\ &\quad + 2[\beta + 2\beta'(1 + k_1^2 + k_2^2)]k_1 k_2 y - \beta k_1 k_3 x^2 \\ &\quad - 2\beta k_1^2 k_2 x y - \beta k_1 k_4 y^2 + \beta k_3^2 x^3 + 3\beta k_1 k_2 k_3 x^2 y \\ &\quad + \beta(k_3 k_4 + 2k_1^2 k_2^2)xy^2 + \beta k_1 k_2 k_4 y^3 \end{aligned} \tag{31}$$

$$\begin{aligned}
\Delta y = & [\beta k_1(k_2 + \tan \delta_0) + 2\beta'(1 + k_1^2 + k_2^2)k_1k_2]x \\
& + [\beta k_3 + 2\beta'(1 + k_1^2 + k_2^2)k_1^2]y \\
& + [\beta + 2\beta'(1 + k_1^2 + k_2^2)](k_2^2 - k_1^2)y \\
& - \beta k_2k_3x^2 - 2\beta k_1k_2^2xy - \beta k_2k_4y^2 + \beta k_1k_2k_3x^3 \\
& + \beta(k_3k_4 + 2k_1^2k_2^2)x^2y + 3\beta k_1k_2k_4xy^2 + \beta k_4^2y^3.
\end{aligned} \tag{32}$$

Let

$$\begin{aligned}
X_R = & -\beta k_1k_3x^2 - 2\beta k_1^2k_2xy - \beta k_1k_4y^2 + \beta k_3^2x^3 \\
& + 3\beta k_1k_2k_3x^2y + \beta(k_3k_4 + 2k_1^2k_2^2)xy^2 + \beta k_1k_2k_4y^3
\end{aligned} \tag{33}$$

and

$$\begin{aligned}
Y_R = & -\beta k_2k_3x^2 - 2\beta k_1k_2^2xy - \beta k_2k_4y^2 + \beta k_1k_2k_3x^3 \\
& + \beta(k_3k_4 + 2k_1^2k_2^2)x^2y + 3\beta k_1k_2k_4xy^2 + \beta k_4^2y^3
\end{aligned} \tag{34}$$

also define

$$\begin{aligned}
A &= \beta k_3 + 2\beta'(1 + k_1^2 + k_2^2)k_1^2 \\
B &= -[\beta k_1(k_2 + \tan) + 2\beta'(1 + k_1^2 + k_2^2)k_1k_2] \\
C &= 2[\beta + 2\beta'(1 + k_1^2 + k_2^2)]k_1k_2y \\
D &= [\beta + 2\beta'(1 + k_1^2 + k_2^2)](k_2^2 - k_1^2).
\end{aligned} \tag{35}$$

Substituting these variables into equation we can rewrite equations (31) and (32) as

$$\begin{aligned}
\Delta x &= Ax + By + C + X_R \\
\Delta y &= -Bx + Ay + D + Y_R.
\end{aligned} \tag{36}$$

Written in this form the refraction terms which cause a change in the scale (A), rotation (B), linear refraction terms (C and D), residual refraction ( $X_R$  and  $Y_R$ ) can be separated. Generally, for small fields and for zenith distance less than  $70^\circ$  the

terms A and B can be neglected. However, this is not so for plates taken at very high declinations. We have included the terms for change of scale and residual refraction, but not rotation. Rotation was not included because the rotation caused by refraction cannot be separated from that caused by the position of the plates in the measuring machine.

Table 2: Refraction Information for plates 1–32

PL	RA0	LMST	MON	DAY	TEMP	HA	Z D	REFR
1	0.0	0.108	10	15	68	0.108	41.15	48.25
2	1.0	1.042	11	11	70	0.042	41.14	48.05
3	2.0	2.058	12	5	70	0.058	41.14	48.06
4	3.0	2.75	11	20	70	23.975	41.14	48.05
5	4.0	4.342	1	6	70	0.342	41.21	48.18
6	5.0	5.408	1	13	75	0.408	41.26	47.78
7	6.0	6.158	1	8	75	0.158	41.16	47.63
8	7.0	7.092	1	8	75	0.092	41.14	47.61
9	8.0	8.092	1	18	77	0.092	41.14	47.43
10	9.0	9.108	1	18	77	0.108	41.15	47.43
11	10.0	10.063	2	7	75	0.063	41.14	47.60
12	11.0	11.258	4	12	65	0.258	41.18	48.58
13	12.0	11.958	4	11	65	23.958	41.14	48.51
14	13.0	13.083	7	3	60	0.083	41.14	48.99
15	14.0	14.008	4	10	65	0.008	41.14	48.51
16	15.0	15.233	6	12	60	0.233	41.17	49.04
17	16.0	16.250	6	12	60	0.250	41.18	49.05
18	17.0	17.150	6	5	60	0.150	41.15	49.00
19	18.0	18.150	6	5	60	0.150	41.15	49.00
20	19.0	18.883	6	5	60	23.883	41.15	48.99
21	20.0	20.238	9	19	60	0.237	41.18	49.04
22	21.0	21.175	10	13	68	0.175	41.16	48.27
23	22.0	22.208	10	15	68	0.208	41.17	48.28
24	23.0	23.275	10	15	68	0.275	41.19	48.32
25	0.0	0.096	11	20	70	0.096	46.14	57.22
26	1.2	1.413	10	13	68	0.212	46.16	57.47
27	2.4	2.496	11	20	70	0.096	46.14	57.22
28	3.6	3.713	11	20	70	0.113	46.14	57.23
29	4.8	4.629	1	13	75	23.829	46.15	56.70
30	6.0	6.213	1	9	75	0.213	46.16	56.71
31	7.2	7.046	1	13	75	23.846	46.15	56.70
32	8.4	8.579	1	18	77	0.179	46.15	56.49

Table 3: Refraction Information for plates 33–64

PL	RA0	LMST	MON	DAY	TEMP	HA	Z D	REFR
33	9.6	9.717	1	18	77	0.117	46.14	56.48
34	10.8	10.967	5	12	65	0.167	46.15	57.79
35	12.0	12.258	4	9	65	0.258	46.17	57.82
36	13.2	13.404	4	12	65	0.204	46.16	57.80
37	14.4	14.729	7	3	60	0.329	46.18	58.41
38	15.6	15.792	6	5	60	0.192	46.15	58.35
39	16.8	16.971	4	19	65	0.171	46.15	57.79
40	18.0	18.088	4	19	60	0.088	46.14	58.33
41	19.2	19.433	6	5	60	0.233	46.16	58.36
42	20.4	20.567	10	11	65	0.167	46.15	57.78
43	21.6	21.746	10	15	68	0.146	46.15	57.45
44	22.8	22.875	10	15	68	0.075	46.14	57.44
45	0.0	0.088	10	18	68	0.088	51.14	68.46
46	1.5	1.583	11	11	70	0.083	51.14	68.20
47	3.0	3.250	11	20	70	0.250	51.15	68.23
48	4.5	4.550	1	7	70	0.050	51.14	68.20
49	6.0	5.900	1	13	75	23.90	51.14	67.56
50	7.5	7.854	2	7	75	0.354	51.16	67.61
51	9.0	9.325	2	7	75	0.325	51.16	67.61
52	10.5	10.575	2	11	75	0.075	51.14	68.90
53	12.0	12.308	4	11	65	0.308	51.16	68.90
54	13.5	13.783	4	12	65	0.283	51.15	68.89
55	15.0	15.183	4	12	65	0.183	51.15	68.87
56	16.5	16.750	6	12	60	0.250	51.15	69.55
57	18.0	18.000	6	12	60	0.000	51.14	69.52
58	19.5	19.771	9	15	60	0.271	51.15	69.55
59	21.0	21.154	9	15	60	0.154	51.14	69.53
60	22.5	22.550	10	18	68	0.050	51.14	68.46
61	0.0	0.133	10	13	68	0.133	56.14	82.15
62	6.0	6.350	1	18	77	0.350	56.14	80.76
63	12.0	12.083	4	12	65	0.083	56.14	82.62
64	18.0	18.263	6	5	60	0.262	56.14	83.42



## CHAPTER 3

### LEAST SQUARES

Since we will use the method of least squares to determine our plate parameters for both the single plate overlapping plate reduction techniques, we will first give an outline of this data analysis method.

#### Theory of Least Squares

Consider a set of  $n$  observations represented in vector form by  $\mathbf{x}_0$ , and assume these observations are unbiased (i.e. without systematic error). The vector of true values is represented by  $\mathbf{x}$  and  $\mathbf{v} = \mathbf{x} - \mathbf{x}_0$  is the vector of errors in the observations. From the assumptions that the observations are unbiased we can assume that the errors will have a Gaussian distribution (multivariate normal distribution) and we will regard their covariance matrix,  $\sigma$ , as being known. Thus we can express the probability density distribution function of the errors as the multivariate gaussian

$$\phi(\mathbf{v}) = C e^{-\frac{1}{2} \mathbf{v}^T \sigma^{-1} \mathbf{v}}. \quad (37)$$

We further assume that the observations satisfy a set of *equations of condition*

$$\mathbf{F}(\mathbf{x}_0 + \mathbf{v}, \mathbf{a}) = 0 \quad (38)$$

where  $\mathbf{a}$  is a vector of  $q$  parameters. Some of the components of the vector equations  $\mathbf{F}=\mathbf{0}$  may not explicitly contain any of the components of  $\mathbf{x}$ ; such equations would be condition equations involving parameters only. In this analysis we will distinguish these from the general condition equations by calling them *parameter constraints*.

If the  $q$  parameters are not mutually independent, the relations existing between them must be included among the parameter constraint equations. The observations must be functionally independent, that is, not one of the  $n$  observations can be derived from any or all of the remaining  $(n-1)$  observations. There must be at least  $n$  observations; in other words,  $n \geq q$ . Otherwise there will be a deficiency in the model. If  $q = n$  then such a circumstance will lead to a unique solution. When  $n > q$ , redundancy is said to exist and adjustment is needed in order to obtain a the best set of estimates for the model variables. Adjustment is meaningful only in those cases in which the data available exceed the minimum necessary for a unique determination. Since the data points are usually obtained from observations, which contain errors, redundant data are usually inconsistent in the sense that each sufficient subset yields different results from another subset. No unique result (no one vector  $\mathbf{a}$ ) will satisfy all the equations, but will give rise to (at least some non-zero) residuals,  $\mathbf{v}$ .

Making the basic assumption, called the *principle of maximum likelihood*, we assume that the set of measurements which we obtain is actually the most probable

set of measurements. Thus the best estimates of the coefficients  $\mathbf{a}$  are the ones that maximize the probability of obtaining the particular set of measurements which we actually obtained. Clearly, the way to maximize  $\phi$  is to minimize the value of the exponent. The principle of maximum likelihood thus leads to the conclusion that we should minimize  $\mathbf{v}^T \sigma^{-1} \mathbf{v}$ .

The principle of least squares consists in finding estimates of  $\mathbf{v}$  and  $\mathbf{a}$  which minimize the quadratic form  $\mathbf{v}^T \sigma^{-1} \mathbf{v}$  while simultaneously satisfying  $\mathbf{F}(\mathbf{x}_0 + \mathbf{v}, \mathbf{a}) = \mathbf{0}$ . Thus if the random variables to which the observations refer are normally distributed, the least squares method will give identical results to those from the maximum likelihood method.

#### Traditional (Linear Least Squares)

Traditional least squares is when we assume that the observation errors are of the same precision and uncorrelated and that exactly one observation occurs in each equation of condition. Since the observations are uncorrelated the covariance matrix  $\sigma$  becomes diagonal. Furthermore, if the observations are of the same precision the covariance matrix will be of the form  $\sigma = \sigma_0 \mathbf{I}$ , where  $\mathbf{I}$  is the identity matrix. The minimum principle of least squares becomes :

$$\begin{aligned} \mathbf{v}^T \sigma^{-1} \mathbf{v} &= \sum_{i=1}^n \sigma^{-1} v_i^2 \\ \mathbf{v}^T \sigma^{-1} \mathbf{v} &= \frac{1}{\sigma_0} \sum_{i=1}^n v_i^2 \rightarrow \text{minimum.} \end{aligned} \tag{39}$$

Thus in this case the minimum of  $\sum_{i=1}^n v_i^2 = \mathbf{v}^T \mathbf{v}$  and  $\mathbf{v}^T \sigma^{-1} \mathbf{v}$  coincide. This last case is the oldest and the most classical, and possibly the one that gave rise to the name “least squares” since in this case we seek the “least” of the sum of the squares of the residuals.

In traditional least squares the condition equations  $\mathbf{F}(\mathbf{x}, \mathbf{a}) = \mathbf{0}$  usually have the form

$$\mathbf{A}\mathbf{a} + \mathbf{x}_0 = -\mathbf{v}. \quad (40)$$

where  $\mathbf{A} = \frac{\partial \mathbf{F}}{\partial \mathbf{a}}$ . In this case the “adjustment unknowns” or “adjustment parameters”,  $\mathbf{a}$ , occur linearly in the condition equation, and each equation contains exactly one observation. The “normal equations” for finding the estimates of  $\mathbf{a}$  are easily found for this case. Multiplying the above equation by its transpose gives:

$$\begin{aligned} (\mathbf{a}^T \mathbf{A}^T + \mathbf{x}_0^T)(\mathbf{A}\mathbf{a} + \mathbf{x}_0) &= (-\mathbf{v}^T)(-\mathbf{v}) \\ \mathbf{a}^T \mathbf{A}^T \mathbf{A} \mathbf{a} + 2\mathbf{a}^T \mathbf{A}^T \mathbf{x}_0 + \mathbf{x}_0^T \mathbf{x}_0 &= \mathbf{v}^T \mathbf{v} \end{aligned} \quad (41)$$

for matrix  $\mathbf{A}$  and vectors  $\mathbf{a}$  and  $\mathbf{x}$ . Also, note that  $\mathbf{v}^T \mathbf{v}$  is not a vector or a matrix, but a number and we may therefore transpose any of the terms without knowing its value. To find the *minimum* of  $\mathbf{v}^T \mathbf{v}$ , we differentiate with respect to each component of  $\mathbf{a}$  and set the derivative equal to zero

$$\begin{aligned} \frac{\partial(\mathbf{v}^T \mathbf{v})}{\partial \mathbf{a}} &= \frac{\partial(\mathbf{a}^T \mathbf{A}^T \mathbf{A} \mathbf{a} + 2\mathbf{a}^T \mathbf{A}^T \mathbf{x}_0 + \mathbf{x}_0^T \mathbf{x}_0)}{\partial \mathbf{a}} = 0 \\ &= 2(\mathbf{a}^T \mathbf{A}^T \mathbf{A} + \mathbf{x}_0^T \mathbf{A}) = 0 \end{aligned} \quad (42)$$

yielding

$$\mathbf{a}^T \mathbf{A}^T \mathbf{A} = -\mathbf{x}_0^T \mathbf{A}. \quad (43)$$

After transposing and rearranging, we get the traditional least squares solution in its simplest form:

$$\mathbf{a} = -(\mathbf{A}^T \mathbf{A})^{-1} \mathbf{A}^T \mathbf{x}_0 \quad (44)$$

the solution of the normal equations.

### Nonlinear Least Squares

The conditional and the constraint equations involved in an adjustment problem can, in general, be nonlinear. However, least squares adjustments are generally performed with linear functions, since it is rather difficult and often impractical, at least at present, to seek a least squares solution of nonlinear equations. Consequently, whenever the equations in the model are originally nonlinear, some means of linearization must be performed on the equations. Series expansions, a Taylor's series in particular, are often used for this purpose, where only the zero and first-order terms are used and all other higher-order terms are neglected.

When applying a series expansion, an initial set of approximate values for the unknowns in the equations must be chosen. The choice of those initial approximations is an important aspect of solving the problem at hand. Unfortunately there is no concrete and unique way of choosing approximations that can be applied to all adjustment problems. In all cases an attempt should be made to obtain

the closest approximations that can be obtained by using relatively simple and uninvolved techniques.

We will now use the more generalized least squares treatment to drop some of the restrictions found in the traditional least squares method. In the following development

1. Observations may be correlated.
2. More than one observation may appear in an equation of condition.
3. The equations of condition are assumed nonlinear in both parameters and observations.
4. Nonlinear constraints among the parameters are allowed.

As before the vector  $\mathbf{x}_0$  is the vector of observations,  $\mathbf{x}$  is the vector of true values  $\mathbf{x}=\mathbf{x}_0 + \mathbf{v}$  , where  $\mathbf{v}$  is the vector of corrections. In order to find estimates of the vector of parameters  $\mathbf{a}$  and  $\mathbf{x}$  in the generalized least squares we will use the method of Laplace multipliers. At the solution the numerical value of  $\mathbf{v}^T \sigma^{-1} \mathbf{v} = S$ . These conditions are the same as  $S^* = \mathbf{v}^T \sigma^{-1} \mathbf{v} - 2\mathbf{F}^T(\mathbf{a}, \mathbf{x}_0 + \mathbf{v})\mathbf{\Lambda}$ , where  $\mathbf{\Lambda}$  is a Lagrange multiplier. This means that the values of  $S$  and  $S^*$  reach their minimum at the same values of  $\mathbf{a}$  and  $\mathbf{v}$ .

As before,  $\mathbf{a}$  has  $q$  components,  $\mathbf{v}$  has  $n$  components and  $\mathbf{F}$  has  $p$  components. Thus there are only  $p+n-q$  free components. Differentiating  $S^*$  with respect to

the components of  $\mathbf{a}$  and  $\mathbf{v}$  gives

$$\begin{aligned}\frac{\partial S^*}{\partial \mathbf{v}} &= 2\sigma^{-1}\mathbf{v} - 2\mathbf{X}^T\mathbf{\Lambda} \\ \frac{\partial S^*}{\partial \mathbf{a}} &= -2\mathbf{A}^T\mathbf{\Lambda}\end{aligned}\quad (45)$$

where

$$\mathbf{X}_{p \times n} = \left( \frac{\partial \mathbf{F}}{\partial \mathbf{v}} \right)_{\mathbf{x}=\mathbf{x}_0, \mathbf{a}=\mathbf{a}_0} = \begin{bmatrix} \frac{\partial f_1}{\partial v_1} & \frac{\partial f_1}{\partial v_2} & \cdot & \cdot & \cdot & \frac{\partial f_1}{\partial v_n} \\ \frac{\partial f_2}{\partial v_1} & \frac{\partial f_2}{\partial v_2} & \cdot & \cdot & \cdot & \frac{\partial f_2}{\partial v_n} \\ \cdot & \cdot & \cdot & \cdot & \cdot & \cdot \\ \cdot & \cdot & \cdot & \cdot & \cdot & \cdot \\ \frac{\partial f_p}{\partial v_1} & \frac{\partial f_p}{\partial v_2} & \cdot & \cdot & \cdot & \frac{\partial f_p}{\partial v_n} \end{bmatrix}_{\mathbf{x}=\mathbf{x}_0, \mathbf{a}=\mathbf{a}_0} \quad (46)$$

$$\mathbf{A}_{p \times q} = \left( \frac{\partial \mathbf{F}}{\partial \mathbf{a}} \right)_{\mathbf{x}=\mathbf{x}_0, \mathbf{a}=\mathbf{a}_0} = \begin{bmatrix} \frac{\partial f_1}{\partial a_1} & \frac{\partial f_1}{\partial a_2} & \cdot & \cdot & \cdot & \frac{\partial f_1}{\partial a_q} \\ \frac{\partial f_2}{\partial a_1} & \frac{\partial f_2}{\partial a_2} & \cdot & \cdot & \cdot & \frac{\partial f_2}{\partial a_q} \\ \cdot & \cdot & \cdot & \cdot & \cdot & \cdot \\ \cdot & \cdot & \cdot & \cdot & \cdot & \cdot \\ \frac{\partial f_p}{\partial a_1} & \frac{\partial f_p}{\partial a_2} & \cdot & \cdot & \cdot & \frac{\partial f_p}{\partial a_q} \end{bmatrix}_{\mathbf{x}=\mathbf{x}_0, \mathbf{a}=\mathbf{a}_0} \quad (47)$$

The following equations must, therefore, be *rigorously* satisfied at the solution

$$\begin{aligned}\sigma^{-1}\mathbf{v} &= \mathbf{X}^T\mathbf{\Lambda} && n \text{ equations} \\ \mathbf{A}^T\mathbf{\Lambda} &= \mathbf{0} && q \text{ equations} \\ \mathbf{F} &= \mathbf{0} && p \text{ equations.}\end{aligned}\quad (48)$$

This means that  $\mathbf{A}$  and  $\mathbf{X}$  must be evaluated at the solution for  $\mathbf{a}$  and for  $\mathbf{x}$ . When one considers that  $\mathbf{\Lambda}$  has  $p$  unknowns, then one can see that there are exactly the same number of unknowns as there are equations.

The equations are in general nonlinear and therefore must be solved by successive approximations. A general rigorous and non-iterative algorithm for the

solution exists only for the case that the elements of  $\mathbf{x}$  and  $\mathbf{a}$  occur linearly in the function  $\mathbf{F}$ . When  $\mathbf{F}$  is nonlinear in the elements of either  $\mathbf{x}$  or  $\mathbf{a}$ , or both, equations which are practically equivalent to the  $\mathbf{F}$  and which are linear in the pertinent variables can be derived, e.g., in the following way: assume that an approximate solution of the above equations has been obtained somehow, linearize these equations about the approximate solution and by iterations determine corrections to it. Start by taking an approximation  $\mathbf{a}_0$  for  $\mathbf{a}$  and using the observations  $\mathbf{x}_0$  as approximations for  $\mathbf{x}$ . If we write  $\mathbf{a} = \mathbf{a}_0 + \alpha$ , with  $\alpha$  being small corrections to  $\mathbf{a}_0$ , the equation  $\mathbf{F}=\mathbf{0}$  can be developed as a Taylor series

$$\begin{aligned} \mathbf{F}(\mathbf{x}, \mathbf{a}) &= \mathbf{F}(\mathbf{x}_0, \mathbf{a}_0) + (\mathbf{x} - \mathbf{x}_0) \frac{\partial \mathbf{F}(\mathbf{x}_0, \mathbf{a}_0)}{\partial \mathbf{x}} + (\mathbf{a} - \mathbf{a}_0) \frac{\partial \mathbf{F}(\mathbf{x}_0, \mathbf{a}_0)}{\partial \mathbf{a}} + O(2) = \mathbf{0} \\ \mathbf{F}(\mathbf{x}, \mathbf{a}) &= \mathbf{F}(\mathbf{x}_0, \mathbf{a}_0) + \mathbf{X}_0 \mathbf{v} + \mathbf{A}_0 \alpha + O(2) = \mathbf{0} \end{aligned} \quad (49)$$

where  $\mathbf{X}_0$  and  $\mathbf{A}_0$  are evaluated at  $\mathbf{x}_0$  and  $\mathbf{a}_0$ ; and also, let  $\mathbf{F}(\mathbf{x}_0, \mathbf{a}_0) = \mathbf{F}_0$ .

From equation (48) we have  $\mathbf{v} = \sigma \mathbf{X}^T \mathbf{\Lambda}$ ; so, by substituting into the above equations we get

$$\mathbf{F}_0 + \mathbf{X}_0 \sigma \mathbf{X}_0^T \mathbf{\Lambda} + \mathbf{A}_0 \alpha = \mathbf{0}. \quad (50)$$

Combining this with  $\mathbf{A}^T \mathbf{\Lambda} = \mathbf{0}$  yields the **Generalized Normal equations**

$$\begin{bmatrix} \mathbf{X}_0 \sigma \mathbf{X}_0^T & \mathbf{A}_0 \\ \mathbf{A}_0^T & \mathbf{0} \end{bmatrix} \begin{bmatrix} \mathbf{\Lambda} \\ \alpha \end{bmatrix} + \begin{bmatrix} \mathbf{F}_0 \\ \mathbf{0} \end{bmatrix} = \begin{bmatrix} \mathbf{0} \\ \mathbf{0} \end{bmatrix}. \quad (51)$$

Note that  $\mathbf{\Lambda}$  is needed for computing the correction  $\mathbf{v}$ . If  $\mathbf{X} \sigma \mathbf{X}^T$  is nonsingular, we can eliminate  $\mathbf{\Lambda}$  from the equation by multiplying the equation (50) by



$\mathbf{A}^T(\mathbf{X}_0\sigma\mathbf{X}_0^T)^{-1}$  yielding

$$\mathbf{A}_0^T(\mathbf{X}_0\sigma\mathbf{X}_0^T)^{-1}\mathbf{F}_0 + \mathbf{A}_0^T\boldsymbol{\Lambda} + \mathbf{A}_0^T(\mathbf{X}_0\sigma\mathbf{X}_0^T)^{-1}\mathbf{A}_0\alpha = \mathbf{0}. \quad (52)$$

Since,  $\mathbf{A}^T\boldsymbol{\Lambda} = \mathbf{0}$ , rearranging gives us

$$\begin{aligned} \mathbf{A}^T(\mathbf{X}_0\sigma\mathbf{X}_0^T)^{-1}\mathbf{A}\alpha &= -\mathbf{A}^T(\mathbf{X}_0\sigma\mathbf{X}_0^T)^{-1}\mathbf{F}_0 \\ \alpha &= -[\mathbf{A}^T(\mathbf{X}_0\sigma\mathbf{X}_0^T)^{-1}\mathbf{A}]^{-1}\mathbf{A}^T(\mathbf{X}_0\sigma\mathbf{X}_0^T)^{-1}\mathbf{F}_0. \end{aligned} \quad (53)$$

Pre-multiplying equation (50) by  $(\mathbf{X}_0\sigma\mathbf{X}_0^T)^{-1}$  and solving for  $\boldsymbol{\Lambda}$  gives

$$(\mathbf{X}_0\sigma\mathbf{X}_0^T)^{-1}\mathbf{F}_0 + \boldsymbol{\Lambda} + (\mathbf{X}_0\sigma\mathbf{X}_0^T)^{-1}\mathbf{A}\alpha = \mathbf{0} \quad (54)$$

$$\boldsymbol{\Lambda} = -(\mathbf{X}_0\sigma\mathbf{X}_0^T)^{-1}\mathbf{A}\alpha - (\mathbf{X}_0\sigma\mathbf{X}_0^T)^{-1}\mathbf{F}_0.$$

$$\boldsymbol{\Lambda} = -\mathbf{W}(\mathbf{A}\alpha + \mathbf{F}_0) \quad (55)$$

where  $\mathbf{W} = (\mathbf{X}_0\sigma\mathbf{X}_0^T)^{-1}$ .  $\mathbf{W}$  is frequently called the weight matrix.

Since we know  $\mathbf{A}^T\boldsymbol{\Lambda} = \mathbf{0}$ , we can pre-multiply equation (55) by  $\mathbf{A}^T$ , and get

$$\mathbf{A}^T\boldsymbol{\Lambda} = -\mathbf{A}^T\mathbf{W}\mathbf{A}\alpha - \mathbf{A}^T\mathbf{W}\mathbf{F}_0 = \mathbf{0}. \quad (56)$$

Solving for  $\alpha$  gives

$$\alpha = -[\mathbf{A}^T\mathbf{W}\mathbf{A}]^{-1}\mathbf{A}^T\mathbf{W}\mathbf{F}_0 \quad (57)$$

It can be shown (Brown 1955; Jefferys 1980, 1981) that  $(\mathbf{A}^T\mathbf{W}\mathbf{A})^{-1}$  is the covariance matrix of  $\alpha$ , so that the square roots of its diagonal terms are the standard deviations of the corresponding terms of  $\alpha$ . Note that  $\mathbf{X}\sigma\mathbf{X}^T$  is not always nonsingular; for instance, when  $\mathbf{F}=\mathbf{0}$  contains equations in which none of

the components of  $\mathbf{x}$  occur explicitly i.e., parameter constraints. This, however, produces in general no essential singularities.

It is now possible to solve for  $\mathbf{v}$ . From  $\mathbf{v} = \sigma \mathbf{X}^T \mathbf{\Lambda}$  we get

$$\mathbf{v} = \sigma \mathbf{X}^T [\mathbf{W} \mathbf{A} [\mathbf{A}^T \mathbf{W} \mathbf{A}]^{-1} \mathbf{A}^T \mathbf{W} - \mathbf{W}] \mathbf{F}_0. \quad (58)$$

Then

$$\begin{aligned} \mathbf{a}_{\text{new}} &= \mathbf{a}_0 + \alpha \\ \mathbf{x}_{\text{new}} &= \mathbf{x}_0 + \mathbf{v} \end{aligned} \quad (59)$$

define the improved solution. If the improved solution is insufficiently accurate, the process should be repeated until satisfactory convergence is attained.

The natural starting point for this scheme is to set  $\mathbf{x}_0 = \mathbf{x}$  as the initial approximation, so that  $\mathbf{v} = \mathbf{0}$ , and to use a vector  $\dot{\mathbf{a}}$  of initial approximations for  $\mathbf{a}$  for  $\mathbf{a}_0$ . Obtaining a suitable  $\dot{\mathbf{a}}$  is sometimes a difficult question, it must be close enough to the solution that the process given above converges.

### Comparison with Traditional Least Squares

It is informative to compare this general method with the results from the traditional least squares method. In the traditional case we are dealing with the a) noncorrelated observations of equal precision (i.e.  $\sigma = \sigma_0 \mathbf{I}_m$ ) of which b) exactly one observation occurs in each equation of condition, and that c) the equation of condition is solved with respect to it, we have  $\mathbf{X} = -\mathbf{I}_m$  and therefore  $(\mathbf{X} \sigma \mathbf{X}^T)^{-1} = \frac{1}{\sigma_0} \mathbf{I}_m$ , so that in this very specialized case  $\alpha = -(\mathbf{A}^T \mathbf{A})^{-1} \mathbf{A}^T \mathbf{F}_0$

Also, the observation errors reduce using this simplification and

$$\begin{aligned} \mathbf{X} &= -\mathbf{I}_m \\ \sigma &= \sigma_o \mathbf{I}_m \\ \mathbf{W} &= \frac{1}{\sigma_o} \mathbf{I}_m \end{aligned} \tag{60}$$

to

$$\begin{aligned} \mathbf{v} &= \sigma \mathbf{X}^T [\mathbf{W} \mathbf{A} [\mathbf{A}^T \mathbf{W} \mathbf{A}]^{-1} \mathbf{A}^T \mathbf{W} - \mathbf{W}] \mathbf{F}_o \\ \mathbf{v} &= \sigma_o \mathbf{I}_m (-\mathbf{I}_m) \left[ \frac{1}{\sigma_o} \mathbf{I}_m \mathbf{A} (\mathbf{A}^T \frac{1}{\sigma_o} \mathbf{I}_m \mathbf{A})^{-1} \mathbf{A}^T \frac{1}{\sigma_o} \mathbf{I}_m - \frac{1}{\sigma_o} \mathbf{I}_m \right] \mathbf{F}_o \\ \mathbf{v} &= \left[ \mathbf{I}_m - \mathbf{A} (\mathbf{A}^T \mathbf{A})^{-1} \mathbf{A}^T \right] \mathbf{F}_o. \end{aligned} \tag{61}$$

This formula is well known from classical least-squares theory and evidently independent of  $\alpha_o$ .

## CHAPTER 4

### METHOD OF PLATE REDUCTIONS

We will now use the theory of least squares for the determination of the plate parameters. Recall that from chapter 2 the determination of the equatorial coordinates is a two-step process. First the reference stars' equatorial coordinates are converted to standard coordinates. Second, after the functional form of a plate model is established between the measured coordinates and the standard coordinates a least squares reduction is performed on the measured and standard coordinates of the reference stars to determine the plate parameters. Usually a great deal of analysis is involved in determining the functional form of the plate model. First a simple 4 or 6-constant model is used and approximate values are obtained for some of the plate parameters. A least squares reduction using only the reference stars on the plate (single plate reduction) is done to find the best values for the parameters. After the reduction, the residuals from the actual measurements ( $x$ ,  $y$ ) and those calculated using these plate parameters and the cataloged equatorial coordinates are studied. From the residual plots it is decided which new terms, if any, need to be added to the plate model. Once the "best" plate model has been established, the plate parameters corresponding to this model are used to determine the equatorial coordinates of all the stars imaged on the plate (not just the reference stars). After position estimates for all the stars have

been determined an overlap solution can be performed. This is because in an overlap solution all the images of stars that occur on at least two plates or are reference stars are considered in the normal equations.

#### Single Plate Reduction: Using Least Squares to Determine the Plate Parameters.

We will first reduce each plate separately. In the next section we will develop a multiple plate reduction technique. We will use the formulation developed by Eichhorn (1985) to set up the equation for a single reduction and also an overlap reduction.

In a least squares adjustment we regard the measured relative coordinates of the images and the position estimates from the reference star catalogue as observables. These two types of observables give rise to two types of condition equations. Consider data from only one plate on which there are  $n$  stars,  $m$  of which are reference stars. Without restricting generality, we may assume that the measured image coordinates of the  $\nu\mu^{\text{th}}$  star,  $x_\mu, y_\mu$  are related to their standard coordinates  $\xi_\mu, \eta_\mu$  by the equation

$$\begin{pmatrix} x_\mu \\ y_\mu \end{pmatrix} = s \begin{pmatrix} \xi_\mu \\ \eta_\mu \end{pmatrix} + \Xi_\mu \mathbf{a}. \quad (62)$$

$\Xi_\nu$  is the model matrix, which depends on  $\xi, \eta$ , and possibly other data pertaining to the star in question, such as magnitude or color index.  $\mathbf{a}$  is the vector of the plate parameters, which constitutes a subset of the adjustment unknowns and is a vector of dimension  $p$ . In what follows, we shall keep the model matrix  $\Xi$

general and hold to the assumption that  $\Xi \mathbf{a}$  is at least one order of magnitude smaller than  $s\xi$  and  $s\eta$ .

Using this relation we establish the first set of condition equations

$$\mathbf{F}_{(2m \times 1)} = \begin{pmatrix} \begin{pmatrix} x_1 \\ y_1 \end{pmatrix} - s \begin{pmatrix} \xi_1(\alpha_1, \delta_1) \\ \eta_1(\alpha_1, \delta_1) \end{pmatrix} - \Xi_1 \mathbf{a} \\ \begin{pmatrix} x_2 \\ y_2 \end{pmatrix} - s \begin{pmatrix} \xi_2(\alpha_2, \delta_2) \\ \eta_2(\alpha_2, \delta_2) \end{pmatrix} - \Xi_2 \mathbf{a} \\ \vdots \\ \begin{pmatrix} x_m \\ y_m \end{pmatrix} - s \begin{pmatrix} \xi_m(\alpha_m, \delta_m) \\ \eta_m(\alpha_m, \delta_m) \end{pmatrix} - \Xi_m \mathbf{a} \end{pmatrix} = 0. \quad (63)$$

In our approach, the observables are  $x_\mu$  and  $y_\mu$  and we regard the adjustment parameters to be not only the plate constants  $\mathbf{a}$ , but also the spherical coordinates  $(\alpha_\mu, \delta_\mu)$  of the stars.  $\xi$  and  $\eta$  are used only as auxiliary quantities. We consider the tangential point,  $\alpha_0$  and  $\delta_0$ , as being known. As stated in Chapter 2 if the assumed tangential point is not the actual one, then this is can be accounted for by an appropriate form of  $\Xi$  and additional components of  $\mathbf{a}$ .

The second type of observations (estimates of the reference star's spherical coordinates from an existing catalogue) states that the actual spherical coordinates  $(\alpha_\mu, \delta_\mu)$  are equal to those estimated in the catalogue plus corrections. To take care of convergence of the meridians, we introduce the factor  $\cos\delta$  in the right

ascension equations yielding

$$\mathbf{G}_{(2m \times 1)} = \begin{pmatrix} (\alpha_{1c} - \alpha_1) \cos \delta_1 \\ \delta_{1c} - \delta_1 \\ (\alpha_{2c} - \alpha_2) \cos \delta_2 \\ \delta_{2c} - \delta_2 \\ \vdots \\ (\alpha_{mc} - \alpha_m) \cos \delta_m \\ \delta_{mc} - \delta_m \end{pmatrix} = \mathbf{0} \quad (64)$$

where  $\alpha_{1c} \dots \delta_{mc}$  are the catalogue positions and  $\alpha_l \dots \delta_m$  are the adjustment unknowns which occur both in  $\mathbf{F}=\mathbf{0}$  and  $\mathbf{G}=\mathbf{0}$ . We will now combine the  $4m$  condition equations  $\mathbf{F}$  and  $\mathbf{G}$  into one set  $\mathbf{H}$ .

$$\mathbf{H}^T = (\mathbf{F}^T, \mathbf{G}^T). \quad (65)$$

Each equation, regardless of whether it belongs to  $\mathbf{F}=\mathbf{0}$  or  $\mathbf{G}=\mathbf{0}$ , contains exactly one observable, therefore

$$\left( \frac{\partial \mathbf{F}}{\partial \mathbf{x}} \right) = \mathbf{X} = \mathbf{I}_{4m}. \quad (66)$$

We assume that the measurements of all the coordinates are free from bias and not correlated. The variance (in units of squares of the units in which  $x_\mu$  and  $y_\mu$  were measured) of  $x_\mu$  is  $\nu_\mu$  and  $y_\mu$  is  $\phi_\mu$ . The covariance matrix of the rectangular coordinate measurements is

$$\sigma_x = \text{diag}(\nu_1, \phi_1, \nu_2, \phi_2, \dots, \nu_m, \phi_m) \quad (67)$$

and in most cases, it will suffice to write

$$\sigma_x = \sigma_m \mathbf{I}_{2m} \quad (68)$$

where  $\sigma_m$  is the common variance of all coordinate measurements and  $\mathbf{I}_{2m}$  is, of course, the identity matrix of order  $2m$ .

Also let's assume that all the reference star coordinate's are uncorrelated, so that the covariance matrix  $\bar{\sigma}_{a\nu}$  of the catalogues reference star coordinate estimates  $\alpha \cos \delta$  and  $\delta$  will be

$$\bar{\sigma}_{a\nu} = \text{diag}(\bar{\rho}_1, \bar{\sigma}_1, \dots, \bar{\rho}_n, \bar{\sigma}_n). \quad (69)$$

The factors  $\cos^2 \delta_\nu$  are introduced in order to make  $\sqrt{\bar{\rho}_\nu}$  the dispersion of  $\alpha_\nu \cos(\delta_\nu)$ , that is, the dispersion on the great circle. Not only will this simplify some of the formulas we need in our calculation, but it compensates for the convergence of the meridians.

Thus, the observations are

$$\mathbf{x}_0^T = (x_1, y_1, x_2, y_2, \dots, x_m, y_m; \alpha_{1c} \cos \delta_1, \delta_1, \dots, \alpha_{mc} \cos \delta_m, \delta_m) \quad (70)$$

and their covariance matrix is

$$\sigma = \text{diag}(\nu_1, \phi_1, \nu_2, \phi_2, \dots, \nu_m, \phi_m; \bar{\rho}_1, \bar{\sigma}_1, \bar{\rho}_2, \bar{\sigma}_2, \dots, \bar{\rho}_m, \bar{\sigma}_m) \quad (71)$$

or

$$\begin{aligned} \sigma &= \begin{pmatrix} \sigma_x & 0 \\ 0 & \alpha_a \end{pmatrix} \\ \sigma_{x\nu} &= \begin{pmatrix} \nu_\mu & 0 \\ 0 & \phi_\mu \end{pmatrix} \\ \sigma_{a\nu} &= \begin{pmatrix} \bar{\rho}_\mu & 0 \\ 0 & \bar{\sigma}_\mu \end{pmatrix}. \end{aligned} \quad (72)$$



The vector  $\mathbf{a}$  of adjustment parameters consists of the corrections to the reference star positions and the initial plate parameters. As approximations for the position we choose their cataloged values which renders  $\mathbf{G}_0 = \mathbf{0}$ . As initial approximations to the vector of the plate parameters we choose 0. Thus we have

$$\begin{aligned} \mathbf{F}_0 &= \mathbf{F}(\alpha_c, \delta_c, 0) = \mathbf{d} \\ \mathbf{H}_0 &= \begin{pmatrix} \mathbf{F}_0 \\ \mathbf{G}_0 \end{pmatrix} = \begin{pmatrix} \mathbf{d} \\ \mathbf{0} \end{pmatrix}. \end{aligned} \quad (73)$$

The vector of the adjustment parameters  $\alpha = \begin{pmatrix} \beta \\ \mathbf{a} \end{pmatrix}$ , with

$$\beta^T = (\cos \delta_1 d\alpha_1, d\delta_1, \dots, \cos \delta_m d\alpha_m, d\delta_m). \quad (74)$$

From our least squares analysis in Chapter 3, the corrections to the parameters  $\alpha$  are given by

$$\alpha = -[\mathbf{A}^T \mathbf{W} \mathbf{A}]^{-1} \mathbf{A}^T \mathbf{W} \mathbf{H}_0 \quad (75)$$

where  $\mathbf{W} = (\mathbf{X} \sigma \mathbf{X}^T)^{-1}$ . Since all the equations have only one observation,  $\mathbf{X} = \mathbf{I}$  and our weight matrix becomes  $\mathbf{W} = \sigma^{-1} \mathbf{I}_m$  so we can write

$$\alpha = -[\mathbf{A}^T \sigma^{-1} \mathbf{A}]^{-1} \mathbf{A}^T \sigma^{-1} \mathbf{H}_0. \quad (76)$$

In order to solve the normal equations, we have to evaluate explicitly the terms of the matrix  $\mathbf{A}$  and since  $\alpha = \begin{pmatrix} \beta \\ \mathbf{a} \end{pmatrix}$ , we can rewrite the above equation as

$$\mathbf{A}^T \sigma^{-1} \mathbf{A} \begin{pmatrix} \beta \\ \mathbf{a} \end{pmatrix} = -\mathbf{A}^T \sigma^{-1} \begin{pmatrix} \mathbf{d} \\ \mathbf{0} \end{pmatrix}. \quad (77)$$

$\mathbf{A}$  is the Jacobian matrix of the condition equations with respect to the adjustment parameters, so we can generally write,

$$\mathbf{A} = \left( \frac{\partial \mathbf{H}}{\partial \alpha} \right) = \left( \frac{\partial(\mathbf{F}, \mathbf{G})}{\partial(\beta, \mathbf{a})} \right) = \begin{pmatrix} \left( \frac{\partial \mathbf{F}}{\partial \beta} \right) & \left( \frac{\partial \mathbf{F}}{\partial \mathbf{a}} \right) \\ \left( \frac{\partial \mathbf{G}}{\partial \beta} \right) & \left( \frac{\partial \mathbf{G}}{\partial \mathbf{a}} \right) \end{pmatrix}. \quad (78)$$

If  $|\alpha| \ll 1$  and if the initial parameter vector is  $\mathbf{a} = \mathbf{0}$  then, the values we obtain for  $\mathbf{a}$  from equation (77) will be the actual parameter values rather than the corrections.

Let's take a closer look at what these partial derivatives equal:

$$\begin{aligned} \left( \frac{\partial F_\mu}{\partial \beta_\mu} \right) &= -s \left( \frac{\partial(\xi_\mu, \eta_\mu)}{\partial(\alpha_\mu \cos \delta_\mu, \delta_\mu)} \right) \\ &= -s \mathbf{B}_\mu, \end{aligned} \quad (79)$$

where  $\mathbf{B} = \left( \frac{\partial(\xi_\mu, \eta_\mu)}{\partial(\alpha_\mu \cos \delta_\mu, \delta_\mu)} \right) \begin{pmatrix} \frac{1}{\cos \delta_\mu} & 0 \\ 0 & 1 \end{pmatrix}$ . When  $\nu$  does not equal  $\mu$ ,  $\left( \frac{\partial F_\mu}{\partial \beta_\nu} \right) = 0$ . Therefore  $\left( \frac{\partial \mathbf{F}}{\partial \beta} \right)$  is block diagonal, consisting of  $m$  blocks of dimension  $2 \times 2$  on the main diagonal; these blocks are  $-s \mathbf{B}_\nu$ . The factor matrix is required because we regard  $\cos \delta \, d\alpha$ , and not  $d\alpha$  as the correction, thus

$$d\xi = \left( \left( \frac{\partial \xi}{\partial \alpha} \right) \frac{1}{\cos \delta} \right) \cos \delta d\alpha + \left( \frac{\partial \xi}{\partial \delta} \right) d\delta. \quad (80)$$

The other elements of  $\mathbf{A}$  are

$$\frac{\partial \mathbf{F}}{\partial \mathbf{a}} = \begin{pmatrix} -\Xi_1 \\ -\Xi_2 \\ \vdots \\ -\Xi_n \end{pmatrix} = -\Xi \quad (81)$$

$$\begin{aligned} \frac{\partial \mathbf{G}}{\partial \beta} &= \begin{pmatrix} \frac{\partial G_1}{\cos \delta_1 \partial \alpha_1} & \frac{\partial G_1}{\partial \delta_1} & \cdots & \frac{\partial G_1}{\cos \delta_n \partial \alpha_n} & \frac{\partial G_1}{\partial \delta_n} \\ \vdots & \vdots & & \vdots & \vdots \\ \frac{\partial G_n}{\cos \delta_1 \partial \alpha_1} & \frac{\partial G_n}{\partial \delta_1} & \cdots & \frac{\partial G_n}{\cos \delta_n \partial \alpha_n} & \frac{\partial G_n}{\partial \delta_n} \end{pmatrix} \\ &= \mathbf{I}_{2n} \end{aligned} \quad (82)$$

and

$$\frac{\partial \mathbf{G}}{\partial \mathbf{a}} = \mathbf{0}. \quad (83)$$

Therefore,

$$\mathbf{A} = - \begin{pmatrix} s\mathbf{B} & \Xi \\ \mathbf{I} & \mathbf{0} \end{pmatrix} \quad (84)$$

We will substitute this into equation (77) and examine the remaining terms.

$$\begin{aligned} \mathbf{A}^T \sigma^{-1} &= - \begin{pmatrix} s\mathbf{B}^T & \mathbf{I} \\ \Xi^T & \mathbf{0} \end{pmatrix} \begin{pmatrix} \sigma_x^{-1} & \mathbf{0} \\ \mathbf{0} & \bar{\sigma}_a^{-1} \end{pmatrix} \\ &= - \begin{pmatrix} s\mathbf{B}^T \sigma_x^{-1} & \bar{\sigma}_a^{-1} \\ \Xi^T \sigma_x^{-1} & \mathbf{0} \end{pmatrix} \end{aligned} \quad (85)$$

$$\begin{aligned} \mathbf{A}^T \sigma^{-1} \mathbf{A} &= \begin{pmatrix} s\mathbf{B}^T \sigma_x^{-1} & \bar{\sigma}_a^{-1} \\ \Xi^T \sigma_x^{-1} & \mathbf{0} \end{pmatrix} \begin{pmatrix} s\mathbf{B} & \Xi \\ \mathbf{I} & \mathbf{0} \end{pmatrix} \\ &= \begin{pmatrix} s^2 \mathbf{B}^T \sigma_x^{-1} \mathbf{B} + \bar{\sigma}_a^{-1} & s\mathbf{B}^T \sigma_x^{-1} \Xi \\ s\Xi^T \sigma_x^{-1} \mathbf{B} & \Xi^T \sigma_x^{-1} \Xi \end{pmatrix} \end{aligned} \quad (86)$$

It is informative to look at the dimensions of  $\mathbf{A}$  and the elements that make up

$\mathbf{A}$ . For  $m$  reference stars and  $p$  plate parameters we have

- $\mathbf{B}$ : block diagonal ( $2m \times 2m$ ), whose elementary matrix is a ( $2 \times 2$ ).
- $\sigma_x^{-1}$ : block diagonal ( $2m \times 2m$ ), whose elementary matrix is a ( $2 \times 2$ ).
- $\sigma_a^{-1}$ : block diagonal ( $2m \times 2m$ ), whose elementary matrix is a ( $2 \times 2$ ).
- $\Xi$ : ( $2m \times p$ )

Therefore the dimensions of the  $2 \times 2$  blocks of  $\mathbf{A}$  are:

- (1,1) position : ( $2m \times 2m$ )
- (1,2) position : ( $2m \times p$ )
- (2,1) position : ( $m \times 2p$ )

- (2.2) position :  $(m \times m)$

After substituting in equation (86) into equation (77) we get

$$\begin{pmatrix} s^2 \mathbf{B}^T \sigma_x^{-1} \mathbf{B} + \bar{\sigma}_a^{-1} & s \mathbf{B}^T \sigma_x^{-1} \Xi \\ s \Xi^T \sigma_x^{-1} \mathbf{B} & \Xi^T \sigma_x^{-1} \Xi \end{pmatrix} \begin{pmatrix} \beta \\ \mathbf{a} \end{pmatrix} = \begin{pmatrix} s \mathbf{B}^T \sigma_x^{-1} & \bar{\sigma}_a^{-1} \\ \Xi^T \sigma_x^{-1} & \mathbf{0} \end{pmatrix} \begin{pmatrix} \mathbf{d} \\ 0 \end{pmatrix} \quad (87)$$

and expanding this gives two equation vectors

$$\left( s^2 \mathbf{B}^T \sigma_x^{-1} \mathbf{B} + \bar{\sigma}_a^{-1} \right) \beta + s \mathbf{B}^T \sigma_x^{-1} \Xi \mathbf{a} = s \mathbf{B}^T \sigma_x^{-1} \mathbf{d} \quad (88)$$

and

$$s \Xi^T \sigma_x^{-1} \mathbf{B} \beta + \Xi^T \sigma_x^{-1} \Xi \mathbf{a} = \Xi^T \sigma_x^{-1} \mathbf{d}. \quad (89)$$

Solving the first for  $\beta$  gives

$$\beta = \left( s^2 \mathbf{B}^T \sigma_x^{-1} \mathbf{B} + \bar{\sigma}_a^{-1} \right)^{-1} s \mathbf{B}^T \sigma_x^{-1} (\mathbf{d} - \Xi \mathbf{a}). \quad (90)$$

Substituting in  $\beta$  to the second equation and letting

$$\mathbf{Y} = s^2 \sigma_x^{-1} \mathbf{B} \left( s^2 \mathbf{B}^T \sigma_x^{-1} \mathbf{B} + \bar{\sigma}_a^{-1} \right)^{-1} \mathbf{B}^T \sigma_x^{-1}, \quad (91)$$

we (after some algebra) get the following

$$\Xi^T (\mathbf{Y} - \sigma_x^{-1}) \mathbf{d} = \Xi^T (\mathbf{Y} - \sigma_x^{-1}) \Xi \mathbf{a}. \quad (92)$$

Let  $\mathbf{J} = \sigma_x^{-1} - \mathbf{Y}$  or

$$\mathbf{J} = \sigma_x^{-1} - s^2 \sigma_x^{-1} \mathbf{B} \left( s^2 \mathbf{B}^T \sigma_x^{-1} \mathbf{B} + \sigma_a^{-1} \right)^{-1} \mathbf{B}^T \sigma_x^{-1} \quad (93)$$

using the inversion lemma (Henderson and Searle, 1981) we get

$$\mathbf{J} = \left( \sigma_x + s^2 \mathbf{B} \sigma_a \mathbf{B}^T \right)^{-1}. \quad (94)$$

Substituting this equation for  $\mathbf{J}$  into equation (92) yielding

$$\Xi^T \mathbf{J} \Xi \mathbf{a} = \Xi^T \mathbf{J} \mathbf{d}. \quad (95)$$

We can solve this equation for  $\mathbf{a}$ :

$$\mathbf{a} = \left( \Xi^T \mathbf{J} \Xi \right)^{-1} \Xi^T \mathbf{J} \mathbf{d}. \quad (96)$$

Note that  $\mathbf{J}$  is also block diagonal, consisting of  $2 \times 2$  blocks on the main diagonal. We can therefore write more explicitly

$$\mathbf{a} = \left( \sum_{\nu=1}^n \Xi_{\nu}^T \mathbf{J}_{\nu} \Xi_{\nu} \right)^{-1} \sum_{\nu=1}^n \Xi_{\nu}^T \mathbf{J}_{\nu} \mathbf{d}_{\nu}. \quad (97)$$

Next, we have to find explicit expression for the terms of  $\mathbf{J}$ . These depend on  $\alpha_x$ ,  $\alpha_a$  and the terms of  $\mathbf{B}$ . The terms of  $\mathbf{B}$  are essentially the terms of  $\left( \frac{\partial(\xi, \eta)}{\partial(\alpha, \delta)} \right)$ . Since we have good approximations of the values of  $\xi$ ,  $\eta$  which are approximately  $(x/s)$  and  $(y/s)$  respectively, we will determine  $\mathbf{J}$  from these quantities. Following the procedure suggested by Eichhorn (1985) we will define

$$\begin{aligned} R^2 &= 1 + \xi^2 + \eta^2 \\ T^2 &= \xi^2 + (\cos \delta_0 - \eta \sin \delta_0)^2 \\ S &= \xi R^2 \sin \delta_0 / T \\ U &= \xi R (\sin \delta_0 + \eta \cos \delta_0) / T \\ V &= R^2 (\cos \delta_0 - \eta \sin \delta_0) / T \\ W &= \xi^2 R \cos \delta_0 / T + V / R \end{aligned} \quad (98)$$

and note that

$$R^3 \equiv SU + VW. \quad (99)$$

$\mathbf{B}$  can now be written as

$$\mathbf{B} = \begin{pmatrix} W & -S \\ U & V \end{pmatrix}. \quad (100)$$

From our earlier discussion we wrote  $\mathbf{J} = (\sigma_x + s^2 \mathbf{B} \sigma_a \mathbf{B}^T)^{-1}$ . However with the formulas above, the elements of  $\mathbf{B}$  can be easily calculated without the explicit knowledge of the star's spherical coordinates. If we further introduce the variables,

$$\begin{aligned} QS &= -\rho UW + \sigma SV \\ Y &= \rho U^2 + \sigma V^2 \\ Z &= \rho W^2 + \sigma S^2 \end{aligned} \quad (101)$$

and introduce

$$\begin{pmatrix} \rho & 0 \\ 0 & \sigma \end{pmatrix} = \sigma_a = s^2 \bar{\sigma} = \begin{pmatrix} s^2 \bar{\rho} & 0 \\ 0 & s^2 \bar{\sigma} \end{pmatrix} \quad (102)$$

the weight matrix  $\mathbf{J}$  can be written in the form

$$\mathbf{J} = \begin{pmatrix} \nu + Z & -Q \\ -Q & \phi + Y \end{pmatrix}^{-1}. \quad (103)$$

Note that for any nonsingular matrix  $\mathbf{D}$  the following is true

$$\mathbf{D}^{-1} = \frac{1}{\Delta} \begin{pmatrix} d_{22} & -d_{12} \\ -d_{21} & d_{11} \end{pmatrix}. \quad (104)$$

Therefore the determinant of  $\mathbf{J}$  is  $\Delta = \nu\phi + Z\phi + Y\nu + R^6\sigma\rho$  and we get the weight matrix belonging to the  $\nu^{\text{th}}$  star as

$$\mathbf{J}_\nu = \frac{1}{\nu_\nu\phi_\nu + Y_\nu\nu_\nu + Z_\nu\phi_\nu + R_\nu^6\sigma_\nu\rho_\nu} \begin{pmatrix} \phi_\nu + Y_\nu & Q_\nu \\ Q_\nu & \nu + Z_\nu \end{pmatrix}. \quad (105)$$

We now need to explore more fully the computation for the corrections to the star positions. We now assume that we have calculated the vector of plate parameters,  $\mathbf{a}$ , from equation (97), and henceforth we consider that the vector  $\mathbf{d} - \Xi\mathbf{a}$  is known. As mentioned before, we have  $m$  different independent sets of equations for calculating the corrections  $\beta_\mu^T = (\cos\delta_\mu d\alpha_\mu, d\delta_\mu)$  for each star. From equation (90) we have the formula for the corrections to the star parameters, expanding this equations out (and substituting  $\bar{\sigma}_a^{-1} = s^2\sigma_a^{-1}$ ) we have

$$\begin{aligned} \beta &= \frac{1}{s} \left( \mathbf{B}^T \sigma_x^{-1} \mathbf{B} + \bar{\sigma}_a^{-1} \right)^{-1} s \mathbf{B}^T \sigma_x^{-1} (\mathbf{d} - \Xi \mathbf{a}) \\ &= \frac{1}{s} \left[ \begin{pmatrix} \frac{1}{\rho} & 0 \\ 0 & \frac{1}{\sigma} \end{pmatrix} + \begin{pmatrix} W & U \\ -S & V \end{pmatrix} \begin{pmatrix} \frac{1}{\nu} & 0 \\ 0 & \frac{1}{\phi} \end{pmatrix} \begin{pmatrix} W & -S \\ U & V \end{pmatrix} \right]^{-1} \\ &\quad \begin{pmatrix} W & U \\ -S & V \end{pmatrix} \begin{pmatrix} \frac{1}{\nu} & 0 \\ 0 & \frac{1}{\phi} \end{pmatrix} (\mathbf{d} - \Xi \mathbf{a}) \end{aligned} \quad (106)$$

Remember that  $\beta$  is different for each star and that the symbols  $W, U, V, S$  above are simple numbers and not matrices. To calculate the inverse of the  $2 \times 2$  matrix in this equation, we need its determinant. After some algebra we get the determinant of  $\beta$  to be

$$\Delta = \frac{1}{\nu\phi\rho\sigma} (\nu\phi + Y\nu + Z\phi + R^6\rho\nu). \quad (107)$$

Except for the factor,  $\frac{1}{\nu\phi\rho\sigma}$ , this is the reciprocal of the determinant of  $\mathbf{J}$ . After multiplying the equation for  $\beta$  (equation 106) by its determinant we get

$$\beta = \frac{1}{s(\nu\phi + Z\phi + Y\nu + R^6\rho\sigma)} \cdot \begin{pmatrix} \rho & 0 \\ 0 & \sigma \end{pmatrix} \left[ \begin{pmatrix} W & U \\ -S & V \end{pmatrix} \begin{pmatrix} \phi & 0 \\ 0 & \nu \end{pmatrix} + R^3 \begin{pmatrix} \sigma & 0 \\ 0 & \rho \end{pmatrix} \begin{pmatrix} V & S \\ -U & W \end{pmatrix} \right] (\mathbf{d} - \Xi \mathbf{a}). \quad (108)$$

Note that  $\beta$  is in radians. Its is (if one investigates more closely ) a sophisticated weighted average of the catalogue positions and that which follows from the plates.

### Final Positions from a Single Plate Reduction,

Once we obtain, by an adjustment procedure, estimates for the plate constants, we use them with an inverse of the plate model to determine estimates for the standard coordinates for all the measured images (reference and non-reference). Then using the inverse gnomonic projection, the equatorial coordinates are determined. One of the drawback of the single plate solution is that if the star occurred on more than one plate, the estimates for the same star's coordinates will, of course, be different depending on which plate they originate from. Thus, the single plate solution does not use the simple fact that a star can at one time occupy only one position. Since all the plates are reduced individually, a star that is found on  $n$  plates will have  $n$  different values for its coordinates. Clearly the star only has one position at one time, but this cannot be obtained without mathematically enforcing this constraint on a multiple plate reduction process. Instead, the



separately computed values are averaged to give the “best” (in the mathematical statistics sense) estimate for the stellar position. In addition, the *random* errors are reduced by a factor of  $\frac{1}{\sqrt{n}}$  but this does not reduce the systematic errors. Another drawback of the single plate solution is that when using only the reference stars in the reduction we would more than likely be extrapolating the magnitude terms to the field stars which are typically fainter than the reference stars.

It was considerations of this kind which led to the method of overlapping plates, in its full form first published by Eichhorn (1960). The method of overlapping plates avoids the multiplicity of several “best” star positions and increases considerably the accuracy of at least some of the plate constants, thus reducing the systematic errors (i.e., increasing the accuracy) of the final positions. However, its implementation requires an arithmetic effort exceeding that which is necessary for traditional plate reductions by a factor of at least 2 orders of magnitude. This task has become possible only within the last few years, because cheap, powerful computers have become easily available, removing the label of “major job” from a complete overlap solution.

### Overlap Plate Reduction

The basic principle of the overlapping plate method is that all the star coordinates, not just the reference stars, are considered together with the plate parameters, as adjustment parameters (unknowns). Since the overlap solution

regards the coordinates of each star as adjustment parameters as long as images of the star were measured on more than one plate, the number of parameters increases in proportion to the ratio of the field stars to the reference stars. Obviously — since the number of unknowns has increased dramatically — the analytical and computational problem is exponentially more complex and time consuming than the single plate reduction. In addition, the adjustments pertaining to individual plates also lose their mutual independence because any two plates which have a star in common can now no longer be reduced individually.

Another unavoidable defect of the single plate reduction is a large parameter variance (Eichhorn and Williams, 1963). Even if the geometry of the imaging system was known precisely and the errors of the measuring machine were modeled exactly, there will still exist unavoidable random errors in the x-y measurements and reference star positions. This leads to an unfavorable error propagation of the resulting star positions, in particular when the number of parameters is large and the number of reference stars per plate is small. The accidental errors of these plate parameter estimates thus reappear as systematic errors in the positions that were calculated with them. Such systematic differences even showing up as functions of model terms are unavoidable (and their magnitudes can even be estimated) for those stars (field stars) which were not involved in the derivation of the single-plate parameter estimates. An overlap solution enforces the constraint that a star can only have one position at one time, producing more accurate plate

parameters, thus inevitably leading to smaller systematic errors in the star positions. Also, since the positions themselves are regarded as adjustment unknowns, there can not be any systematic residuals between plates (except those introduced by model deficiencies). In addition, when there is a strong overlap between plates, fewer reference stars are needed per square degree to obtain the same accuracy since, in effect, the total area covered by the overlapping plates is treated as one large plate.

We assume that there are altogether  $m$  stars involved in the adjustment, including both reference and field stars found on more than one plate. Each star number:  $\mu = 1, 2, \dots, m$ . The numbers  $\mu$  are assigned to the stars in some organized fashion. There are  $n$  plates and each plate is assigned a number  $\nu = 1, 2, \dots, n$ . On the  $\nu^{\text{th}}$  plate there are  $m_\nu$  stars. For example,  $(x_{\mu\nu}, y_{\mu\nu})$  are the measured rectangular coordinates of the images of the  $\mu^{\text{th}}$  star on the  $\nu^{\text{th}}$  plate.  $m_r$  of the  $m$  stars are reference stars and the reference stars are assigned a number  $\mu_{r_1}, \mu_{r_2}, \dots, \mu_{r_{m_r}}$ .

The stars used in a overlap reduction are either field stars which occur on at least two plates or reference stars. The estimates for the field stars' equatorial coordinates are found from the single plate solution. When the star appears on more than one plate the average of the single plate solution is used. Thus the averaged  $\alpha_\mu, \delta_\mu$  of the field stars are used to find the standard coordinates  $\xi_{\mu\nu}, \eta_{\mu\nu}$  on all plates on which the star appears. However, for the reference stars

the catalogued values  $\alpha_{c\mu}$ ,  $\delta_{c\mu}$  are used as initial approximations to these stars' spherical coordinates.

For the establishment of the condition equations, it is important to fix the order of the equations and the order of the adjustment parameters. The condition equations are arranged in the following order. Plate by plate we establish the F-type equations for each star on that plate which either occurs on at least on other plate or as a reference star in order of increasing star number. These are followed by the G-type equations which are produced by the estimates of the spherical coordinates of the reference stars, also in the order of increasing star numbers. The order of the observations is the same as the order of the equations which they generate. We chose the order of the parameters as follows: star by star, in numerical order, corrections to the coordinates, i.e.  $\cos \delta_{\mu} d\alpha_{\mu}$  and  $d\delta_{\mu}$  with  $\mu = 1, 2, \dots, m$  are followed by the frame parameters  $\mathbf{a}_1, \dots, \mathbf{a}_n$ .

The equations of condition are identical to those in the single plate solution. As before the total vector of conditions equations  $\mathbf{H}=\mathbf{0}$  consists of "plate equations",  $\mathbf{F}=\mathbf{0}$  and "catalogue equations",  $\mathbf{G}=\mathbf{0}$ . First let's discuss the  $\mathbf{F}=\mathbf{0}$  equations. Plate by plate we establish the F-type equations for each star on that plate which either occurs on at least one other plate or as a reference star. The observations are  $x_{\mu\nu}$  and  $y_{\mu\nu}$ , the measured coordinates of the image of the  $\mu^{\text{th}}$  star on the  $\nu^{\text{th}}$  plate. Exactly one observation occurs in each equation of condition, as before.

The frame equations for the  $\nu$  plate are

$$F_\nu = \begin{pmatrix} x_{\mu\nu} \\ y_{\mu\nu} \end{pmatrix} - s_\nu \begin{pmatrix} \xi_{\mu\nu} \\ \eta_{\mu\nu} \end{pmatrix} - \Xi_{\mu\nu} \mathbf{a}_\nu. \quad (109)$$

There are  $m_\nu$  such equations for each plate, for a total of  $2m_\nu$  equations.  $\xi_{\mu\nu}$  and  $\eta_{\mu\nu}$  are the standard coordinates of the  $\mu^{\text{th}}$  star with respect to the assumed tangential point of the  $\nu^{\text{th}}$  plate.  $\Xi_{\mu\nu}$  is the model matrix for the  $\mu^{\text{th}}$  star on the  $\nu^{\text{th}}$  plate and  $\mathbf{a}_\nu$  is the vector of plate parameters on the  $\nu^{\text{th}}$  plate. Expanding the above equation, we get

$$\mathbf{F}_\nu = \begin{bmatrix} \begin{pmatrix} x_{\mu_{\nu_1}\nu} - s\xi_{\mu_{\nu_1}\nu} \\ y_{\mu_{\nu_1}\nu} - s\eta_{\mu_{\nu_1}\nu} \end{pmatrix} - \Xi_{\mu_{\nu_1}\nu} \mathbf{a}_\nu \\ \begin{pmatrix} x_{\mu_{\nu_2}\nu} - s\xi_{\mu_{\nu_2}\nu} \\ y_{\mu_{\nu_2}\nu} - s\eta_{\mu_{\nu_2}\nu} \end{pmatrix} - \Xi_{\mu_{\nu_2}\nu} \mathbf{a}_\nu \\ \vdots \\ \begin{pmatrix} x_{\mu_{\nu_{m_\nu}}\nu} - s\xi_{\mu_{\nu_{m_\nu}}\nu} \\ y_{\mu_{\nu_{m_\nu}}\nu} - s\eta_{\mu_{\nu_{m_\nu}}\nu} \end{pmatrix} - \Xi_{\mu_{\nu_{m_\nu}}\nu} \mathbf{a}_\nu \end{bmatrix}. \quad (110)$$

At first glance the above notation looks rather confusing. However,  $x_{\mu_{\nu_1}\nu}$  is the first star on the  $\nu^{\text{th}}$  plate. Since all the stars are given a particular number designation numbered 1, 2, ...,  $m$ . There has to be a way to keep up with the running star number  $\mu$  and the star number on each plate, which we will refer to as  $\nu_k$ . The number of stars on the  $\nu^{\text{th}}$  plate run from  $\mu_{\nu_1}$  to  $\mu_{\nu_{m_\nu}}$ . These subscripts are useful in designating the total running star number and the star number on a particular plate. See the example at end of this chapter on how to assign the running star number.

The entire vector  $\mathbf{F}$  is

$$\mathbf{F} = \begin{pmatrix} \mathbf{F}_1 \\ \mathbf{F}_2 \\ \vdots \\ \mathbf{F}_n \end{pmatrix} = \mathbf{0}. \quad (111)$$

Each vector  $\mathbf{F}_\nu$  has the dimension  $2m_\nu \times 1$  and the dimension of the total vector is  $\sum_{\nu=1}^n (2m_\nu \times 1)$ .

Now on to the reference star condition equations. There are a total of  $m_r$  reference stars, numbered  $\mu_{r1}, \mu_{r2}, \dots, \mu_{rm_r}$ . For each reference star we have an estimated value of its position  $(\alpha_{c\mu}, \delta_{c\mu})$  from the catalog. The  $\mathbf{G}=\mathbf{0}$  equations look like this:

$$G = \begin{bmatrix} (\alpha_{c\mu_{r1}} - \alpha_{\mu_{r1}}) \cos \delta_{\mu_{r1}} + \varepsilon_{\mu_{r1}} \\ \delta_{c\mu_{r1}} - \delta_{\mu_{r1}} + \varepsilon_{\mu_{r1}} \\ (\alpha_{c\mu_{r2}} - \alpha_{\mu_{r2}}) \cos \delta_{\mu_{r2}} + \varepsilon_{\mu_{r2}} \\ \delta_{c\mu_{r2}} - \delta_{\mu_{r2}} + \varepsilon_{\mu_{r2}} \\ \vdots \\ (\alpha_{c\mu_{rm_r}} - \alpha_{\mu_{rm_r}}) \cos \delta_{\mu_{rm_r}} + \varepsilon_{\mu_{rm_r}} \\ \delta_{c\mu_{rm_r}} - \delta_{\mu_{rm_r}} + \varepsilon_{\mu_{rm_r}} \end{bmatrix}. \quad (112)$$

Since only a small fraction of all stars are reference stars, it follows that  $\mu_{rk}$  and  $\mu_{rk+1}$  of two neighboring reference stars normally do not have the same number. That means that the subscript  $r$  is just to keep track of reference stars, but just because a star has a subscript  $r$  it does not mean that it is given a different number from that of a field star.  $\mathbf{G}$  does not consist of a separate equations for each plate, as they do for the equations  $\mathbf{F}$ , it has a dimension of  $2m_r \times 1$ .

As before, the total vector  $\mathbf{H}$  consists of the plate equations  $\mathbf{F}$  and the catalog equations  $\mathbf{G}$ .

$$\mathbf{H} = \begin{pmatrix} \mathbf{F} \\ \mathbf{G} \end{pmatrix} = \mathbf{0}. \quad (113)$$

Likewise the vector of residuals is

$$\mathbf{H}_0^T = (\mathbf{d}^T, \mathbf{0}) \quad (114)$$

The covariance matrix is similar to that in a single plate setup, except that  $\sigma_x$  is broken down into blocks belonging to the various frames. Again we are assuming no correlation between observations, so the covariance matrix is diagonal. It consists of  $\nu_{\mu\nu}$ ,  $\phi_{\mu\nu}$ , the variances of  $x_{\mu\nu}$  and  $y_{\mu\nu}$ , and the  $\rho_\mu, \sigma_\mu$  which are  $\cos^2 \delta_\mu$  times the variance of  $\alpha_\mu$  and the variance of  $\delta_\mu$ , respectively, for those  $\mu$  which belong to a reference star

$$\sigma = \text{diag}(\sigma_{x_1}, \sigma_{x_2}, \dots, \sigma_{x_n}; \sigma_a) = \begin{pmatrix} \sigma_x & 0 \\ 0 & \sigma_a \end{pmatrix}. \quad (115)$$

The dimensions of each  $\sigma_{x_k} : 2m_\nu \times 2m_\nu$ , so the dimension of the total matrix  $\sigma_x : \sum_{\nu=1}^n (2m_\nu \times 2m_\nu)$ , while the dimension of  $\sigma_a : 2m_r \times 2m_r$ .

As with the single plate each equation contains only one observation so,  $\mathbf{X} = \left( \frac{\partial \mathbf{F}}{\partial \mathbf{x}} \right) = \mathbf{I}$ , where  $\mathbf{x} = (x_1, y_1, x_2, y_2, \dots, x_m, y_m; \alpha_{1c} \cos \delta_1, \delta_1, \dots, \alpha_{mc} \cos \delta_m, \delta_m)$ , so  $\mathbf{X}\sigma\mathbf{X}^T = \sigma = \begin{pmatrix} \sigma_x & 0 \\ 0 & \sigma_a \end{pmatrix}$ .

The mathematical development of an overlap solution is very similar to the single plate method discussed in the last section. The major difference is the

increase in the observations (all the stars), which enormously increase, the size and structure of the matrices. We will present the mathematical development similar to the single plate development, noting the changing the structure of the matrices.

As before, the correction to the parameters is given by

$$\alpha = -\left(\mathbf{A}^T \sigma^{-1} \mathbf{A}\right)^{-1} \mathbf{A}^T \sigma^{-1} \mathbf{H}_0 \quad (116)$$

where  $\alpha = \begin{pmatrix} \beta \\ \mathbf{a} \end{pmatrix}$  and  $\beta$  is the vector of corrections to the spherical coordinates  $(\alpha_\mu \cos \delta_\mu, \delta_\mu)$ . The total vector of plate parameters for all the plates is  $\mathbf{a}$ , which is made up of the individual vectors for each plate

$$\mathbf{a} = \begin{pmatrix} \mathbf{a}_1 \\ \mathbf{a}_2 \\ \vdots \\ \mathbf{a}_n \end{pmatrix}. \quad (117)$$

Our primary concern is the establishment of the matrix  $\mathbf{A}$  for the overlap case:

$$\mathbf{A} = \left( \frac{\partial \mathbf{H}}{\partial \alpha} \right) = \left( \frac{\partial (\mathbf{F}, \mathbf{G})}{\partial (\beta, \mathbf{a})} \right) = \begin{pmatrix} \left( \frac{\partial \mathbf{F}}{\partial \beta} \right) & \left( \frac{\partial \mathbf{F}}{\partial \mathbf{a}} \right) \\ \left( \frac{\partial \mathbf{G}}{\partial \beta} \right) & \left( \frac{\partial \mathbf{G}}{\partial \mathbf{a}} \right) \end{pmatrix}. \quad (118)$$

Similar to the single plate reduction we have for each star

$$\frac{\partial \mathbf{F}_{\mu\nu}}{\partial \beta_{\mu\nu}} = \frac{\partial (\xi_{\mu_{\nu_k} \nu}, \eta_{\mu_{\nu_k} \nu})}{\partial (\alpha_{\mu_{\nu_k} \nu} \cos \delta_{\mu_{\nu_k} \nu}, \delta_{\mu_{\nu_k} \nu})} = -s \mathbf{B}_{\mu_{\nu_k} \nu} \quad (119)$$



where each  $\mathbf{B}_{\mu_{\nu_k}\nu}$  is a  $2 \times 2$  matrix. For each plate we get

$$\frac{\partial \mathbf{F}_\nu}{\partial \beta} = -s\mathbf{B}_\nu = -s \begin{pmatrix} 0 & 0 & \mathbf{B}_{\mu_{\nu_1}\nu} & \dots & \dots & \dots & \dots & \dots & 0 \\ 0 & 0 & \dots & 0 & \mathbf{B}_{\mu_{\nu_2}\nu} & \dots & \dots & \dots & 0 \\ \vdots & \vdots & \vdots & \vdots & \vdots & \vdots & \vdots & \vdots & \vdots \\ 0 & \dots & \dots & \dots & \dots & \dots & \mathbf{B}_{\mu_{\nu_{m_\nu}}\nu} & \dots & 0 \end{pmatrix} \quad (120)$$

where the dimension of each  $\mathbf{B}_\nu$  matrix is  $(2m_\nu \times 2m)$ . Thus each line pair contains exactly one  $\mathbf{B}_{\mu_{\nu_k}\nu}$  matrix (of dimension  $2 \times 2$ ) but only in those column pairs which belong to a star whose image was measured on the  $\nu^{\text{th}}$  plate. In other words, the rows correspond to the stars on plate  $\nu$ , while the columns are for all the stars, therefore  $\mathbf{B}_{\mu_{\nu_k}\nu}$  is not the null matrix only when the  $\mu^{\text{th}}$  star is on the  $\nu^{\text{th}}$  plate. The entire matrix  $\mathbf{B}$  for all the plates is written as

$$s\mathbf{B} = \begin{pmatrix} s\mathbf{B}_1 \\ s\mathbf{B}_2 \\ \vdots \\ s\mathbf{B}_n \end{pmatrix} \quad (121)$$

and this matrix is of dimension  $\sum_{\nu=1}^n 2m_\nu \times 2m$ .

Furthermore, we have

$$\frac{\partial \mathbf{F}_\nu}{\partial \mathbf{a}_\nu} = -\Xi_\nu \quad (122)$$

where  $\Xi_\nu$  is of dimension  $2m_\nu \times l_\nu$ ,  $l_\nu$  being the number of components of the vector  $\mathbf{a}$  on the  $\nu^{\text{th}}$  plate. In  $\Xi_\nu$ , each star with number  $\mu$  that occurs on the  $\nu^{\text{th}}$

frame generates a  $2 \times l_\nu$  matrix  $\Xi_{\mu\nu}$ . Thus

$$\Xi_\nu = \begin{pmatrix} \Xi_{\mu_{\nu_1}\nu} \\ \Xi_{\mu_{\nu_2}\nu} \\ \vdots \\ \Xi_{\mu_{\nu_n}\nu} \end{pmatrix} \quad (123)$$

and the total matrix  $\Xi$  is of the form

$$\frac{\partial \mathbf{F}}{\partial \mathbf{a}} = -\Xi = - \begin{pmatrix} \Xi_1 & \cdots & 0 \\ \vdots & \Xi_2 & \vdots \\ & \ddots & \\ 0 & \cdots & \Xi_n \end{pmatrix} \quad (124)$$

and has dimension  $\sum_{\nu=1}^n 2m_\nu \times \sum_{\nu=1}^n l_\nu$ .

Furthermore,

$$\frac{\partial \mathbf{G}_\nu}{\partial \beta} = \frac{\partial \mathbf{G}_\nu}{\cos \delta_{\mu\nu} \partial \alpha_{\mu\nu}} \frac{\partial \mathbf{G}_\nu}{\partial \delta_{\mu\nu}} = -\mathbf{K}. \quad (125)$$

All nonzero elements of the matrix  $\mathbf{K}$  are 1. However, since not all stars are reference stars,  $\mathbf{K}$  is not the identity matrix.  $\mathbf{K}$  has the dimension of  $2m_r \times 2m$ . If the  $\mu^{\text{th}}$  star is also a reference star then the row pair corresponding to this reference star and the column pair for this  $\mu^{\text{th}}$  star will contain the  $\mathbf{I}_2$  identity matrix.

Since  $\mathbf{G}$  is independent of the plate parameters, we have (as in the single plate result)

$$\frac{\partial \mathbf{G}}{\partial \mathbf{a}} = \mathbf{0}. \quad (126)$$

Combining all these results (as in the single plate reduction), the matrix  $\mathbf{A}$  can be written as

$$\mathbf{A} = - \begin{pmatrix} s\mathbf{B} & \Xi \\ \mathbf{K} & \mathbf{0} \end{pmatrix} \quad (127)$$

and has dimension  $2\left(\sum_{\nu=1}^n m_\nu + m_r\right) \times 2m + \sum_{\nu=1}^n l_\nu$ .

Now that we have looked at the various matrices that make up the matrix  $\mathbf{A}$ , let's look at the structure of the normal equations. The structure of the normal equations looks the same as in the single plate solution:

$$\left(\mathbf{A}^T \sigma^{-1} \mathbf{A}\right) \begin{pmatrix} \beta \\ \alpha \end{pmatrix} = -\mathbf{A}^T \sigma^{-1} \begin{pmatrix} \mathbf{d} \\ \mathbf{0} \end{pmatrix}. \quad (128)$$

However, these equations are much more complicated than in the single plate case. In detail

$$\begin{aligned} \mathbf{A}^T \sigma^{-1} \mathbf{A} &= \begin{pmatrix} s\mathbf{B}^T \sigma_x^{-1} & \mathbf{K}^T \sigma_a^{-1} \\ \Xi^T \sigma_x^{-1} & \mathbf{0} \end{pmatrix} \begin{pmatrix} s\mathbf{B} & \Xi \\ \mathbf{K} & \mathbf{0} \end{pmatrix} \\ &= \begin{pmatrix} s^2 \mathbf{B}^T \sigma_x^{-1} \mathbf{B} + \mathbf{K}^T \sigma_a^{-1} \mathbf{K} & s^2 \mathbf{B}^T \sigma_x^{-1} \Xi \\ s \Xi^T \sigma_x^{-1} \mathbf{B} & \Xi^T \sigma_x^{-1} \Xi \end{pmatrix} \end{aligned} \quad (129)$$

which can also be written as

$$\begin{aligned} \mathbf{A}^T \sigma^{-1} \mathbf{A} &= \begin{pmatrix} s^2 \sum_{\nu=1}^n \mathbf{B}_\nu^T \sigma_\nu^{-1} \mathbf{B}_\nu + \mathbf{K}^T \sigma_a^{-1} \mathbf{K} & s\mathbf{B}_1^T \sigma_1^{-1} \Xi_1 & \dots & s\mathbf{B}_n^T \sigma_n^{-1} \Xi_n \\ s\Xi_1^T \sigma_1^{-1} \mathbf{B}_1 & \Xi_1^T \sigma_1^{-1} \mathbf{B}_1 & \dots & \mathbf{0} \\ \vdots & \vdots & & \vdots \\ s\Xi_n^T \sigma_n^{-1} \mathbf{B}_n & \mathbf{0} & & \Xi_n^T \sigma_n^{-1} \mathbf{B}_n \end{pmatrix} \\ &= \begin{pmatrix} \mathbf{L} & s\mathbf{B}^T \sigma_x^{-1} \Xi \\ s\Xi^T \sigma_x^{-1} \mathbf{B} & \Xi^T \sigma_x^{-1} \Xi \end{pmatrix} \end{aligned} \quad (130)$$

with  $\mathbf{L} = \mathbf{K}^T \sigma_a^{-1} \mathbf{K} + s^2 \mathbf{B}^T \sigma_x^{-1} \mathbf{B}$ .

Now let's take a closer look at structure of the matrices that make up equation (130). The example given later on will help to clarify these matrices, so the reader may want to refer to this example. Because  $\sigma_x$  is a diagonal matrix,

multiplication by this matrix leaves the structure of the matrix by which it is multiplied unchanged.

We noted from the discussion above that the  $\mathbf{B}_\nu$  ( $2m_\nu \times 2m$ ) are very sparse matrices and have a structure similar to that of  $\mathbf{K}$ . Each row pair contains exactly one non-zero  $2 \times 2$  matrix, however not every column pair has one of these blocks, (i.e. some of the column pairs contain all zero elements). Nonzero elements occur in a column pair of  $\mathbf{B}_\nu$  only if the corresponding star occurs on the plate corresponding to the row for that plate. Compact blocks with nonzero elements in  $\mathbf{B}_\nu^T$  will interact with compact blocks in  $\mathbf{B}_\nu$ , wherever the  $\mu^{\text{th}}$  star's image was measured on the  $\nu^{\text{th}}$  plate. The result of the interaction will result in a  $2 \times 2$  block in the  $\mu^{\text{th}}$  row pair — and column pair — of  $\mathbf{L}$ . The structure of  $\mathbf{B}^T \sigma_x^{-1} \mathbf{B}$  is thus similar to that of  $\mathbf{B}^T$ , except that the  $\nu^{\text{th}}$  column pair would be “replaced” by a matrix of the width  $l_\nu$ . The matrix  $\mathbf{K}^T \sigma_a^{-1} \mathbf{K}$  will be a diagonal matrix, however some of the elements on the diagonal may be zero. The result of adding this matrix to  $s^2 \mathbf{B}^T \sigma_x^{-1} \mathbf{B}$  is that the diagonal blocks  $(\rho_\mu, \sigma_\mu)$  will add to the diagonal blocks in the  $\mu^{\text{th}}$  double row and column.  $\mathbf{L}$  is thus a block-diagonal.

Since the dimensions of the matrices  $\mathbf{B}_\nu^T$  are  $2m \times 2m_\nu$  and those of  $\Xi_\nu$  are  $2m_\nu \times l_\nu$ , the product  $s \mathbf{B}_\nu^T \sigma_\nu^{-1} \Xi_\nu$  is a sparse matrix of dimensions  $2m \times l_\nu$ , whose nonzero  $2 \times 2$  elements  $s \mathbf{B}_{\mu\nu}^T \sigma_{\mu\nu}^{-1} \Xi_{\mu\nu}$  occur only on those of its line pairs whose numbers correspond to a star which occurs on the  $\nu^{\text{th}}$  plate.

$\Xi^T \sigma_x^{-1} \Xi$  is block-diagonal, the individual blocks being  $\Xi_\nu^T \sigma_\nu^{-1} \Xi_\nu$ , the matrices of the product sums of each plate's model matrix with the covariance matrix.

Finally, consider the right hand side of the normal equations (equation 128),  $\mathbf{A}^T \sigma^{-1} \mathbf{H}$ . The resulting vector has the dimension  $(2m + \sum_{\nu=1}^n l_\nu) \times 1$  which is a vector of the order of twice the number of stars plus the total number of plate parameters.

$$\begin{aligned} \mathbf{A}^T \sigma^{-1} \mathbf{H} &= - \begin{pmatrix} s\mathbf{B}^T & \mathbf{K}^T \\ \Xi^T & \mathbf{0} \end{pmatrix} \begin{pmatrix} \sigma_x^{-1} & \mathbf{0} \\ \mathbf{0} & \sigma_a^{-1} \end{pmatrix} \begin{pmatrix} \mathbf{d} \\ \mathbf{0} \end{pmatrix} \\ &= \begin{pmatrix} -s\mathbf{B}^T \\ \Xi^T \end{pmatrix} \sigma_x^{-1} \mathbf{d} \end{aligned} \quad (131)$$

Consider the  $2 \times 1$  vector:  $s \sum_{\nu=1}^n \mathbf{B}_{\mu\nu}^T \sigma_{\mu_n}^{-1} \mathbf{d}_{\mu\nu}$ . Nonzero contributions to these sums are made only when images of the  $\mu^{\text{th}}$  star were measured on the  $\nu^{\text{th}}$  plate.

Substituting equation (130) and (131) in the normal equations (128) yields

$$\begin{pmatrix} \mathbf{L} & s\mathbf{B}^T \sigma_x^{-1} \Xi \\ s\Xi^T \sigma_x^{-1} \mathbf{B} & \Xi^T \sigma_x^{-1} \Xi \end{pmatrix} \begin{pmatrix} \beta \\ \mathbf{a} \end{pmatrix} = \begin{pmatrix} s\mathbf{B}^T \\ \Xi^T \end{pmatrix} \sigma_x^{-1} \mathbf{d}. \quad (132)$$

The first row gives  $\mathbf{L}\beta + s\mathbf{B}^T \sigma_x^{-1} \Xi \mathbf{a} = s\mathbf{B}^T \sigma_x^{-1} \mathbf{d}$  and the second row gives  $s\Xi^T \sigma_x^{-1} \mathbf{B}\beta + \Xi^T \sigma_x^{-1} \Xi \mathbf{a} = \Xi^T \sigma_x^{-1} \mathbf{d}$ . As before, the solution to the normal equations is done in steps. First we eliminate the star parameters,  $\beta$ , and solve for the plate parameters  $\mathbf{a}$ . Solving the first equation for  $\beta$  gives :

$$\beta = s\mathbf{L}^{-1} \mathbf{B}^T \sigma_x^{-1} (\mathbf{d} - \Xi \mathbf{a}). \quad (133)$$

Substituting  $\beta$  into the second row of the normal equations yields

$$\Xi^T \left( \sigma_x^{-1} - s^2 \sigma_x^{-1} \mathbf{B} \mathbf{L}^{-1} \mathbf{B}^T \sigma_x^{-1} \right) (\mathbf{d} - \Xi \mathbf{a}) = \mathbf{0}. \quad (134)$$

Let

$$\mathbf{J}' = \sigma_{\mathbf{x}}^{-1} - s^2 \sigma_{\mathbf{x}}^{-1} \mathbf{B} \mathbf{L}^{-1} \mathbf{B}^T \sigma_{\mathbf{x}}^{-1} \quad (135)$$

Then

$$\begin{aligned} \Xi^T (\mathbf{J}') (\mathbf{d} - \Xi \mathbf{a}) &= 0 \\ \Xi^T \mathbf{J}' \mathbf{d} &= \Xi^T \mathbf{J}' \Xi \mathbf{a} \\ \mathbf{a} &= \left( \Xi^T \mathbf{J}' \Xi \right)^{-1} \Xi^T \mathbf{J}' \mathbf{d}. \end{aligned} \quad (136)$$

The inversion lemma cannot be used to simplify  $\mathbf{J}'$  as it was used to simplify  $\mathbf{J}$  because the  $2m \times 2m$  matrix  $\mathbf{K}^T \sigma^{-1} \mathbf{K}$  term in  $\mathbf{L}$  is a diagonal matrix with nonzero elements on the diagonal only in those double blocks whose ordinal numbers correspond to reference stars, thus it is *singular*. Unlike the matrix  $\mathbf{J}'$ ,  $\mathbf{J}$  is not block-diagonal. Since we have established above that  $\mathbf{L}$  is block-diagonal with blocks of dimension  $2 \times 2$ , the structure of  $\mathbf{J}'$  is the same as that of  $\mathbf{B} \mathbf{B}^T$ . Thus the resulting  $\Xi^T \mathbf{J}' \Xi$  is “banded-bordered” (De Vegt and Ebner, 1972) and thus there are simplified routines to invert it.

Now that we have determined (i.e., estimated) the plate parameters, we can use them to find the star parameters by equation (133). In terms of the individual stars

$$\beta_{\mu} = s \left( \delta_{\mu, \mu_n} \sigma_{\mu_n}^{-1} + s^2 \sum_{\nu=1}^n \mathbf{B}_{\mu\nu}^T \sigma_{\mu\nu}^{-1} \mathbf{B}_{\mu\nu} \right)^{-1} \sum_{\nu=1}^n \mathbf{B}_{\mu\nu}^T \sigma_{\mu\nu}^{-1} (\mathbf{d}_{\mu\nu} - \Xi_{\mu\nu} \mathbf{a}_{\nu}). \quad (137)$$

The symbol  $\delta_{\mu\nu}$  is of Kronecker type, it equals zero if the  $\mu^{\text{th}}$  star is not a reference star, and it equals 1 for reference stars. The  $2 \times 1$  vector  $\beta_{\mu} = (d\alpha_{\mu} \cos \delta_{\mu}, d\delta_{\mu})^T$

is a sub-matrix of the previously encountered  $2m_\nu \times 1$  vector  $\beta_\nu$  which stands for the pairs  $(d\alpha \cos \delta, d\delta)$  of all the stars which occur on the  $\nu^{\text{th}}$  frame. Thus if a star occurs on  $n$  plates, there will be  $n$  different  $\beta$ 's after the reduction, whereas in the case  $\beta_\mu$ , all the star parameters for one star are calculated after all the plate parameters have been calculated. This substantially amounts to taking a weighted mean for all the contributions of all frames on which images of the star were measured.

#### Example of Overlap Reduction.

Although the solution of the normal equations in the overlap case is very similar tot that of the single plate case, the interaction of the stars imaged on more than one plate complicates the reduction. It is therefore extremely useful to illustrate the method with an example.

We will use a *very simple* example. Consider the case where we have 8 stars imaged on 2 plates, 6 stars on the first plate and 6 stars on the second. Let three of the stars be reference stars.

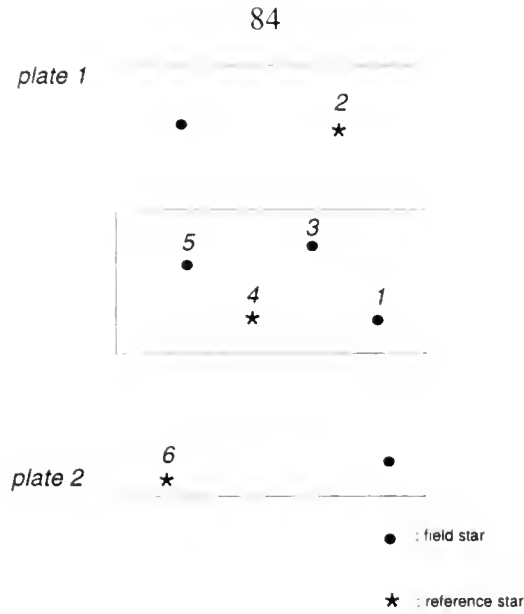


Figure 9: Example of two overlapping plates

One can see that each plate has a star in the corner to which no number has been assigned. Each of these two stars occurs on only one plate, and none is a reference star, thus in the overlap reduction they are ignored. After the reduction has been performed, the plate parameters are used to calculate the equatorial coordinates of these isolated stars.

Using our notation established earlier we have

$$m = 6$$

$$n = 2$$

$$m_r = 3$$

$$m_l = 5$$



$$m_2 = 5$$

Indexing for the stars on plate 1 is  $\mu_{\nu_k} \nu$

- Star 1 : the first star on plate 1,  $\mu_{1_1} 1 = 1_1 1 = 1, 1$
- Star 2 : the second star on plate 2,  $\mu_{1_2} 1 = 2_2 1 = 2, 1$  or  $\mu_{r_1} = 2$
- Star 3 : the third star on plate 1,  $\mu_{1_3} 1 = 3_3 1 = 3, 1$
- Star 4 : the forth star on plate 1,  $\mu_{1_4} 1 = 4_4 1 = 4, 1$  or  $\mu_{r_2} = 4$
- Star 5 : the fifth star on plate 1,  $\mu_{1_5} 1 = 5_5 1 = 5, 1$

Indexing for the stars on plate 2 is

- Star 1: the first star on plate 2,  $\mu_{2_1} 2 = 1_1 2 = 1, 2$
- Star 3 : the second star on the second plate,  $\mu_{2_2} 2 = 3_2 2 = 3, 2$
- Star 4 : the third star on the second plate,  $\mu_{2_3} 2 = 4_3 2 = 4, 2$   $\mu_{r_2} = 4$
- Star 5 : the forth star on the second plate,  $\mu_{2_4} 2 = 5_4 2 = 5, 2$
- Star 6 : the fifth star on the second plate  $\mu_{2_5} 2 = 6_5 2 = 6, 2$  or  $\mu_{r_3} = 6$

We have four prime goals:

1. Set up the equations of condition.
2. Use these equations to find  $\mathbf{J}'$ .
3. Use  $\mathbf{J}'$ , to determine  $\mathbf{a}$ .
4. Use  $\mathbf{a}$ , to find  $\beta$ .

Set up the equations of condition

The equations **F** have the form

$$\mathbf{F}_\nu = \begin{pmatrix} \mathbf{x}_{\mu\nu} \\ \mathbf{y}_{\mu\nu} \end{pmatrix} - s_\nu \begin{pmatrix} \xi_{\mu\nu} \\ \eta_{\mu\nu} \end{pmatrix} - \Xi_{\mu\nu} \mathbf{a}_\nu = \mathbf{0} \quad (138)$$

and the equations **G** become

$$\mathbf{G} = \begin{pmatrix} (\alpha_{c\mu_{r_k}} - \alpha_{\mu_{r_k}}) - \cos \delta_{\mu_{r_k}} \\ (\delta_{c\mu_{r_k}} - \delta_{\mu_{r_k}}) \end{pmatrix} = \mathbf{0}, \quad (139)$$

where  $k$  goes from 1 to  $m_r$ , the total number of reference stars. The index  $\alpha_{c\mu_{r_k}}$  is the  $\mu^{\text{th}}$  number of the  $k^{\text{th}}$  reference star. Therefore in our example:

- $\mu_{r_1} = 2$
- $\mu_{r_2} = 4$
- $\mu_{r_3} = 6$

It is important to fix the order of the equations. In the last section we stated that the equations were ordered plate by plate and within a plate, in order of increasing star number. However, from a programming point of view we found it simpler to order the equations star by star. In other words we group all the stars together that occur on the separate plates. This is equivalent to ordering the equations plate by plate (the row and columns of the matrices are interchanged). Therefore the equations are ordered star by star in order of increasing star number.

The total vector  $\mathbf{H}$  becomes

$$\mathbf{H} = \begin{pmatrix} \begin{pmatrix} X_{11} - s\xi_{11} \\ Y_{11} - s\eta_{11} \end{pmatrix} - \Xi_{11}\mathbf{a}_1 \\ \begin{pmatrix} X_{12} - s\xi_{12} \\ Y_{12} - s\eta_{12} \end{pmatrix} - \Xi_{12}\mathbf{a}_2 \\ \begin{pmatrix} X_{21} - s\xi_{21} \\ Y_{21} - s\eta_{21} \end{pmatrix} - \Xi_{21}\mathbf{a}_1 \\ \begin{pmatrix} X_{31} - s\xi_{31} \\ Y_{31} - s\eta_{31} \end{pmatrix} - \Xi_{31}\mathbf{a}_1 \\ \begin{pmatrix} X_{32} - s\xi_{32} \\ Y_{32} - s\eta_{32} \end{pmatrix} - \Xi_{32}\mathbf{a}_2 \\ \begin{pmatrix} X_{41} - s\xi_{41} \\ Y_{41} - s\eta_{41} \end{pmatrix} - \Xi_{41}\mathbf{a}_1 \\ \begin{pmatrix} X_{42} - s\xi_{42} \\ Y_{42} - s\eta_{42} \end{pmatrix} - \Xi_{42}\mathbf{a}_2 \\ \begin{pmatrix} X_{51} - s\xi_{51} \\ Y_{51} - s\eta_{51} \end{pmatrix} - \Xi_{51}\mathbf{a}_1 \\ \begin{pmatrix} X_{52} - s\xi_{52} \\ Y_{52} - s\eta_{52} \end{pmatrix} - \Xi_{52}\mathbf{a}_2 \\ \begin{pmatrix} X_{62} - s\xi_{62} \\ Y_{62} - s\eta_{62} \end{pmatrix} - \Xi_{62}\mathbf{a}_2 \\ (\alpha_{c2} - \alpha_2) - \cos \delta_2 \\ (\delta_{c2} - \delta_2) \\ (\alpha_{c4} - \alpha_4) - \cos \delta_4 \\ (\delta_{c4} - \delta_4) \\ (\delta_{c6} - \delta_6) - \cos \delta_6 \\ (\delta_{c6} - \delta_6) \end{pmatrix} = \begin{pmatrix} d_{11} \\ d_{12} \\ d_{21} \\ d_{31} \\ d_{32} \\ d_{41} \\ d_{42} \\ d_{51} \\ d_{52} \\ d_{62} \\ 0 \\ 0 \\ 0 \end{pmatrix}. \quad (140)$$

The (total) covariance matrix is  $\sigma = \begin{pmatrix} \sigma_x & 0 \\ 0 & \sigma_a \end{pmatrix}$  where the covariance matrix of

the measurements is

$$\sigma_x = \begin{pmatrix} \sigma_{11} & 0 & 0 & 0 & 0 & 0 & 0 & 0 & 0 & 0 \\ 0 & \sigma_{12} & 0 & 0 & 0 & 0 & 0 & 0 & 0 & 0 \\ 0 & 0 & \sigma_{21} & 0 & 0 & 0 & 0 & 0 & 0 & 0 \\ 0 & 0 & 0 & \sigma_{31} & 0 & 0 & 0 & 0 & 0 & 0 \\ 0 & 0 & 0 & 0 & \sigma_{32} & 0 & 0 & 0 & 0 & 0 \\ 0 & 0 & 0 & 0 & 0 & \sigma_{41} & 0 & 0 & 0 & 0 \\ 0 & 0 & 0 & 0 & 0 & 0 & \sigma_{42} & 0 & 0 & 0 \\ 0 & 0 & 0 & 0 & 0 & 0 & 0 & \sigma_{51} & 0 & 0 \\ 0 & 0 & 0 & 0 & 0 & 0 & 0 & 0 & \sigma_{61} & 0 \\ 0 & 0 & 0 & 0 & 0 & 0 & 0 & 0 & 0 & \sigma_{62} \end{pmatrix}. \quad (141)$$

Each sub-matrix in  $\sigma_x$  is a  $2 \times 2$  diagonal matrix of the form  $\sigma_{\mu\nu} = \begin{pmatrix} \rho_\mu & 0 \\ 0 & \sigma_\mu \end{pmatrix}$ .

The matrix  $\sigma_x$  then has dimensions  $\sum_{\nu=1}^n 2m_\nu \times \sum_{\nu=1}^n 2m_\nu$ . The covariance matrix of the reference stars has the form

$$\sigma_a = \begin{pmatrix} \sigma_2 & 0 & 0 \\ 0 & \sigma_4 & 0 \\ 0 & 0 & \sigma_6 \end{pmatrix}, \quad (142)$$

where the diagonal elements are  $2 \times 2$  block matrices of the form

$$\sigma_{a\mu} = \begin{pmatrix} \alpha_\mu \cos^2 \delta_\mu & 0 \\ 0 & \delta_\mu \end{pmatrix} \quad (143)$$

so the dimension of  $\sigma_a$  is  $2m_r \times 2m_r$ .

$\mathbf{B}_\nu$  has dimension  $2m_\nu \times 2m$ , so in this example the total matrix  $\mathbf{B}$  is a

20×12 matrix.

$$\mathbf{B} = \begin{pmatrix} \mathbf{B}_{11} & 0 & 0 & 0 & 0 & 0 \\ \mathbf{B}_{12} & 0 & 0 & 0 & 0 & 0 \\ 0 & \mathbf{B}_{21} & 0 & 0 & 0 & 0 \\ 0 & 0 & \mathbf{B}_{31} & 0 & 0 & 0 \\ 0 & 0 & \mathbf{B}_{32} & 0 & 0 & 0 \\ 0 & 0 & 0 & \mathbf{B}_{41} & 0 & 0 \\ 0 & 0 & 0 & \mathbf{B}_{42} & 0 & 0 \\ 0 & 0 & 0 & 0 & \mathbf{B}_{51} & 0 \\ 0 & 0 & 0 & 0 & \mathbf{B}_{52} & 0 \\ 0 & 0 & 0 & 0 & 0 & \mathbf{B}_{62} \end{pmatrix}. \quad (144)$$

The matrix  $\mathbf{K}$  has the dimension  $2m_r \times 2m_r$ , in this case it is a  $6 \times 12$  matrix:

$$\mathbf{K} = \begin{pmatrix} 0 & \mathbf{I}_2 & 0 & 0 & 0 & 0 \\ 0 & 0 & 0 & \mathbf{I}_2 & 0 & 0 \\ 0 & 0 & 0 & 0 & 0 & \mathbf{I}_2 \end{pmatrix}. \quad (145)$$

$\Xi_\nu$  is of dimension  $2m_\nu \times l_\nu$ . Let's take a 6-constant model, thus  $\Xi_1$  and  $\Xi_2$  have the dimension  $10 \times 6$ . Thus the total matrix  $\Xi$  is a  $20 \times 12$ . For each star we have a model matrix of the form:

$$\Xi_{\mu\nu} = \begin{pmatrix} \xi_{\mu\nu} & \eta_{\mu\nu} & 1 & 0 & 0 & 0 \\ 0 & 0 & 0 & \xi_{\mu\nu} & \eta_{\mu\nu} & 1 \end{pmatrix} \quad (146)$$

and for all the stars the total model matrix is,

$$\Xi = \begin{pmatrix} \Xi_{11} & 0 \\ 0 & \Xi_{12} \\ \Xi_{21} & 0 \\ \Xi_{31} & 0 \\ 0 & \Xi_{32} \\ \Xi_{41} & 0 \\ 0 & \Xi_{42} \\ \Xi_{51} & 0 \\ 0 & \Xi_{52} \\ 0 & \Xi_{62} \end{pmatrix}. \quad (147)$$

Altogether the matrix  $\mathbf{A}$  is

$$\mathbf{A} = - \begin{pmatrix} s\mathbf{B} & \Xi \\ \mathbf{K} & 0 \end{pmatrix} \quad (148)$$

or expanded

$$\mathbf{A} = \begin{pmatrix} s\mathbf{B}_{11} & 0 & 0 & 0 & 0 & 0 & \Xi_{11} & 0 \\ s\mathbf{B}_{12} & 0 & 0 & 0 & 0 & 0 & 0 & \Xi_{12} \\ 0 & s\mathbf{B}_{21} & 0 & 0 & 0 & 0 & \Xi_{21} & 0 \\ 0 & 0 & s\mathbf{B}_{31} & 0 & 0 & 0 & \Xi_{31} & 0 \\ 0 & 0 & s\mathbf{B}_{32} & 0 & 0 & 0 & 0 & \Xi_{32} \\ 0 & 0 & 0 & s\mathbf{B}_{41} & 0 & 0 & \Xi_{41} & 0 \\ 0 & 0 & 0 & s\mathbf{B}_{42} & 0 & 0 & 0 & \Xi_{42} \\ 0 & 0 & 0 & 0 & s\mathbf{B}_{51} & 0 & \Xi_{51} & 0 \\ 0 & 0 & 0 & 0 & s\mathbf{B}_{52} & 0 & 0 & \Xi_{52} \\ 0 & 0 & 0 & 0 & 0 & s\mathbf{B}_{62} & 0 & \Xi_{62} \\ 0 & \mathbf{I}_2 & 0 & 0 & 0 & 0 & 0 & 0 \\ 0 & 0 & 0 & \mathbf{I}_2 & 0 & 0 & 0 & 0 \\ 0 & 0 & 0 & 0 & 0 & \mathbf{I}_2 & 0 & 0 \end{pmatrix}. \quad (149)$$

Determine  $\mathbf{J}'$

Now let's go back to  $\mathbf{L} = \mathbf{K}^T \sigma_a^{-1} \mathbf{K} + s^2 \mathbf{B}^T \sigma_x^{-1} \mathbf{B}$  and look at the second term:  $\mathbf{B}^T \sigma_x^{-1} \mathbf{B}$ . Since the covariance matrix is diagonal, each  $p$  diagonal element is multiplied by the  $p^{\text{th}}$  column. The matrix dimension is  $\mathbf{B}_{(12 \times 20)}^T \sigma_{x(20 \times 20)}^{-1} \mathbf{B}_{(20 \times 12)} = (12 \times 12)$ . This matrix has to compact blocks wherever the  $\mu^{\text{th}}$  star was measured on the  $\nu^{\text{th}}$ , plate.

$$\mathbf{B}^T \sigma_x^{-1} \mathbf{B} = \text{diag} \begin{pmatrix} \mathbf{B}_{11}^T \sigma_{11}^{-1} \mathbf{B}_{11} + \mathbf{B}_{12}^T \sigma_{12}^{-1} \mathbf{B}_{12} \\ \mathbf{B}_{21}^T \sigma_{21}^{-1} \mathbf{B}_{21} \\ \mathbf{B}_{31}^T \sigma_{31}^{-1} \mathbf{B}_{31} + \mathbf{B}_{32}^T \sigma_{32}^{-1} \mathbf{B}_{32} \\ \mathbf{B}_{41}^T \sigma_{41}^{-1} \mathbf{B}_{41} + \mathbf{B}_{42}^T \sigma_{42}^{-1} \mathbf{B}_{42} \\ \mathbf{B}_{51}^T \sigma_{51}^{-1} \mathbf{B}_{51} + \mathbf{B}_{52}^T \sigma_{52}^{-1} \mathbf{B}_{52} \\ \mathbf{B}_{62}^T \sigma_{62}^{-1} \mathbf{B}_{62} \end{pmatrix}^T \quad (150)$$

The matrix has dimension of  $\mathbf{K}_{(12 \times 6)}^T \sigma_a^{-1} \mathbf{K}_{(6 \times 12)} = (12 \times 12)$ .

$$\begin{aligned} \mathbf{K}^T \sigma_a^{-1} \mathbf{K} &= \begin{pmatrix} 0 & 0 & 0 \\ \mathbf{I}_2 & 0 & 0 \\ 0 & 0 & 0 \\ 0 & \mathbf{I}_2 & 0 \\ 0 & 0 & 0 \\ 0 & 0 & \mathbf{I}_2 \end{pmatrix} \begin{pmatrix} \sigma_2^{-1} & 0 & 0 \\ 0 & \sigma_4^{-1} & 0 \\ 0 & 0 & \sigma_6^{-1} \end{pmatrix} \begin{pmatrix} 0 & \mathbf{I}_2 & 0 & 0 & 0 & 0 \\ 0 & 0 & 0 & \mathbf{I}_2 & 0 & 0 \\ 0 & 0 & 0 & 0 & 0 & \mathbf{I}_2 \end{pmatrix} \\ &= \begin{pmatrix} 0 & 0 & 0 & 0 & 0 & 0 \\ 0 & \sigma_2^{-1} & 0 & 0 & 0 & 0 \\ 0 & 0 & 0 & 0 & 0 & 0 \\ 0 & 0 & 0 & \sigma_4^{-1} & 0 & 0 \\ 0 & 0 & 0 & 0 & 0 & 0 \\ 0 & 0 & 0 & 0 & 0 & \sigma_6^{-1} \end{pmatrix}. \end{aligned} \quad (151)$$

Adding the two equations above yields  $\mathbf{L}$ :

$$\mathbf{L} = \text{diag} \left( \begin{pmatrix} \mathbf{B}_{11}^T \sigma_{11}^{-1} \mathbf{B}_{11} + \mathbf{B}_{12}^T \sigma_{12}^{-1} \mathbf{B}_{12} \\ \mathbf{B}_{21}^T \sigma_{21}^{-1} \mathbf{B}_{21} + \sigma_2^{-1} \\ \mathbf{B}_{31}^T \sigma_{31}^{-1} \mathbf{B}_{31} + \mathbf{B}_{32}^T \sigma_{32}^{-1} \mathbf{B}_{32} \\ \mathbf{B}_{41}^T \sigma_{41}^{-1} \mathbf{B}_{41} + \mathbf{B}_{42}^T \sigma_{42}^{-1} \mathbf{B}_{42} + \sigma_4^{-1} \\ \mathbf{B}_{51}^T \sigma_{51}^{-1} \mathbf{B}_{51} + \mathbf{B}_{52}^T \sigma_{52}^{-1} \mathbf{B}_{52} \\ \mathbf{B}_{62}^T \sigma_{62}^{-1} \mathbf{B}_{62} + \sigma_6^{-1} \end{pmatrix}^T \right) \quad (152)$$

Using this form of  $\mathbf{L}$  we can now find  $\mathbf{J}'$ :  $\mathbf{J}' = \sigma_x^{-1} - s^2 \sigma_x^{-1} \mathbf{B} \mathbf{L}^{-1} \mathbf{B}^T \sigma_x^{-1}$ .

In our example,  $\mathbf{J}'$  has a dimension of

$$\sum_{\nu=1}^2 2m_\nu \times \sum_{\nu=1}^2 2m_\nu = 20 \times 20 \quad (153)$$

From this equation we see that we first need to find the inverse of  $\mathbf{L}$ . Since  $\mathbf{L}$  is

block diagonal, its inverse is just the inverse of the individual block components.

$$L^{-1} = \text{diag} \left( \begin{pmatrix} (B_{11}^T \sigma_{11}^{-1} B_{11} + B_{12}^T \sigma_{12}^{-1} B_{12})^{-1} \\ (B_{21}^T \sigma_{21}^{-1} B_{21} + \sigma_2^{-1})^{-1} \\ (B_{31}^T \sigma_{31}^{-1} B_{31} + B_{32}^T \sigma_{32}^{-1} B_{32})^{-1} \\ (B_{41}^T \sigma_{41}^{-1} B_{41} + B_{42}^T \sigma_{42}^{-1} B_{42} + \sigma_4^{-1})^{-1} \\ (B_{51}^T \sigma_{51}^{-1} B_{51} + B_{52}^T \sigma_{52}^{-1} B_{52})^{-1} \\ (B_{62}^T \sigma_{62}^{-1} B_{62} + \sigma_6^{-1})^{-1} \end{pmatrix}^T \right) \quad (154)$$

So we get  $BL^{-1}B^T =$

$$\begin{pmatrix} B_{11} L_{11}^{-1} B_{11}^T & B_{11} L_{11}^{-1} B_{12}^T & 0 & 0 & 0 & 0 & 0 & 0 & 0 & 0 \\ B_{12} L_{11}^{-1} B_{11}^T & B_{12} L_{11}^{-1} B_{12}^T & 0 & 0 & 0 & 0 & 0 & 0 & 0 & 0 \\ 0 & 0 & B_{21} L_{22}^{-1} B_{21}^T & 0 & 0 & 0 & 0 & 0 & 0 & 0 \\ 0 & 0 & 0 & B_{31} L_{33}^{-1} B_{31}^T & B_{31} L_{33}^{-1} B_{32}^T & 0 & 0 & 0 & 0 & 0 \\ 0 & 0 & 0 & B_{32} L_{33}^{-1} B_{31}^T & B_{32} L_{33}^{-1} B_{32}^T & 0 & 0 & 0 & 0 & 0 \\ 0 & 0 & 0 & 0 & 0 & B_{41} L_{44}^{-1} B_{41}^T & B_{41} L_{44}^{-1} B_{42}^T & 0 & 0 & 0 \\ 0 & 0 & 0 & 0 & 0 & B_{42} L_{44}^{-1} B_{41}^T & B_{42} L_{44}^{-1} B_{42}^T & 0 & 0 & 0 \\ 0 & 0 & 0 & 0 & 0 & 0 & 0 & B_{51} L_{55}^{-1} B_{51}^T & B_{51} L_{55}^{-1} B_{52}^T & 0 \\ 0 & 0 & 0 & 0 & 0 & 0 & 0 & B_{52} L_{55}^{-1} B_{51}^T & B_{52} L_{55}^{-1} B_{52}^T & 0 \\ 0 & 0 & 0 & 0 & 0 & 0 & 0 & 0 & 0 & B_{62} L_{66}^{-1} B_{62}^T \end{pmatrix} \quad (155)$$

and substituting this into  $J' = \sigma_x^{-1} - s^2 \sigma_x^{-1} BL^{-1}B^T \sigma_x^{-1}$  yields

$$J' = \begin{pmatrix} J_{111} & J_{112} & 0 & 0 & 0 & 0 & 0 & 0 & 0 & 0 \\ J_{121} & J_{122} & 0 & 0 & 0 & 0 & 0 & 0 & 0 & 0 \\ 0 & 0 & J_{211} & 0 & 0 & 0 & 0 & 0 & 0 & 0 \\ 0 & 0 & 0 & J_{311} & J_{312} & 0 & 0 & 0 & 0 & 0 \\ 0 & 0 & 0 & J_{321} & J_{322} & 0 & 0 & 0 & 0 & 0 \\ 0 & 0 & 0 & 0 & 0 & J_{411} & J_{412} & 0 & 0 & 0 \\ 0 & 0 & 0 & 0 & 0 & J_{421} & J_{422} & 0 & 0 & 0 \\ 0 & 0 & 0 & 0 & 0 & 0 & 0 & J_{511} & J_{512} & 0 \\ 0 & 0 & 0 & 0 & 0 & 0 & 0 & J_{521} & J_{522} & 0 \\ 0 & 0 & 0 & 0 & 0 & 0 & 0 & 0 & 0 & J_{622} \end{pmatrix} \quad (156)$$

The notation above is as follows.  $J_{abc}$ ,  $a$  is the  $\mu$  number of the star,  $b$  and  $c$  are plate numbers. One can think of it as the  $b^{th}$  plate crossed with the  $c^{th}$  plate. For



example,  $\mathbf{J}_{112}$  is the  $\mu=1$  star on the first plate crossed with the second plate. As one can see  $\mathbf{J}_{212}$  does not exist, because the second star is not found on the second plate. In this example, this star is a reference star. In the equation above, the main diagonal terms

$$\mathbf{J}'_{abc} = \sigma_{rab}^{-1} - s^2 \sigma_{xab}^{-1} \mathbf{B}_{ab} \mathbf{L}_{aa}^{-1} \mathbf{B}_{ac} \sigma_{xac}^{-1} \quad (157)$$

and the off diagonal terms (where  $b$  does not equal  $c$ ) so  $\sigma_{rab}^{-1} = 0$ , equation (157) becomes

$$\mathbf{J}_{abc} = -s^2 \sigma_{xab}^{-1} \mathbf{B}_{ab} \mathbf{L}_{aa}^{-1} \mathbf{B}_{ac}^T \sigma_{xac}^{-1}. \quad (158)$$

As we stated earlier,  $\mathbf{J}'$  is not block-diagonal.  $\mathbf{J}'$  will have a  $2 \times 2$  block of nonzero elements only at the intersection of those line pairs and column pairs which belong to stars that were measured on the  $\nu^{\text{th}}$  as well as on the  $\mu^{\text{th}}$  frame.

### Determine a

Now we are ready to calculate the vector  $\mathbf{a}$ . From the overlap theory we have

$$\Xi^T (\mathbf{J}') (\mathbf{d} - \Xi \mathbf{a}) = 0$$

$$\Xi^T \mathbf{J}' \mathbf{d} = \Xi^T \mathbf{J}' \Xi \mathbf{a} \quad (159)$$

$$\mathbf{a} = \left( \Xi^T \mathbf{J}' \Xi \right)^{-1} \Xi^T \mathbf{J}' \mathbf{d}.$$

$$\Xi^T \mathbf{J} =$$

$$\begin{pmatrix} \Xi_{11}^T \mathbf{J}_{111} & \Xi_{11}^T \mathbf{J}_{112} & \Xi_{21}^T \mathbf{J}_{211} & \Xi_{31}^T \mathbf{J}_{311} & \Xi_{31}^T \mathbf{J}_{312} & \Xi_{41}^T \mathbf{J}_{411} & \Xi_{41}^T \mathbf{J}_{412} & \Xi_{51}^T \mathbf{J}_{511} & \Xi_{51}^T \mathbf{J}_{512} & 0 \\ \Xi_{12}^T \mathbf{J}_{121} & \Xi_{12}^T \mathbf{J}_{122} & 0 & \Xi_{32}^T \mathbf{J}_{321} & \Xi_{32}^T \mathbf{J}_{322} & \Xi_{42}^T \mathbf{J}_{421} & \Xi_{42}^T \mathbf{J}_{422} & \Xi_{52}^T \mathbf{J}_{521} & \Xi_{52}^T \mathbf{J}_{522} & \Xi_{62}^T \mathbf{J}_{622} \end{pmatrix} \quad (160)$$

$$\Xi^T \mathbf{J} \Xi = \begin{pmatrix} \Pi_{11} & \Pi_{12} \\ \Pi_{21} & \Pi_{22} \end{pmatrix} \quad (161)$$

where

$$\begin{aligned} \Pi_{11} &= \Xi_{11}^T \mathbf{J}_{111} \Xi_{11} + \Xi_{21}^T \mathbf{J}_{211} \Xi_{21} + \Xi_{31}^T \mathbf{J}_{311} \Xi_{31} + \Xi_{41}^T \mathbf{J}_{411} \Xi_{41} + \Xi_{51}^T \mathbf{J}_{511} \Xi_{51} \\ \Pi_{21} &= \Xi_{12}^T \mathbf{J}_{121} \Xi_{11} + \Xi_{32}^T \mathbf{J}_{321} \Xi_{31} + \Xi_{42}^T \mathbf{J}_{421} \Xi_{41} + \Xi_{52}^T \mathbf{J}_{521} \Xi_{51} \\ \Pi_{12} &= \Xi_{11}^T \mathbf{J}_{112} \Xi_{12} + \Xi_{31}^T \mathbf{J}_{312} \Xi_{32} + \Xi_{41}^T \mathbf{J}_{412} \Xi_{42} + \Xi_{51}^T \mathbf{J}_{512} \Xi_{52} \\ \Pi_{22} &= \Xi_{12}^T \mathbf{J}_{122} \Xi_{12} + \Xi_{32}^T \mathbf{J}_{322} \Xi_{32} + \Xi_{42}^T \mathbf{J}_{422} \Xi_{42} + \Xi_{52}^T \mathbf{J}_{522} \Xi_{52} + \Xi_{62}^T \mathbf{J}_{622} \Xi_{62} \end{aligned} \quad (162)$$

$\Xi^T \mathbf{J} \mathbf{d}$  is found by multiplying  $\Xi^T \mathbf{J}$  with the vector  $\mathbf{d}$ .

$$\begin{aligned} \Xi^T \mathbf{J} \mathbf{d} &= \\ &= \begin{pmatrix} \Xi_{11}^T \mathbf{J}_{111} d_{11} + \Xi_{12}^T \mathbf{J}_{112} d_{12} + \Xi_{21}^T \mathbf{J}_{211} d_{21} + \Xi_{31}^T \mathbf{J}_{311} d_{31} + \Xi_{32}^T \mathbf{J}_{312} d_{32} + \Xi_{41}^T \mathbf{J}_{411} d_{41} + \Xi_{42}^T \mathbf{J}_{412} d_{42} + \Xi_{51}^T \mathbf{J}_{511} d_{51} + \Xi_{52}^T \mathbf{J}_{512} d_{52} \\ \Xi_{12}^T \mathbf{J}_{121} d_{11} + \Xi_{12}^T \mathbf{J}_{122} d_{12} + \Xi_{32}^T \mathbf{J}_{321} d_{31} + \Xi_{32}^T \mathbf{J}_{322} d_{32} + \Xi_{42}^T \mathbf{J}_{421} d_{41} + \Xi_{42}^T \mathbf{J}_{422} d_{42} + \Xi_{52}^T \mathbf{J}_{521} d_{51} + \Xi_{52}^T \mathbf{J}_{522} d_{52} + \Xi_{62}^T \mathbf{J}_{622} d_{62} \end{pmatrix} \end{aligned}$$

Finally we are able to find the parameters  $\mathbf{a}$  from

$$\mathbf{a} = \left( \Xi^T \mathbf{J}' \Xi \right)^{-1} \Xi^T \mathbf{J}' \mathbf{d}. \quad (164)$$

From our earlier discussion  $\Xi^T \mathbf{J} \Xi$  does not have the same form as in the single plate case (i.e. block diagonal). In this case the matrix is banded bordered and there are simplifying routines to invert this matrix.

Determine  $\beta$

Now let's find  $\beta$  from

$$\beta = s \mathbf{L}^{-1} \mathbf{B}^T \sigma_x^{-1} (\mathbf{d} - \Xi \mathbf{a}) \quad (165)$$

$$sL^{-1}B^T\sigma_x^{-1} = \begin{pmatrix} L_{11}^{-1}B_{11}^T\sigma_{11}^{-1} & L_{11}^{-1}B_{12}^T\sigma_{12}^{-1} & 0 & 0 & 0 & 0 & 0 & 0 & 0 & 0 \\ 0 & 0 & L_{22}^{-1}B_{21}^T\sigma_{21}^{-1} & 0 & 0 & 0 & 0 & 0 & 0 & 0 \\ 0 & 0 & 0 & L_{33}^{-1}B_{31}^T\sigma_{31}^{-1} & L_{33}^{-1}B_{32}^T\sigma_{32}^{-1} & 0 & 0 & 0 & 0 & 0 \\ 0 & 0 & 0 & 0 & 0 & L_{44}^{-1}B_{41}^T\sigma_{41}^{-1} & L_{44}^{-1}B_{42}^T\sigma_{42}^{-1} & 0 & 0 & 0 \\ 0 & 0 & 0 & 0 & 0 & 0 & 0 & L_{55}^{-1}B_{51}^T\sigma_{51}^{-1} & L_{55}^{-1}B_{52}^T\sigma_{52}^{-1} & 0 \\ 0 & 0 & 0 & 0 & 0 & 0 & 0 & 0 & 0 & L_{66}^{-1}B_{62}^T\sigma_{62}^{-1} \end{pmatrix} \quad (166)$$

$$d - \Xi a = \begin{pmatrix} d_{11} \\ d_{12} \\ d_{12} \\ d_{31} \\ d_{32} \\ d_{41} \\ d_{42} \\ d_{51} \\ d_{52} \\ d_{62} \end{pmatrix} - \begin{pmatrix} \Xi_{11} & 0 \\ 0 & \Xi_{12} \\ \Xi_{21} & 0 \\ \Xi_{31} & 0 \\ 0 & \Xi_{32} \\ \Xi_{41} & 0 \\ 0 & \Xi_{42} \\ \Xi_{51} & 0 \\ 0 & \Xi_{52} \\ 0 & \Xi_{62} \end{pmatrix} \begin{pmatrix} a_1 \\ a_2 \end{pmatrix} \quad (167)$$

$$d - \Xi a = \begin{pmatrix} d_{11} - \Xi_{11}a_1 \\ d_{12} - \Xi_{12}a_2 \\ d_{21} - \Xi_{21}a_1 \\ d_{31} - \Xi_{31}a_1 \\ d_{32} - \Xi_{32}a_2 \\ d_{41} - \Xi_{41}a_1 \\ d_{42} - \Xi_{42}a_2 \\ d_{51} - \Xi_{51}a_1 \\ d_{52} - \Xi_{52}a_2 \\ d_{62} - \Xi_{62}a_2 \end{pmatrix}.$$

Finally,

$$\beta = \begin{pmatrix} sL_{11}^{-1}B_{11}^T\sigma_{11}^{-1}(d_{11} - \Xi_{11}a_1) + sL_{11}^{-1}B_{12}^T\sigma_{12}^{-1}(d_{12} - \Xi_{12}a_2) \\ sL_{22}^{-1}B_{21}^T\sigma_{21}^{-1}(d_{21} - \Xi_{21}a_1) \\ sL_{33}^{-1}B_{31}^T\sigma_{31}^{-1}(d_{31} - \Xi_{31}a_1) + sL_{33}^{-1}B_{32}^T\sigma_{32}^{-1}(d_{32} - \Xi_{32}a_2) \\ sL_{44}^{-1}B_{41}^T\sigma_{41}^{-1}(d_{41} - \Xi_{41}a_1) + sL_{44}^{-1}B_{42}^T\sigma_{42}^{-1}(d_{42} - \Xi_{42}a_2) \\ sL_{55}^{-1}B_{51}^T\sigma_{51}^{-1}(d_{51} - \Xi_{51}a_1) + sL_{55}^{-1}B_{52}^T\sigma_{52}^{-1}(d_{52} - \Xi_{52}a_2) \\ sL_{66}^{-1}B_{62}^T\sigma_{62}^{-1}(d_{62} - \Xi_{62}a_2) \end{pmatrix}. \quad (168)$$

This concludes the example.

## CHAPTER 5 OBSERVATIONS

### Observations for the Southern Polar Zone

The Southern Polar Zone plates were exposed between September 15, 1955 and August 7, 1956 at Sydney, Australia, where the Yale southern astrograph had been temporarily mounted. The focal length of the telescope is 206 cm and the lens is an 8-in Ross, stopped to 4-inches aperture to assure good definition at the plate edges. The measured plate area is  $11^{\circ} \times 11^{\circ}$  on 17-inch plates with a plate scale of  $100''/\text{mm}$ . An objective grating gave short first-order spectral images three magnitudes fainter than the primary, to be measured for the brighter stars. Exposure times ranged from three to ten minutes. In all, 93 plates were exposed on the 64 regions, but only the best plate on each region was selected for measurement. Dirk Brouwer exposed 60 of the plates on the 41 regions. The remainder of the plates were exposed by Harley Wood (21 plates) and his staff, W. H. Robertson (5 plates) and K.P. Sims (7 plates). Brouwer planned the observing program so as to provide that in each declination zone successive plates overlap 50% in right ascension and each declination zone also overlaps 50% (Hoffleit, 1971). This overlap pattern is illustrated in Figure 1. As one can see from the figures this arrangement provides that a star should occur on two plates for the

stars located at  $-70^\circ$ , whereas closer to the pole a star should be found on a minimum of 4 plates. Some stars occur on up to 20 different plates. This strong overlap feature is one the prime reason we are reducing this catalog.

### Measurement of Stars

The plates were measured between 1963 and 1965 with two different measuring machines. Between August 1963 and early 1965, eighteen of the twenty plates centered at  $-80^\circ$  were measured with a single screw Gaertner engine (equipped with a digitizer and automatic IBM key-punch). This machine was used for most of the Yale zone catalogs since 1932 and was designed by Schlesinger and described by him in Schlesinger and Barney (1933), and the remaining 46 plates were measured with a 2-screw Mann machine installed in 1965. This was a Type 880 Comparator, built to hold plates up to  $18 \times 18$  inches, equipped with a DATA LOGGER Model 1045 for automatically displaying the measured coordinates to the nearest micron and automatically transferring the coordinates to punched cards (Hoffleit, 1971).

Table 6 gives the plate center, epoch of observation, and measuring machine used for the 64 Yale plates.

Table 4: The Yale Plates

Plate	RA	Dec	Epoch	Engine	Plate	RA	Dec	Epoch	Engine		
1	0	0	-75	1955.79	M	33	9	36	-80	1956.05	G
2	1	0	-75	1955.86	M	34	10	48	-80	1956.28	G
3	2	0	-75	1955.93	M	35	12	0	-80	1956.27	G
4	3	0	-75	1955.88	M	36	13	12	-80	1956.28	G
5	4	0	-75	1956.01	M	37	14	24	-80	1956.50	G
6	5	0	-75	1956.03	M	38	15	36	-80	1956.51	G
7	6	0	-75	1956.03	M	39	16	48	-80	1956.30	G
8	7	0	-75	1956.02	M	40	18	0	-80	1956.30	G
9	8	0	-75	1956.05	M	41	19	12	-80	1956.43	G
10	9	0	-75	1956.05	M	42	20	24	-80	1956.78	G
11	10	0	-75	1956.10	M	43	21	36	-80	1956.79	G
12	11	0	-75	1956.28	M	44	22	48	-80	1956.79	G
13	12	0	-75	1956.28	M	45	0	0	-85	1955.79	M
14	13	0	-75	1956.50	M	46	1	30	-85	1955.86	M
15	14	0	-75	1956.27	M	47	3	0	-85	1955.88	M
16	15	0	-75	1956.45	M	48	4	30	-85	1956.02	M
17	16	0	-75	1956.45	M	49	6	0	-85	1956.03	M
18	17	0	-75	1956.43	M	50	7	30	-85	1956.09	M
19	18	0	-75	1956.43	M	51	9	0	-85	1956.10	M
20	19	0	-75	1956.43	M	52	10	30	-85	1956.11	M
21	20	0	-75	1955.72	M	53	12	0	-85	1956.28	M
22	21	0	-75	1955.78	M	54	13	30	-85	1956.28	M
23	22	0	-75	1955.79	M	55	15	0	-85	1956.28	M
24	23	0	-75	1955.79	M	56	16	30	-85	1956.45	M
25	0	0	-80	1955.88	M	57	18	0	-85	1956.45	M
26	1	12	-80	1955.78	G	58	19	30	-85	1955.70	M
27	2	24	-80	1955.88	G	59	21	0	-85	1955.70	M
28	3	36	-80	1955.88	G	60	22	30	-85	1955.79	M
29	4	48	-80	1956.03	G	61	0	0	-90	1955.78	M
30	6	0	-80	1956.02	G	62	6	0	-90	1956.05	M
31	7	12	-80	1956.03	G	63	12	0	-90	1956.28	M
32	8	24	-80	1956.05	G	64	18	0	-90	1956.43	M

Not all star images on the plates were measured. A list of target stars was chosen beforehand. These target stars to be measured were chosen from the Cape Photographic Durchmusterung (CPD, Gill and Kapteyn, 1899) to cover nine to ten stars per square degree. Following a suggestion of Heinrich Eichhorn, approximately 3000 mainly fainter stars, chosen from the Melbourne Astrographic Catalog, were added to the selection list in order to improve the astrometric accuracy by means of a more thorough investigation of the magnitude effect. For the stars north of  $-80^\circ$ , including stars as far north as  $-69^\circ$ , all of the stars in the

Cape Photographic Catalogue for 1950.0, zones  $-64^{\circ}$  to  $-80^{\circ}$  (Stoy, 1966) were included. For stars south of  $-80^{\circ}$  all the stars in the CPD were included, amounting to 50% more stars than are included in the corresponding Cape Photographic Catalogue for 1950.0, zones  $-80^{\circ}$  to  $-90^{\circ}$  (Stoy, 1968). Only about 10 percent of the selected faint stars were bright enough to also be in the CPD. According to the program originally envisioned by Brouwer, 11600 stars were to be measured. The original catalog lists 18702 stars of which 2891 are selected faint Melbourne stars. The limiting magnitude of the catalog is 13.6

Before the selected stars can be measured, predicted rectangular coordinates ( $x$ ,  $y$ ) for each star to be measured were computed from the right ascensions and declinations from the source catalogs and the positions of the plate centers. These positions were precessed to the equinox 1950.0 and whenever possible, proper motion corrections are applied to bring the predicted positions into the best possible agreement with the observed coordinates on the plates. For half of the stars south of  $-80^{\circ}$ , no proper motions are available. In case of the stars selected for the Melbourne Astrographic Catalogues, no right ascension and declination were given, only the measured rectangular coordinates on the Melbourne plates, and the plate constants. For these stars the plate constants and plate scale were used to find the rectangular coordinates.

On both measuring machines the operator using the predicted coordinates searched for the target stars and bisected the image, usually by manually operating

the screws. Once a setting had been achieved, the operator depressed a lever which automatically activated the keypunch to record the screw reading. The Gaertner machine has a single screw — so measures in  $x$  and  $y$  had to be made independently, with the plate rotated  $90^\circ$  in the machine for the  $y$ -reading after all the  $x$ -measurements were completed (Hoffleit, 1967). The Mann machine is a 2 screw measuring machine so both coordinates were recorded at the same time. Each plate was measured only once in each coordinate. In accordance with Schlesinger's precepts (Schlesinger and Barney, 1933) alternate regions (odd numbered) were measured "direct", i.e., in order of increasing right ascension; the other (even numbered) were measured "reversed". This was done to reduce systematic errors.

Many of the selected faint stars were evidently too faint to be measurable on the Yale plates. Occasionally two stars were found close to the predicted coordinates for one star. Many of these were faint stars. In these cases both positions were measured and given the same CPD number with an additional designation of 1 or 2. Many program stars had to be omitted because of overlapping images. Nearly 100 secondaries of double stars were measured in order to avert the possibility of misidentification of the components. These stars were also given the same CPD number with a designation of 1 or 2. Since the plates were taken through an objective grating, the bright stars in the field all have first-order spectral images that are three magnitudes fainter than the central image.



In these cases all 3 positions were given the same CPD number with a designation of 0 for the central image, 1 for the 2 primary images and 2 for the first order images. Higher-order spectral images, even when present, were not measured. For the fainter stars on our program, the spectral images are not visible. The measurer decided in every case in the course of measuring which spectral images are suitable to be measured. From an analysis of the percentages of stars of successively fainter magnitude for which spectral images have been successfully measured at the Yale engine, Dorrit Hoffleit found only a small number of stars as bright as  $8.0^m$  for which the spectra were not measurable, whereas very few stars as faint as  $9.0^m$  have measurable spectra. A practical magnitude limit seemed to be  $8.3^m$  (Hoffleit, 1962).

### Magnitude System

No photometry was performed on the images, so the magnitudes of the stars were taken directly from the input catalogs. In fact, the magnitudes as well as color indices and spectral types were taken from the input catalog, the CPD and the Cape Zone Catalogues. In the case of the faint stars where the input catalog was the Melbourne catalog in which only image diameters are given, the stars's magnitudes were derived from the published image diameters on the Melbourne plates and calibrated according to the reduction tables included in the Melbourne Astrographic Catalogs, having a limiting photographic magnitude of 13.0

## CHAPTER 6

### PLATE REDUCTIONS

#### Reference Catalog

As we stated in Chapter 1, in order to reduce photographic plates a set of reference stars must be used whose images are on the plate. The adopted reference catalog is the United States Naval Observatory's International Reference Star Catalog (IRS, Corbin, 1991), provided in two versions FK4/B 1950 and FK5/J2000. The IRS is an all-sky catalog of positions and proper motions that is based on the AGK3R (Corbin 1977, 1978) in the northern hemisphere and the newly completed SRS (Southern Reference Stars, Smith et al. 1990) in the south. The IRS has a density of 1 star/deg<sup>2</sup> with most of the stars primarily in the magnitude range 7<sup>m</sup>.0 to 9<sup>m</sup>.0. It was compiled by matching 122 meridian circle catalogs with the AGK3R and the SRS to provide the base. South of  $-60^\circ$ , the IRS, has a mean error in position of 0".09 and 0".10 for right ascension and declination, respectively. The mean errors in proper motion are  $\pm 0.50$  arcsec per century and  $\pm 0.51$  arcsec per century in right ascension and declination, respectively. We have the fortunate occurrence that the mean epoch of the reference catalog ( 1956.6 for right ascension and 1954.4 for declination) falls extremely close to the average

epoch of the Yale observations, 1956.13. Because of this short time interval, the errors on the IRS proper motions can be neglected.

In order to determine which images on the plate are IRS stars, we applied proper motions to the IRS stars to the average epoch of Yale Observations, determined the standard coordinates by the gnomonic projection, and then determined preliminary  $x$  and  $y$  values by using plate parameters determined from the original reduction by Ľu. However, while the original solution used a 20-constant model (see equation 175), we only used the constants corresponding to the 6-constant model. After a preliminary match of the reference stars using these approximate plate parameters, we performed a single plate adjustment determining more accurate plate parameters, and with these improved plate parameters we then re-matched the reference stars. A total of 1121 IRS stars were found on the plates, with an average of approximately 70 IRS stars per plate. If we were only doing a single plate reduction, we would first apply the proper motions to the IRS stars to bring them to the epoch of each plate, find the matches, and perform the adjustment at the epoch of each plate. However, this leaves the positions determined from the reduction process dependent on which plate they are photographed on. A star found on different plates will have different positions depending on the epoch of the observation, again causing a problem for the overlap solution. Since we have a short time interval between the epochs of observation of Yale plates (maximum 0.83 years) we assumed the proper motion over this time to be

negligible and simply apply the proper motion of the stars to bring them to the average epoch of the plates.

Though there are other denser reference catalogs —ACRS and the PPM— both of these catalogs are compilation catalogs and contain the original positions from Yale catalog, so their use as a reference catalog would have been circular and introduced correlations.

### External Catalog

In order independently to analyze the results we use an external reference catalog, the 90,000 Star Supplement to the Positions and Proper Motions Supplement Catalog (we refer to this catalog as, PPM-S, Roeser, et al., 1993). These stars are *not* used in the plate reduction. We chose the PPM-S because it is one of the few reference catalogs in the southern celestial hemisphere which is dense and accurate enough to give us a meaningful estimate of the accuracy of our results and which was not compiled using the original Southern Polar Zone Catalogue. The mean error in position (at the average epoch of the Yale plates) for those PPM-S stars located on plates is 0."097 in right ascension and 0."094 in declination. The mean epoch for these stars is 1951.64 for right ascension and 1951.65 for declination. Once again, we have the favorable circumstance that the mean epoch of the catalog is close to the mean epoch of the Yale plates, so proper motion errors (0."34 and 0".33, for right ascension and declination, respectively)

can be considered negligible. Using the same procedures for the reference stars we found 8,768 PPM-S stars on the Yale plates, with an average of 150 PPM-S stars per plate.

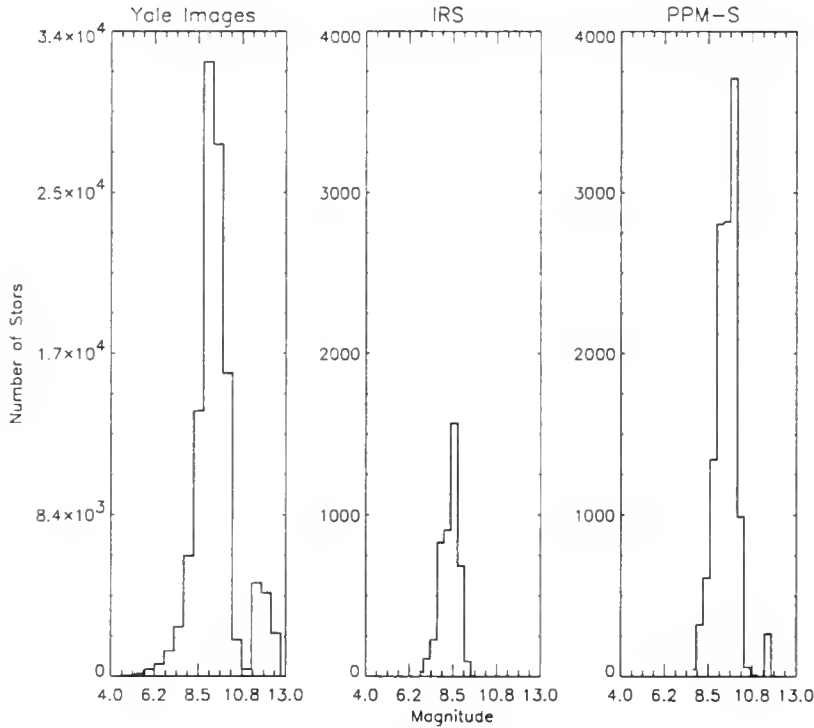


Figure 10: Distribution of Magnitudes

PPM-S stars are used as an external check on the accuracy of our solution in both the single plate and overlap reductions. After a plate reduction we calculate the right ascension and declination of these stars using the measured  $x$  and  $y$  values, the plate parameters, and a gnomonic projection. We then compare these calculated positions to the cataloged positions, subtracting in quadrature the mean

error of the PPM-S star positions. This gives a independent check on our solution.

One problem of using an external catalog as a check on the solution is that since the reference catalog is the IRS, the plate parameters establish a system based on the IRS reference system. There will inevitably be small systematic effects between the PPM-S and the IRS reference systems. When using an external catalog the difference between the cataloged right ascension and declination and the values calculated with the plate constants will be made up of two parts: a small part which represents the difference between the reference catalog, and a larger part which determines how accurate our positions are. The majority of the stars in the PPM-S are fainter than those in the IRS. The average magnitude of the Yale stars is  $9.^m64$ , for the PPM-S it is  $9.^m57$ , and for the IRS stars it is  $8.^m31$ . In fact the distribution of the magnitudes is very similar between the PPM-S and the Yale stars (see Figure 10). This is good from the standpoint that most of the Yale stars are fainter than the IRS stars so we can probe a magnitude effect better with the PPM-S. However, from the standpoint of comparing the results this difference in magnitude may introduce a magnitude effect into our comparison. The PPM-S does not contain any stars that are also in the IRS catalog, therefore it is difficult to check for systematic differences between the reference systems. Because the PPM-S is an extension of the PPM system, we can use the PPM (which contains stars that also appear in the IRS catalog) as a check of systematic differences. It is probably safe to say that the PPM and PPM-S are based on the same system.

We compared 1804 stars in common between the PPM and IRS catalogs for the  $-60^\circ$  to  $-90^\circ$  region. After proper moving both catalogs to the average epoch of the plates we found a difference of  $-0.''0072$  and  $-0.''0049$  in right ascension and declination, respectively. So we can safely use the PPM-S as an external check on our solution since these differences are at least a factor of 10 below the mean error of the PPM-S.

### Determining the Plate Model

The choice of the model is one of the most important steps in reducing photographic plates. With  $11^\circ \times 11^\circ$  plates the relationship between the measured and standard coordinates can be rather complex. The model will invariably not account for all of the contributing effects. Our task is to determine the model that best represents the physical situation. We start out by making an adjustment using a simple 6-constant model, plot the residuals to check for correlations, and then add terms to the model in an attempt to eliminate the correlations. We analyzed common optical effects such as coma and optical distortion, and other possible errors producing a non-orthogonal system, such as plate tilt and rotation. We must be careful when analyzing the terms to be included in the model and include terms for which we have a "physical" understanding. In Chapter 2 we pointed out that many of the effects we are trying to model often produce similar and/or correlated terms in the model and therefore it is difficult, if not impossible, to



separate different contributions and evaluate the physical meaning of the plate parameters in detail. In addition, we have the problem of parameter variance: when the number of parameters is large, an unfavorable error propagation of the resulting star positions in the plate field due to the random errors in the  $x,y$  measurements and the reference star positions is introduced (Eichhorn & Williams 1963). Our approach for the plate reduction is therefore to set up a minimal plate model by taking the physical meaning of the plate parameters into consideration and applying known transformations and corrections to the  $x,y$  measurements a priori. This minimal plate model then is restricted to describe the properties of the mapping and measuring process.

### Single Plate Reduction

We first determine the model using single plate adjustments. The starting point is the basic 6-constant model (Chapter 2) and terms are added to this model appropriately. We perform a weighted least squares reduction, pre-correcting the  $x,y$  positions of the measured stars for refraction. The weights for the reference stars' equatorial coordinates are taken from the reference catalog, and for the measurement errors we first assumed an approximation of 4 microns. Later we use a more sophisticated method for determining the measuring errors. Since the single plate adjustment only uses the reference stars, reference stars with large residuals (this could be due to bad matches) will significantly effect the results.



After the adjustment we determined the residuals using the newly determined plate parameters. All reference stars with residuals greater than 3 standard deviations from the mean were eliminated and a new reduction was performed. In total three adjustments were done. The first two were for the purpose of removing high residual stars, and the last reduction determined the final plate parameters. Using this scheme we were able to improve upon the precision of our solution by only removing a few stars. For example, in the case of the 13-constant model adjustment we started with 4510 measurements, and by the last adjustment we had eliminated 137 measurements, most of these come from a handful of plates, and the average number of reference stars was 68 per plate. In all iterations, the catalogued right ascension and declination values were used in the reduction; we did *not* iterate on the solution.

After every reduction we used the reference stars and the PPM-S stars and compared the cataloged right ascension and declination with the computed values. The average rms for a single measurement for some of the different reductions we performed are given in Table 5. We want to point out that these values are actually the precision of a single measurement and not the averaged position. Since – on the average– a star is imaged on 6.97 different plates, we expect that after the average positions of each star is found these values will decrease by  $\frac{1}{\sqrt{6.97}}$ . So in the case of the 13-constant single plate adjustment the rms values for average position should roughly be (from the above reasoning) 0."22 for right

ascension and declination.

Table 5: Single Plate RMS Results

<u>Model</u>	<u>IRS REF RMS</u>	<u>PPM-S EXT</u>
6-constant	RA : 0." 67	0." 93
	DEC: 0." 66	1." 00
8-constant	RA : 0." 46	0." 66
	DEC: 0." 49	0." 71
13-constant	RA : 0." 41	0." 58
	DEC: 0." 43	0." 62
15-constant	RA : 0." 40	0." 55
	DEC: 0." 42	0." 57
18-constant	RA : 0." 39	0." 59
	DEC: 0." 42	0." 62
20-constant	RA : 0." 42	0." 70
	DEC: 0." 44	0." 72

Besides checking the cataloged positions against the computed positions we determined the best model by computing the following residuals for the reference stars:

$$\begin{pmatrix} \Delta x \\ \Delta y \end{pmatrix} = \begin{pmatrix} x_m \\ y_m \end{pmatrix} - \begin{pmatrix} x_c \\ y_c \end{pmatrix} \quad (169)$$

where  $x_m$  and  $y_m$  are the measured  $x$  and  $y$  values (pre-corrected for refraction) and  $x_c$  and  $y_c$  are calculated from the cataloged using the plate parameters. We use

these residuals to determine if we need to add terms to the model. The residuals are plotted against possible terms which we might want to add to our model. If we find a correlation, then we add the term or terms to the model and re-run the plate reduction, determining new plate parameters and then replotting the graphs. The terms we looked at are :

$$\begin{aligned} & x, y, xy, x^2, y^2, (x^2 + y^2), x(x^2 + y^2), y(x^2 + y^2), \\ & m, mx, my, mx^2, my^2, m^2, m^2x, m^2y, ci, x^3, y^3, x^2y, y^2x \end{aligned} \quad (170)$$

where  $m$  is magnitude and  $ci$  is the color index. These terms allow us to check for coma, radial distortion, magnitude effects, and other second and third order effects.

Figures 14–18 are the residuals for the 6–constant model for all the reference stars on all the plates (after a 3 sigma elimination test). A third degree polynomial was fit to the points, for the purpose of analyzing the trends in the data. The left-hand side of the plots are for  $dx$  and right-hand side for  $dy$ . From these figures we can make the following conclusions: there is a strong correlation of  $dy$  with  $y$ , there is a strong indicator for the inclusion of a plate tilt term because  $dx$  is correlated with both  $xy$  and  $x^2$  and  $dy$  is correlated with  $xy$  and  $y^2$ , and there also is a good indication that a distortion term should be included because of the correlation of both  $dx$  and  $dy$  with  $x(x^2 + y^2), y(x^2 + y^2)$ . Because of the complicated way the residuals interact we will say nothing else about the other plots until we have included the above terms.

In Figures 19–23 we included the terms only for plate tilt. This model is an 8–constant model has the form

$$\Xi = \begin{pmatrix} \xi & \eta & 1 & 0 & 0 & 0 & \xi^2 & \xi\eta \\ 0 & 0 & 0 & \xi & \eta & 1 & \xi\eta & \eta^2 \end{pmatrix}. \quad (171)$$

This dramatically improved the results and demonstrates the cross interaction these terms have on one another. However, there is still a radial distortion term that should be included. Using a 13–constant model (equation 172) we included the radial distortion term and split the second order effects for both dx and dy, see figures 24–28. This model has the form:

$$\Xi = \begin{pmatrix} \xi & \eta & 1 & 0 & 0 & 0 & \xi^2 & \xi\eta & \eta^2 & 0 & 0 & 0 & \xi(\xi^2 + \eta^2) \\ 0 & 0 & 0 & \xi & \eta & 1 & 0 & 0 & 0 & \xi^2 & \xi\eta & \eta^2 & \eta(\xi^2 + \eta^2) \end{pmatrix}. \quad (172)$$

Though we added a term for radial distortion the residual plots for this term still show a systematic trend. However, this is probably due to the interaction of the  $x^2y$  and  $y^2x$  terms. After adding these terms to the 13–constant model we have a 15–constant model of the form

$$\Xi = \begin{pmatrix} \xi & \eta & 1 & 0 & 0 & 0 & \xi^2 & \xi\eta & \eta^2 & 0 & 0 & 0 & \xi(\xi^2 + \eta^2) & \xi(\xi\eta) & 0 \\ 0 & 0 & 0 & \xi & \eta & 1 & 0 & 0 & 0 & \xi^2 & \xi\eta & \eta^2 & \eta(\xi^2 + \eta^2) & 0 & \eta(\xi\eta) \end{pmatrix}. \quad (173)$$

From the residual plots (figures 29–33) we have graphed, we see that all the correlations are essentially eliminated:

We tested many different models, including an 18–constant model which added first-order magnitude terms to the 15–constant model:

$$\Xi = \begin{pmatrix} \xi & \eta & 1 & 0 & 0 & 0 & \xi^2 & \xi\eta & \eta^2 & 0 & 0 & 0 & \xi(\xi^2 + \eta^2) & \xi(\xi\eta) & 0 & (m - m_0) & 0 & \xi(m - m_0) \\ 0 & 0 & 0 & \xi & \eta & 1 & 0 & 0 & 0 & \xi^2 & \xi\eta & \eta^2 & \eta(\xi^2 + \eta^2) & 0 & \eta(\xi\eta) & 0 & (m - m_0) & \eta(m - m_0) \end{pmatrix} \quad (174)$$

and the original 20-constant model adopted by Lü:

$$\Xi = \begin{pmatrix} \xi & \eta & 1 & 0 & 0 & 0 & \xi^2 & \xi\eta & \eta^2 & 0 & 0 & 0 & (m - m_0) & 0 & (m - m_0)\xi & 0 & (c - c_0)\xi & 0 & (m - m_0)\eta & 0 \\ 0 & 0 & 0 & \xi & \eta & 1 & 0 & 0 & 0 & \xi^2 & \xi\eta & \eta^2 & 0 & (m - m_0) & 0 & (m - m_0)\eta & 0 & (c - c_0)\eta & 0 & (m - m_0)\xi \end{pmatrix} \quad (175)$$

However, we have only shown the residual plots for 20-constant model Figures 34–38). We determined that the “best” model for the single plate solutions was the 15-constant model. From Table 5 we can see that this model gives the smallest rms and basically removes all the systematic trends in the residual plots. However, the difference between this model and the 18-constant model is quite small. The main difference between these two models is with the magnitude terms. The magnitude range of the IRS catalog is roughly 2 magnitudes ( $7^m$ – $9^m$ ), [see Figure 10], and with this small range it is difficult to test for a magnitude term. The situation will improve for the overlap solution, where all the stars are used in the reduction, so our magnitude range increases to 5 magnitudes ( $7^m$ – $12^m$ ) and the usage of the grating images allows us to explore magnitude effect in greater detail. For this reason and the desire to have as few plate parameters as needed we chose the 15-constant model to determine the positions for the single plate solution. We found that our model fit the data better than the 20-constant model adopted by Lü. We did not find any justification for the inclusion of the magnitude nor color terms.

### Final Positions from the Single Plate Solution

As we stated before, the major problem with the single plate approach is that a star located on  $n$  different plates has  $n$  different position estimates. In Figure 11 we demonstrated this by comparing the positions from plates 1 and plate 24 (top) and plates 1 and 25 (bottom) after a single plate reduction using the plate constants from a 15-constant model. In Figure 12 we show three of the polar plates, plate 61 overlapped with plate 64 and plate 62 overlapped with 63. In the bottom left hand corner a scale of 2 arcseconds is given. The values given on the upper right are the average standard deviation in the positions from the two different plates. RMS ALL is the average difference in the position. In other words, it is the average length of the lines. The plates overlapped with plate 1 have on the average about 0."8 difference in position, while for the polar plates we have closer to 1". Though these differences appear large, these are the individual differences in position from one plate to the other and not the difference between the individual value and the average value.

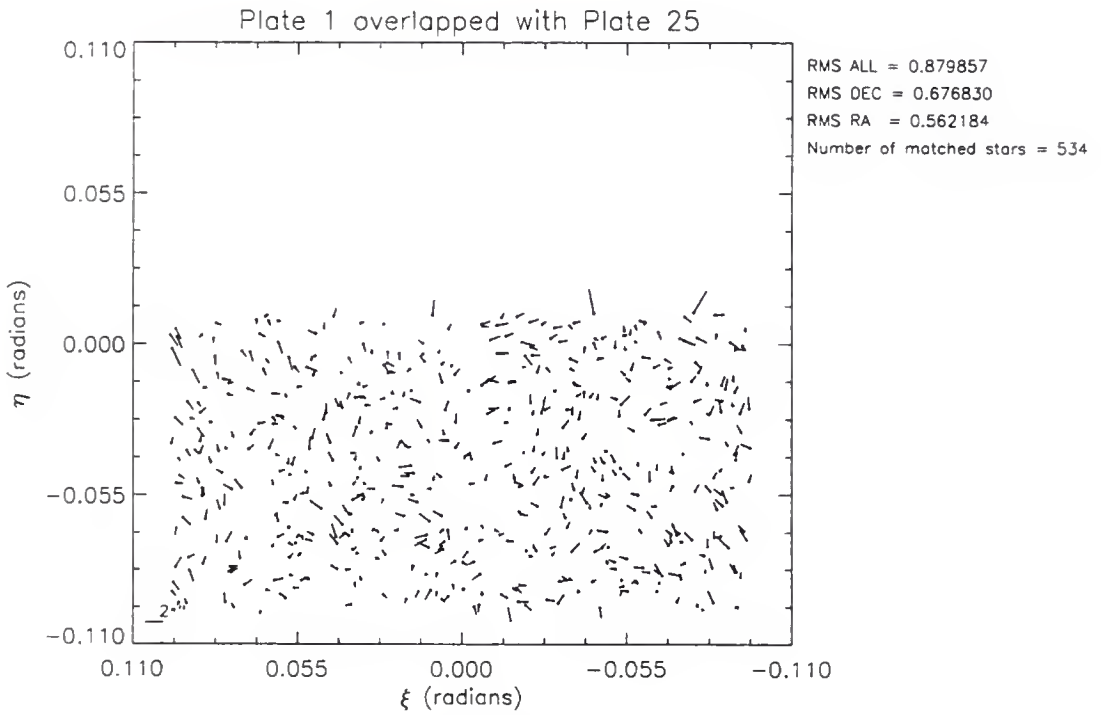
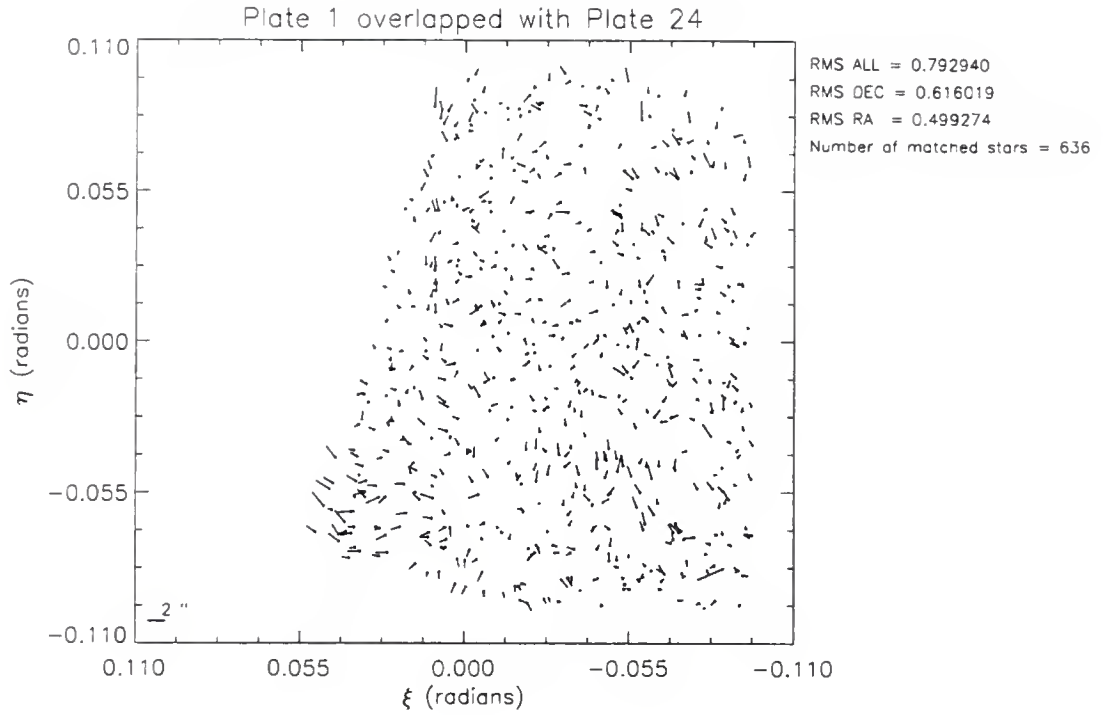


Figure 11: The different in positions found from the single plate adjustment for plates 1 and 24 and plates 1 and 25.

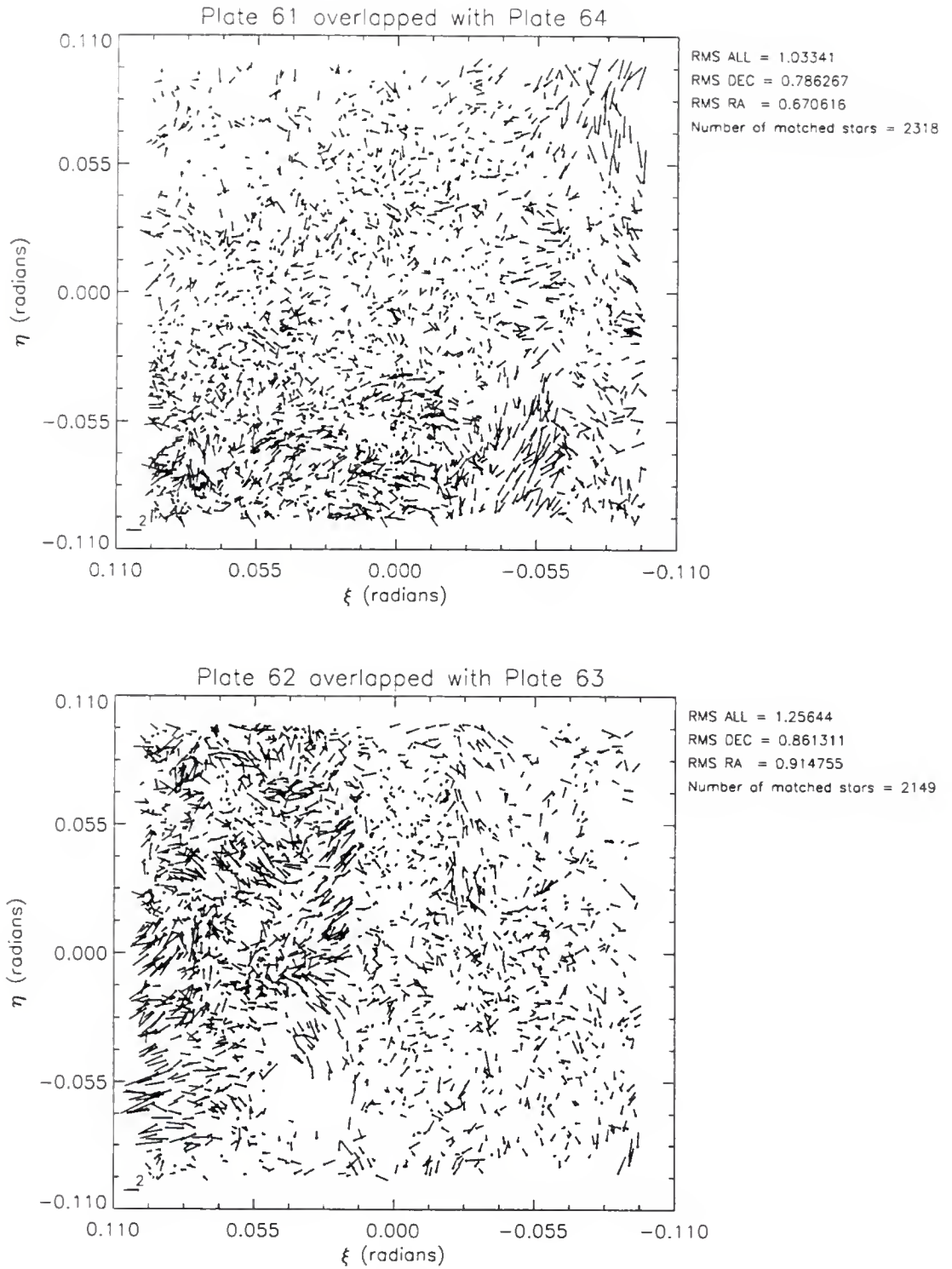


Figure 12: The different in positions found from the single plate adjustment for plates 61 and 64 and plates 62 and 63.



After determining all the stars' equatorial coordinates (using the plate parameters from the single plate adjustment) we then matched the images of the same star on different plates and averaged these positions together. This step is probably the most frustrating and time consuming. The data for the Yale plates were measured on semi-automatic measuring machines and much of the information concerning the observations and measuring has been lost. A great deal of time (and patience) was required in cleaning up this data and matching the star images. When the plates were measured there were hundreds of "possible target stars" which were close to the program stars and therefore were measured in addition to the probable target star to avert any confusion. Part of the "cleaning" process involved determining which of these measurements were truly images of the intended program stars. We also had to eliminate other images either because they were imperfections on plate, bad measurements or repeated measurements. In addition there were numerous cases where only one measurement was given or where the magnitude of a star was definitely incorrect. We deleted the images with only one measurement and corrected the magnitudes by cross referencing them with the CPD catalog.

The choice for the matching tolerance, of course, determines which images we call the same star. It is extremely important to correctly match the images of the same stars from different plates. If there is too low a matching tolerance, then not all the images of the same star will be matched together and this will result

in artificially increasing the total number of stars we determine. If we have too high a tolerance then “bad” data and images which really belong to other stars will be combined together. This will artificially decrease the total number of stars we determine and weaken the solution.

In total there are 124,229 star images of 17506 stars. We found 3831 stars were averaged together because they were measured twice by accident and 1600 possible double stars which were removed. We do not want to include double stars in the overlap solution so we removed them and treat these stars separately. There were a number of images that were on only one plate (2,752) either because they occurred at the borders of the Southern Polar Zone (so they are only imaged on one plate) or they were simply bad data points. These measurements are not used in the overlap solution. Their positions are determined from the plate parameters after the overlap solution.

After cleaning the data and matching and averaging the images together we compared the average position with the individual values from the plates and found the rms in right ascension to be 0."54 and in declination 0."55. These values are the precision of the individual measurements and are consistent with the values from Table 5.

We also compared our averaged single plate position with those found in the PPM-S catalog. For 1874 stars in common we obtained an rms in right

ascension of  $0''.28$  and in declination  $0''.32$ . After quadratically subtracting the error due to the PPM-S we get  $0''.26$  and  $0''.31$ , for right ascension and declination, respectively. These values are roughly the mean error in our positions after the single plate solution.

### Overlapping Plate Reduction

As we stated earlier an overlap adjustment uses all the stars that either occur on more than one plate or are reference stars. This dramatically increases the number of observations used in the adjustment. In the case of the single plate method we had roughly 70 reference stars per plate; however, now we have 124,229 star images of 17,506 stars greatly increasing the computational effort.

Besides using the PPM-S stars as a means of evaluating the accuracy of our solution we also randomly pulled approximately 10 IRS stars on each plate which were flagged not to be used as a reference stars. So as not to confuse these stars with IRS reference stars we call these flagged stars “external” IRS stars. After every reduction we use the reference stars, external IRS stars and the PPM-S stars and compare the cataloged right ascension and declination with the computed ones. The average for all the plates of the rms values for some of the different reductions we performed is given in Table 6

As in the single plate analysis we tested various different models, starting with the 6-constant model and adding terms appropriately. In this case we iterated on

the solution three times; after every iteration we added the correction to the positions to the field stars, but not the reference stars. In addition, instead of assuming a measuring error of 4 microns we used a measuring error dependent on magnitude. The measuring error associated with a measuring machine depends on how precisely the measuring machine can determine the center of the image. If the image is large (i.e., a bright star) or if the image is very small (i.e., a faint star) the center is difficult to determine. Therefore, bright and faint stars generally have a larger measuring error associated with them. Every measuring machine has its own characteristic range of image diameters where its measuring error is at a minimum. In order to find a relationship to characterize the magnitude-dependent measuring error we used the stars in the PPM-S and the PPM. Here we have included the stars in the PPM because they are brighter than the PPM-S and we want to adequately cover the entire magnitude range found on the plates. We calculated the predicted  $x$  and  $y$  values for the stars in these catalogs and compared them to the measured  $x$  and  $y$  values and subtracted the error in the positions from the reference catalog. We have assumed that most of the remaining error is due to measuring error and not systematic errors remaining from incorrect modeling. In this case, we used the plate parameters that included terms for linear magnitude effects so that our results would not be corrupted by a magnitude term. Since the plates were measured on two different measuring machines we performed the analysis separately for each. We fit a third-degree polynomial through the points

and used this as our function to estimate the measuring error for the overlap reduction. The graph of these results is shown in Figure 13 (after the points were binned). The binned points are shown as circles — with large circles indicating few points are contained in the final binned point and small circles indicating a large number of points make up the binned point. The function representing the magnitude-dependent measuring error for the two machines is roughly the same. However, for determining the measuring error for the overlap we used the function corresponding to the appropriate measuring machine.

One other change we made for the overlap reduction was the inclusion of the grating images for the purpose of eliminating magnitude effects. There are 6901 stars with grating images. With ideal magnitude-independent imaging, the primary stellar image will be at the average of the first order images positions. Coma and magnitude effects will cause deviations from an exact agreement of the average of the grating images and the primary image. By examining this deviation we can model the magnitude dependent terms. The stars with grating images are brighter than the average field stars ( $m < 9.0$ ) and the grating images themselves are three magnitudes fainter than the primary. Therefore we can use the grating image information to ensure that any magnitude effects are equally modeled for the whole stellar magnitude range (i.e.  $9^m$  to  $12^m$ ). We do this by averaging the x and y positions of the grating images and assign a fictitious star to the average which is also three magnitudes fainter than the primary and has the same right

ascension and declination as the primary. We treat data for these fictitious stars as additional information in the overlap, but in the theoretical framework of the overlap solution they are treated as the same star as the primary.

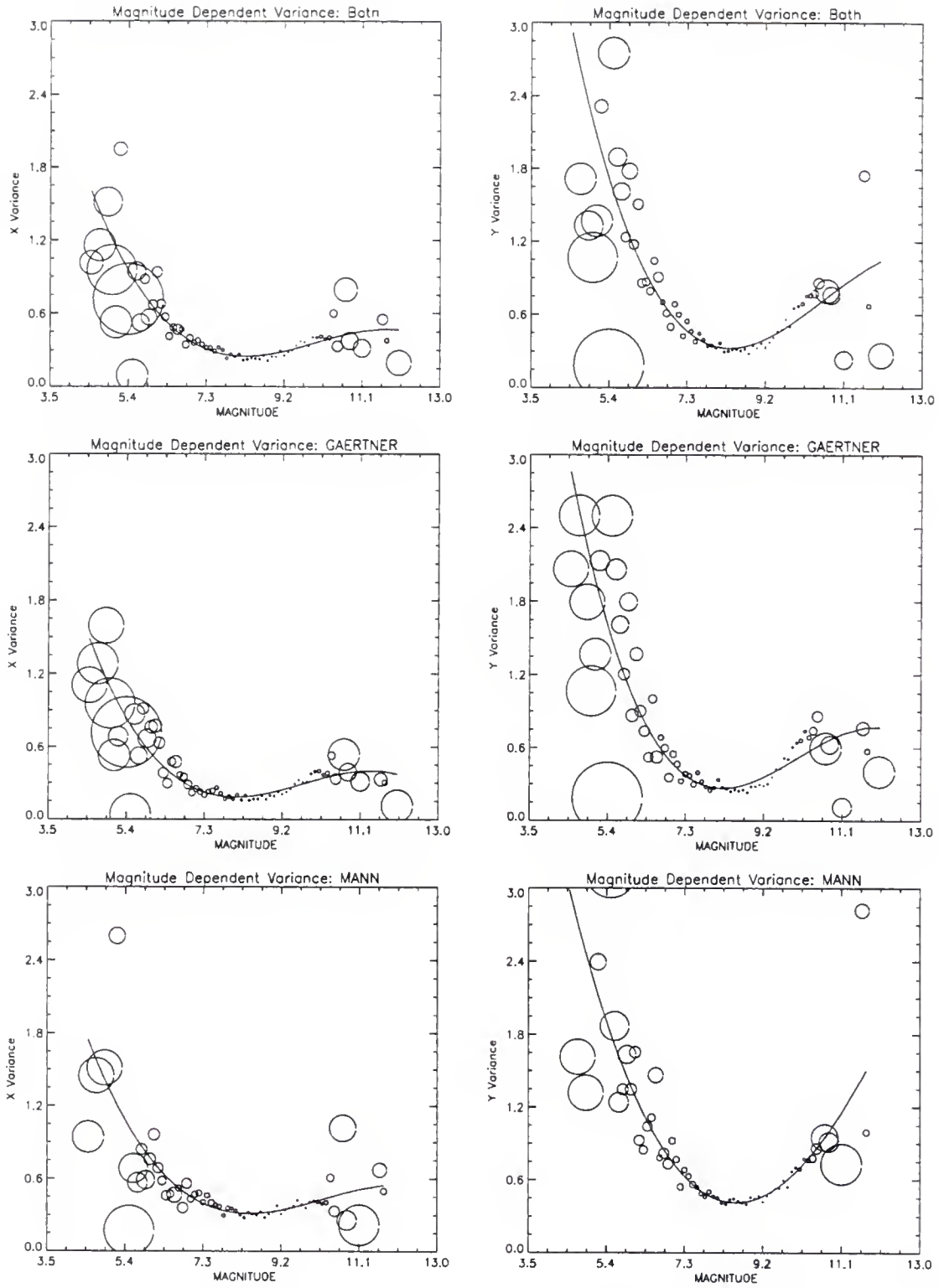


Figure 13: Magnitude Dependent Measuring Error,  
the units of the variances are arcseconds squared.

Table 6 lists the results of some of the models. The columns 2–4 are the rms values of comparing the position determined from the plate parameters to the position from a reference catalog. The reference catalogs are as follows: IRS REF the IRS stars used in the reduction, IRS EXT, the IRS stars not used in the reduction, PPM–S IND the PPM–S compared to the individual value, and PPM–S AVE the PPM–S compared to the average position. The last columns is the comparison of a star to its individual plate values.



Table 6: Overlap Plate RMS Results

<u>Model</u>	<u>IRS REF</u>	<u>IRS EXT</u>	<u>PPM-S IND</u>	<u>PPM-S AVE</u>	<u>IND to AVE</u>
6-constant	RA: 0." 84	0." 72	0.87"	0.51"	0."72
	DEC:1.32	1." 13	1".48	1." 22	0." 76
8-constant	RA: 0." 50	0." 41	0." 61	0." 33	0." 52
	DEC: 0." 54	0." 33	0." 66	0." 37	0." 56
13-constant	RA: 0." 45	0." 38	0." 53	0." 28	0." 46
	DEC: 0."48	0." 34	0." 56	0." 32	0." 49
15-constant	RA: 0." 42	0." 35	0." 50	0." 24	0." 43
	DEC: 0."43	0." 31	0." 53	0." 29	0." 46
18-constant	RA: 0." 41	0." 35	0." 49	0." 24	0." 43
	DEC: 0."43	0." 31	0." 51	0." 27	0." 46

Since in the single plate adjustment each solution was dependent on only 60–70 observations, the solutions could be somewhat loose and therefore some of the systematic effects could be hidden in the noise. In the case of an overlap solution the restriction that a star have the same position from plate to plate makes the solution much stronger and the systemic effects more noticeable. The residual plot for the overlap solution only contains the weighted least squares curve and not the actual data points (with 124,229 images the graphs would have been black bands). We did not include the residual plots for the 6 or 8–constant model. The systematic trends for these graphs are similar to the single plate results: after a reduction with a 6–constant model the residual plots showed a strong indication for the inclusion of full second order terms and radial distortion. The 8–constant model improved the situation but a distortion term still needed to be included. Following the procedure from the single plate we tested the main models including our 13–constant (Figures 39–42) 15 (Figures 43–46) and 18–constant models (Figure 47–50).

### Conclusions

From Table 6 we can see that the 15–constant and 18–constant model give roughly the same values. However, we feel that the coma term and linear magnitude terms should be included. First of all, it is very likely that with such large plates ( $11^\circ \times 11^\circ$ ) a coma term, though small, exists. In addition,

technically since we have included the grating images as additional information, not including a magnitude term like coma will probably add to the noise of the other parameters. A linear magnitude term corrects for guiding error which can vary greatly from plate to plate. Though this coefficient might be near zero on most of the plates, it is wise to include it in case it is large on a few plates. Though we are not as limited in the single plate case to keep the number of parameters to the absolute minimum, including too many terms will cause problems in our inversion process, leading to either a non-invertible matrix or at best a poorly determined matrix. From Table 6 and the residual plots we decided the “best” model was the 18-constant model. Using this model we determined the positions for all the stars and in Tables 7 and 8 we compared our results for the single plate and overlap solutions.

Table 7: RMS Single Plate Comparisons: 15-constant model

	<u>RA (")</u>	<u>DEC (")</u>
IRS REF TO IND	0.40	0.42
PPM-S TO IND	0.55	0.57
PPM-S TO AVE	0.27	0.29
IND TO AVE	0.54	0.55

Table 8: RMS Overlap Plate Comparisons: 18-constant model

	<u>RA (")</u>	<u>DEC (")</u>
IRS REF TO AVE	0.41	0.43
PPM-S TO IND	0.49	0.51
PPM-S TO AVE	0.24	0.27
IND TO AVE	0.43	0.46

The 18% improvement in the precision of the average position over that the individual measurement between the overlap and single solutions shows an improvement in the precision of positions due to a stronger adjustment producing better determined plate parameters. In the original reduction quoted this value at 0."55. The original reduction used the Second Cape Catalogue as the reference catalog. Using this catalog there was approximately 100–200 stars per plate. We have on the average 70 stars per plate. Thus, though we have a better-determined reduction model the results are roughly the same between the two reductions because of the dense reference catalog used in the original reduction. There is an improvement of 11% from the single plate reduction and the overlap in the comparison of the PPM-S to the average vaule. This improvement would be larger if the effect of parameter variance were removed In addition, the measuring error of 4 microns is now dominate and it is difficult to obtain much more improvement.

Future Work

The positions estimates derived in this investigation would be improved if the plates were remeasured. We have thoroughly tested the improvement in the precision attainable by the overlapping plate reduction method. An interesting addition to the reduction method would be to restrict the plate parameters which do not vary much from plate to plate to a constant value. Alternately, these plate parameters could be constrained to an average value which is only allowed to vary according known distribution, (i.e. stochastically constrained). In theory, by stochastically constraining the parameters we can find estimates for parameters that would be more accurate than those obtained by ignoring the fact that they are samples of a population with known characteristics. For example, if the plates were all taken with the same telescope then we would expect the plate parameters corresponding to a scale, coma, and distortion could possibly be restricted to a constant value or constrained to an average value which is allow to vary according to a known distribution.

Though these are interesting additions to the adjustment method and we did test constraining some of the parameters to constant values, this data set is simply not accurate or precise enough to warrant such additions. However, if the plates were remeasured or if we used data from one of the current measuring machines with a measuring error of 1 micron then the incorporation of these constraints

might lead to a substantial improvement. We considered remeasuring the plates. However, because of the large size of the plates and because of the large number of them this has proved beyond the scope of this dissertation. There are very few measuring faculties that could be used for this project. Hopefully, in the future these plates can be remeasured.

The obvious next step is to determine the proper motions for the stars located on the plates. The best usage of this newly compiled catalog is as a mid-epoch or a first epoch source. The Astrographic Catalogue has been transferred to machine-readable form and would serve as an excellent first epoch with either the CPC-2 (the Second Cape Photographic Catalog, Zacharias, 1992) or the FOCAT-S (Bystrov et al., 1989) catalog as the third epoch.

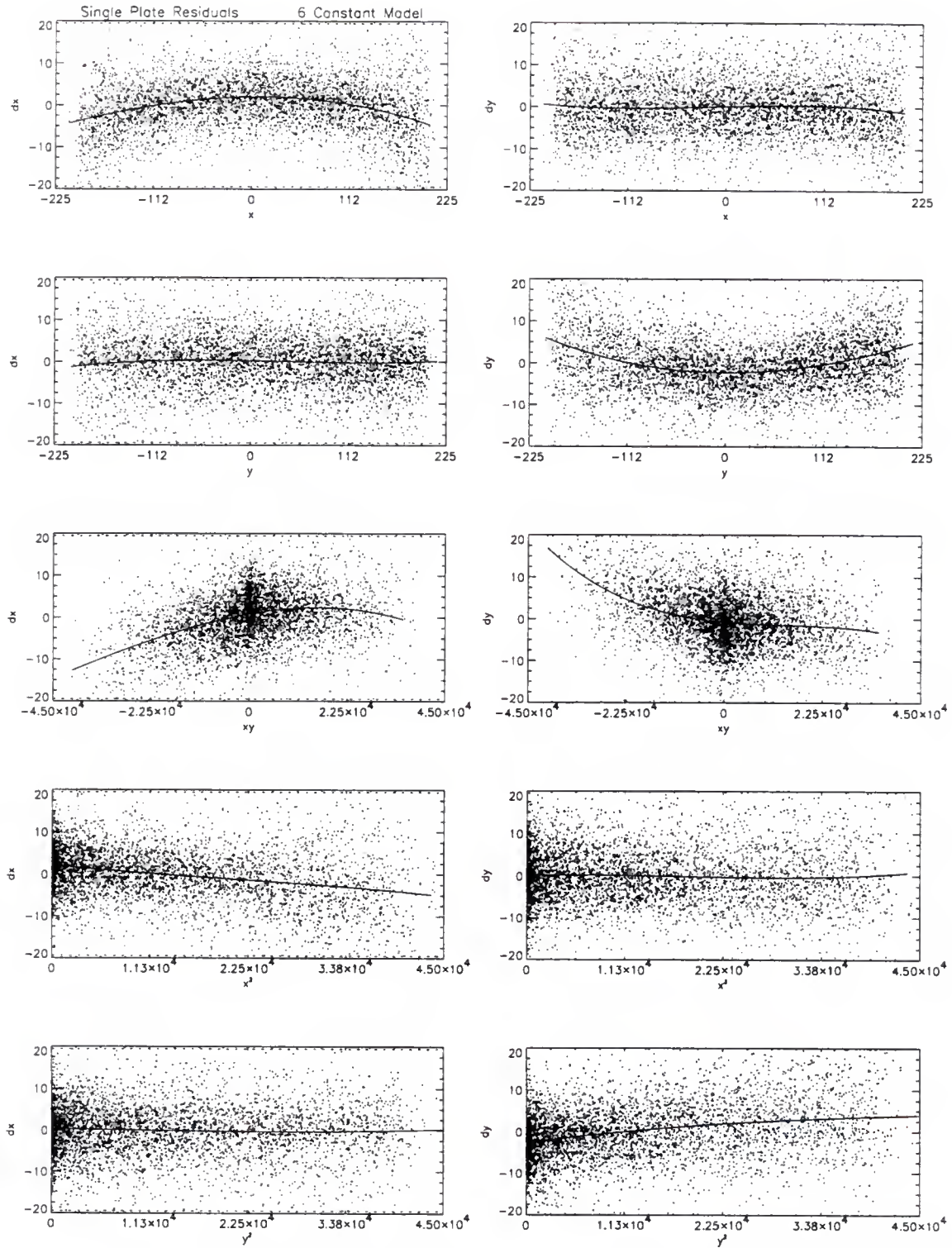


Figure 14: 6-Constant Single Plate Residuals



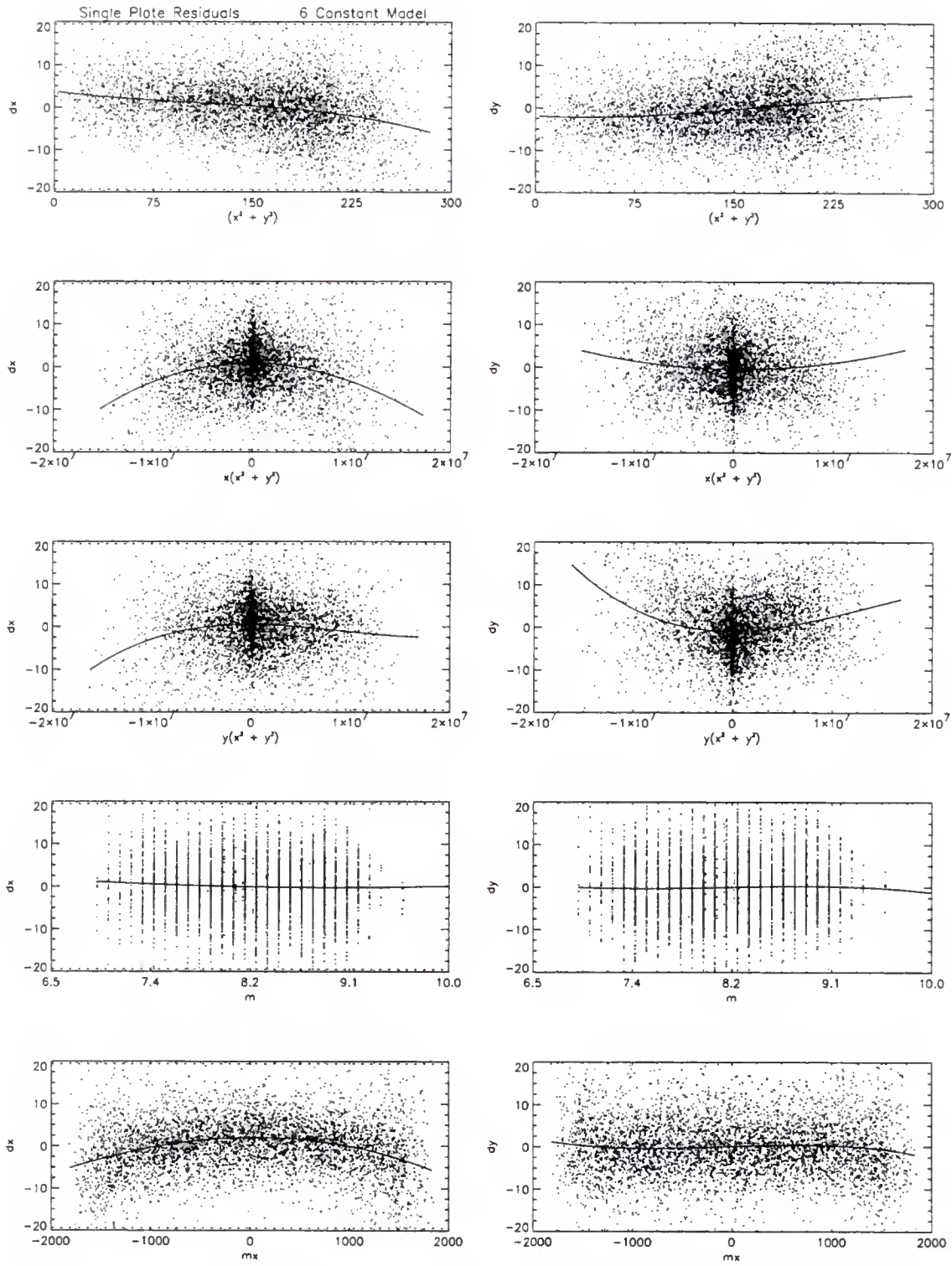


Figure 15: 6-Constant Single Plate Residuals



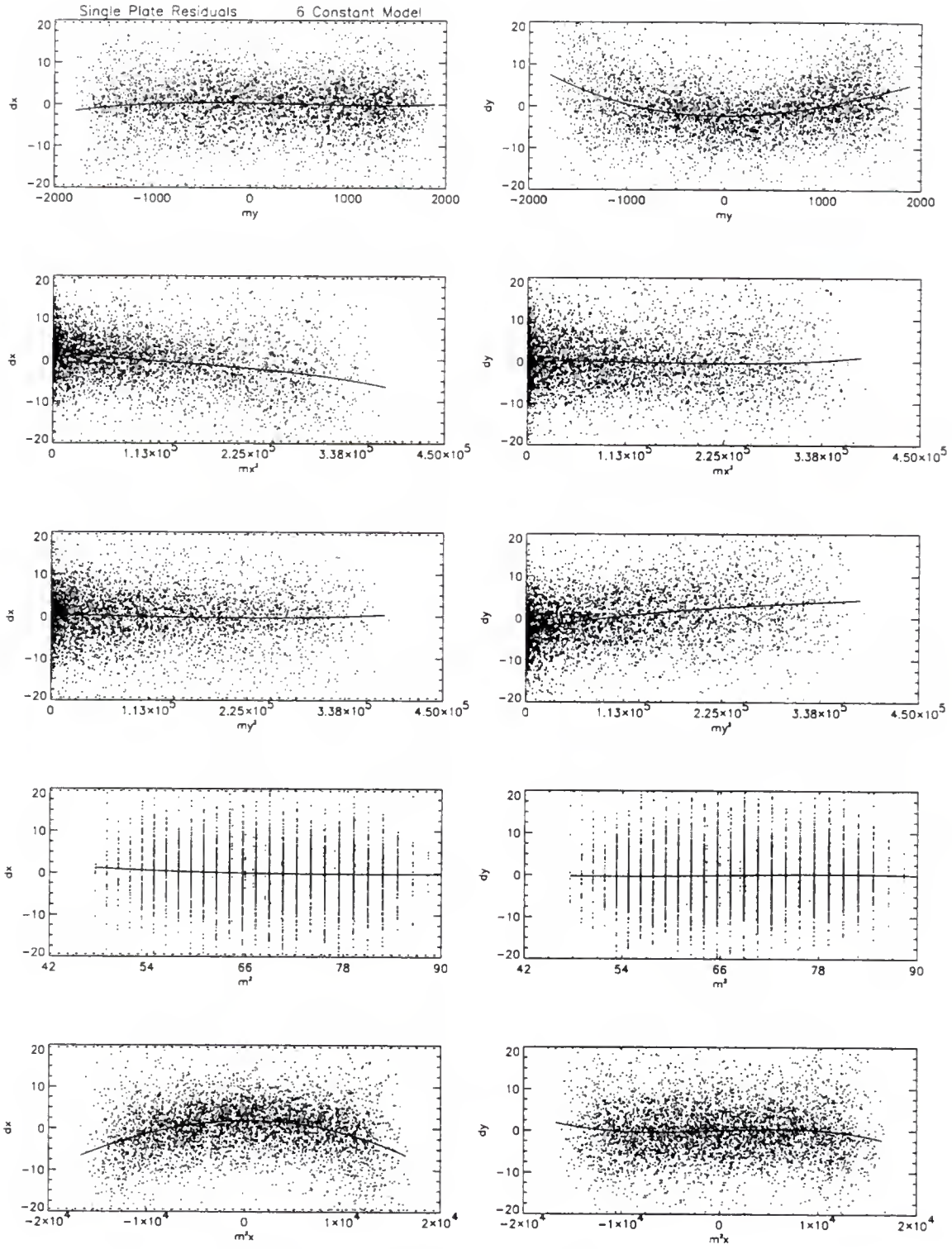


Figure 16: 6-Constant Single Plate Residuals

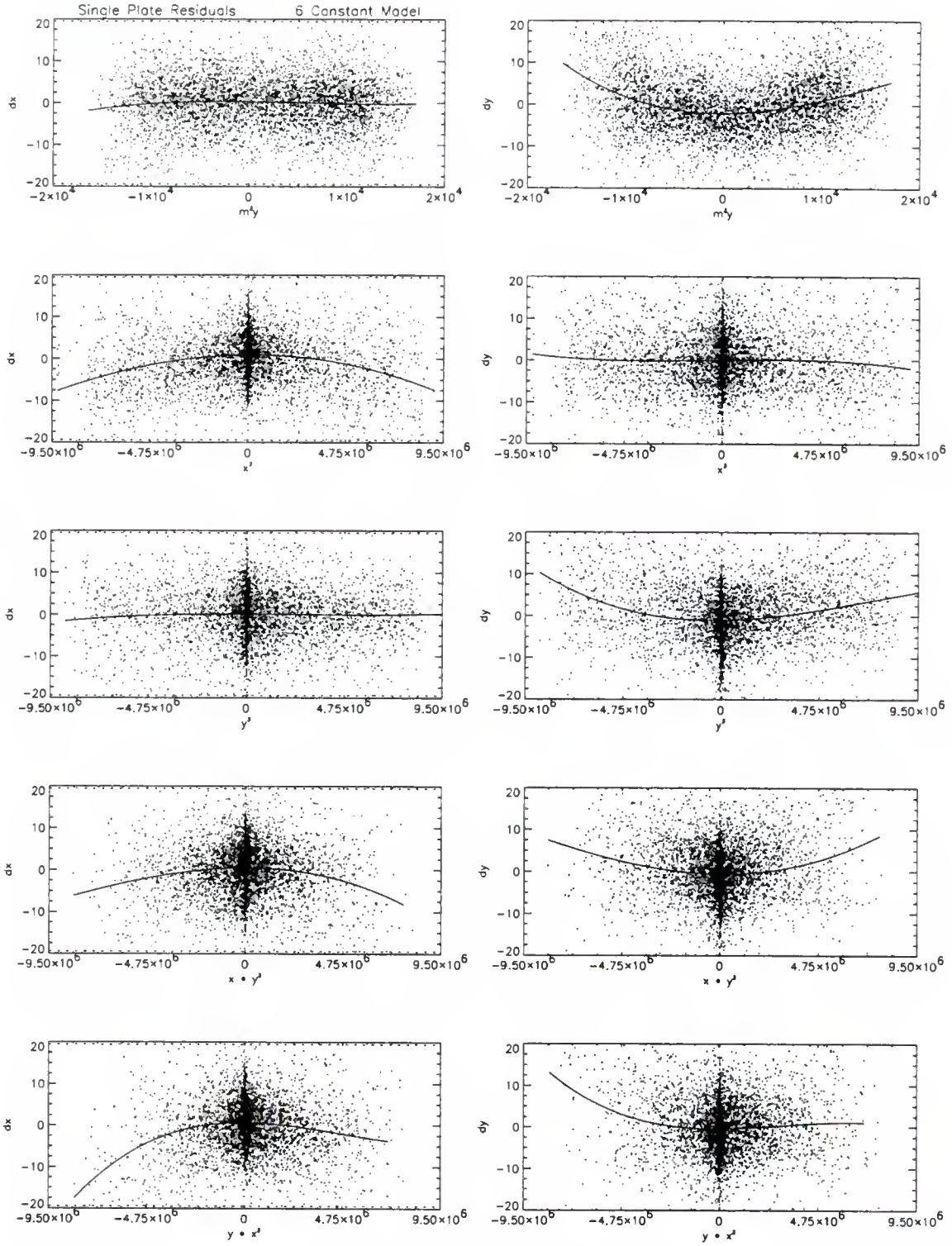


Figure 17: 6-Constant Single Plate Residuals

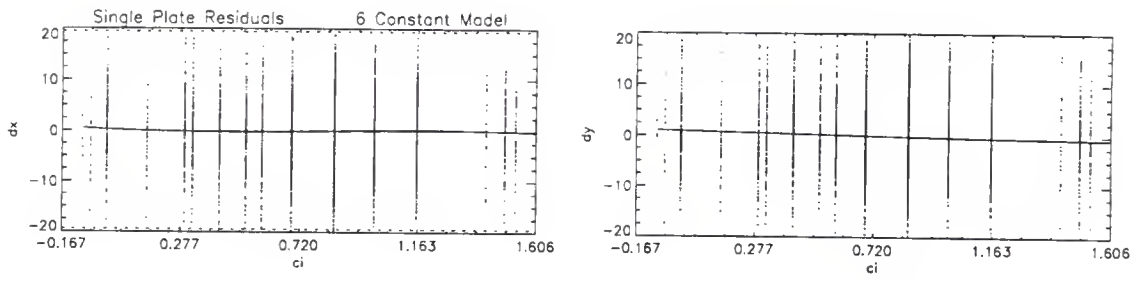


Figure 18: 6-Constant Single Plate Residuals

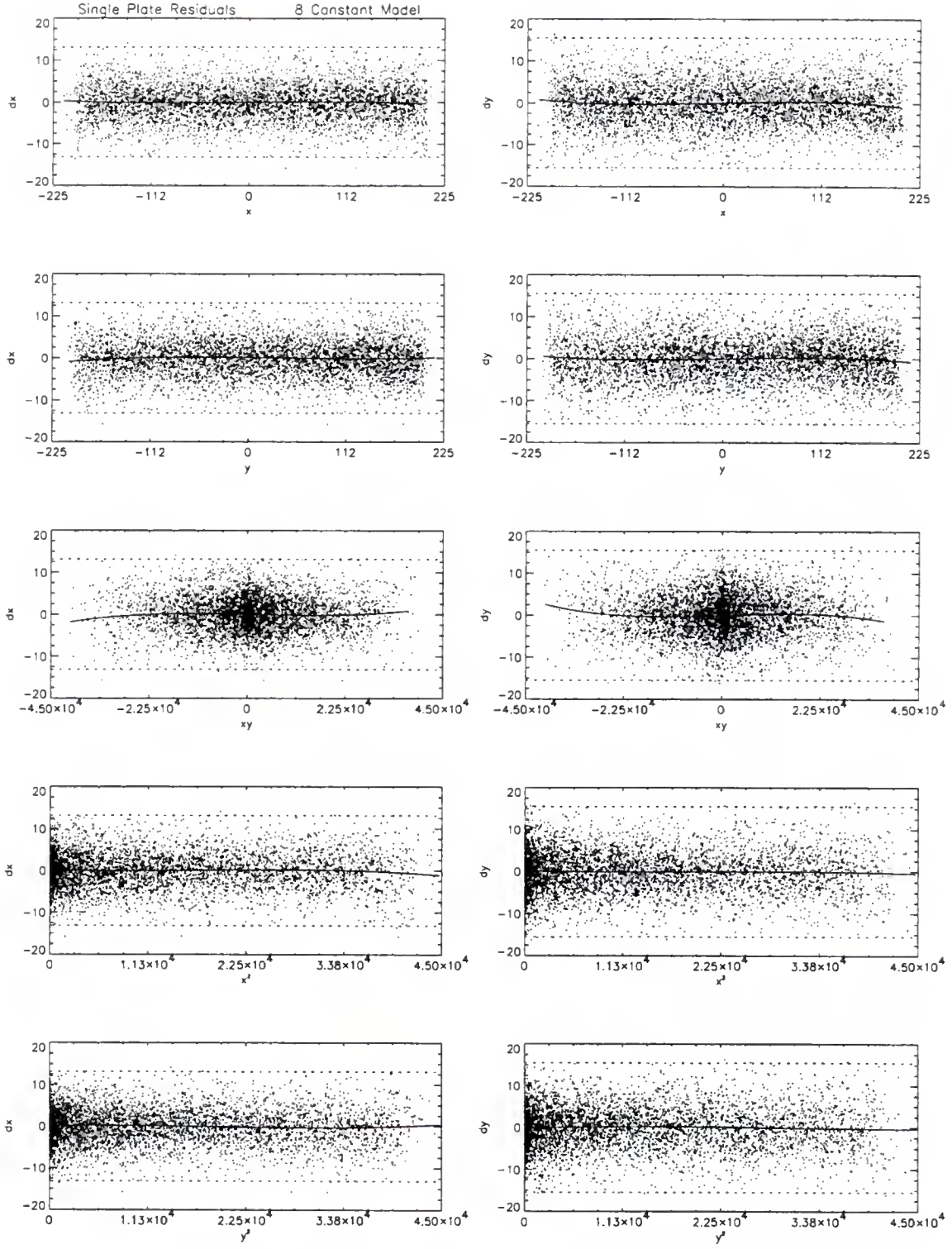


Figure 19: 8-Constant Single Plate Residuals



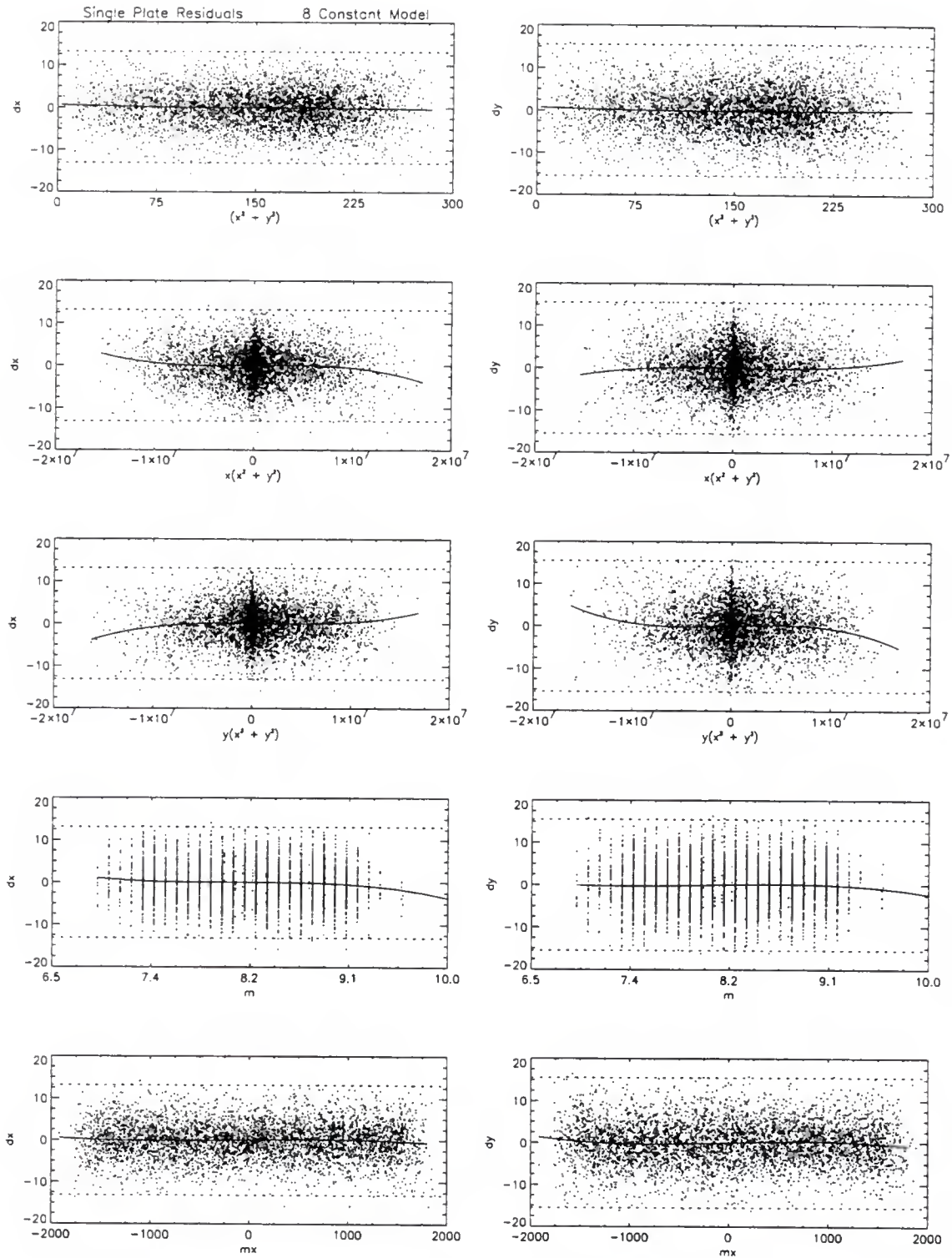


Figure 20: 8-Constant Single Plate Residuals

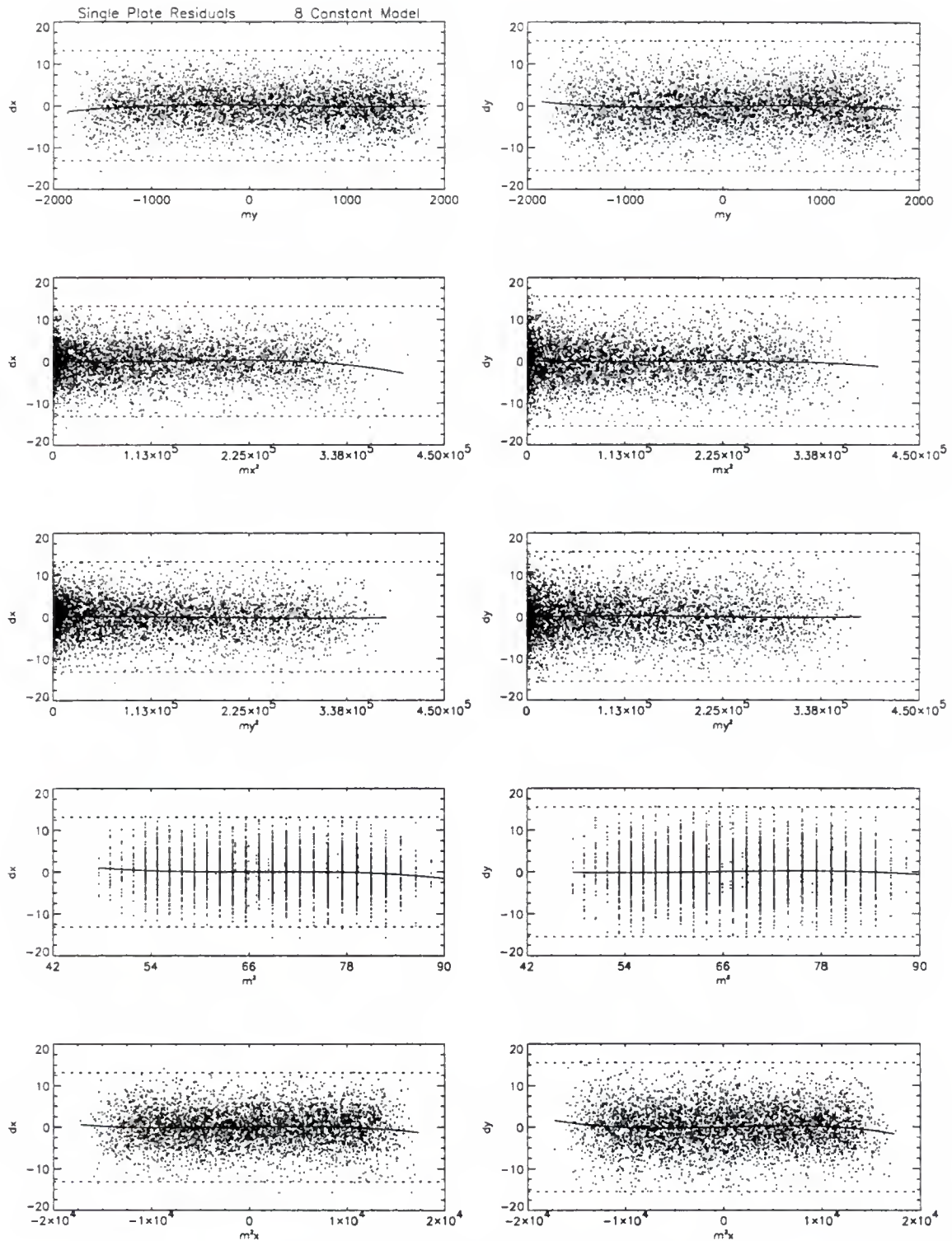


Figure 21: 8-Constant Single Plate Residuals

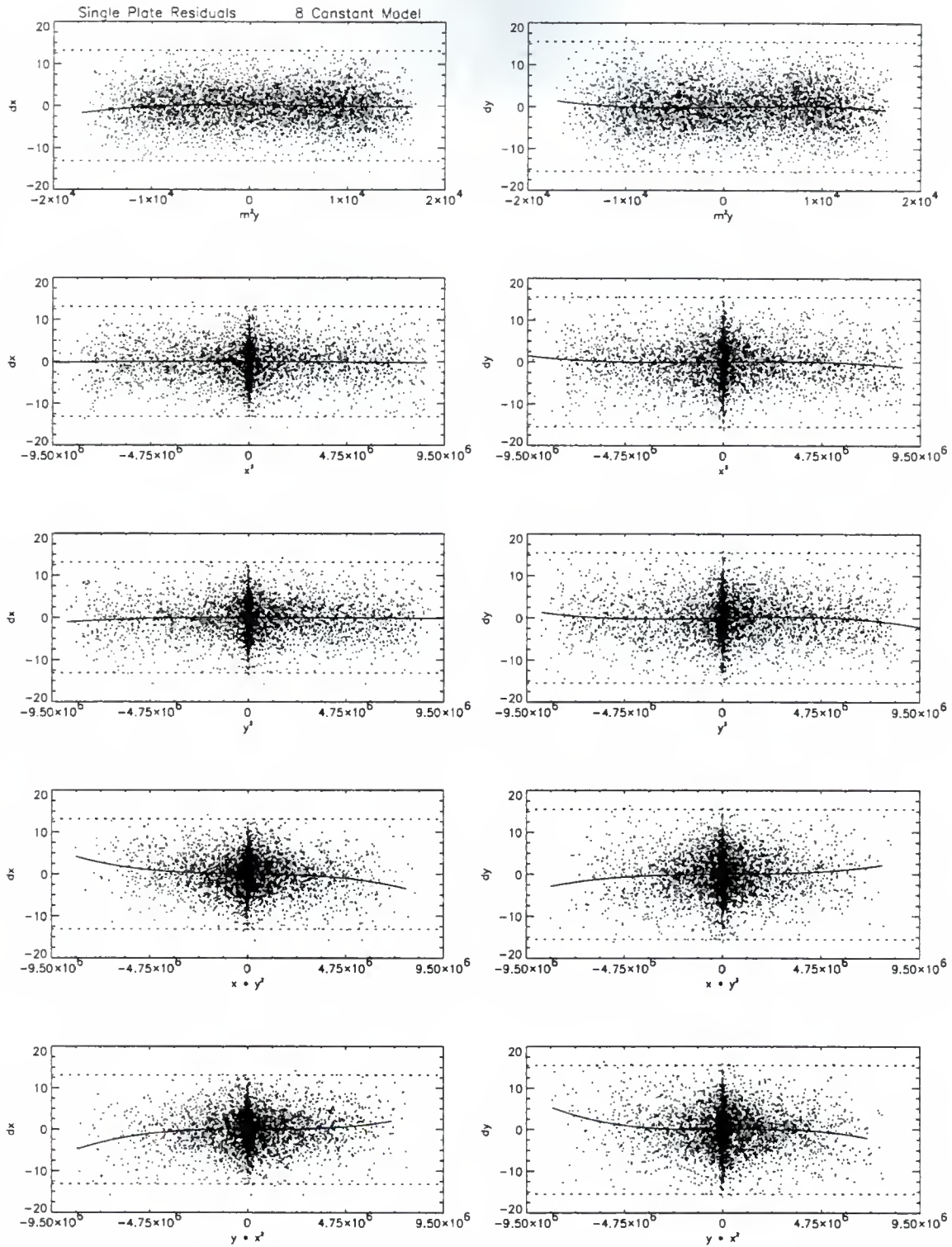


Figure 22: 8-Constant Single Plate Residuals

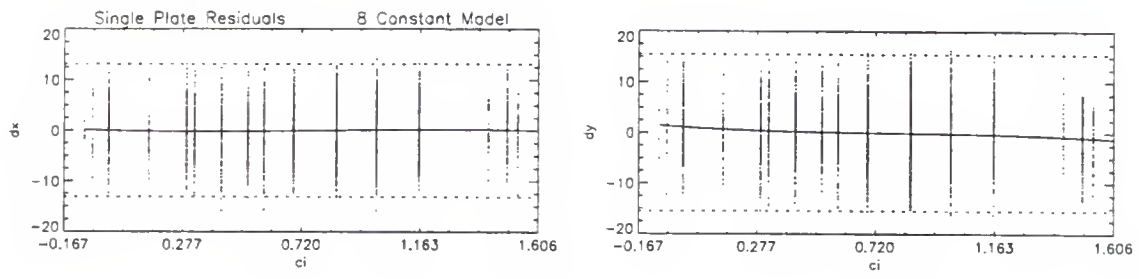


Figure 23: 8-Constant Single Plate Residuals



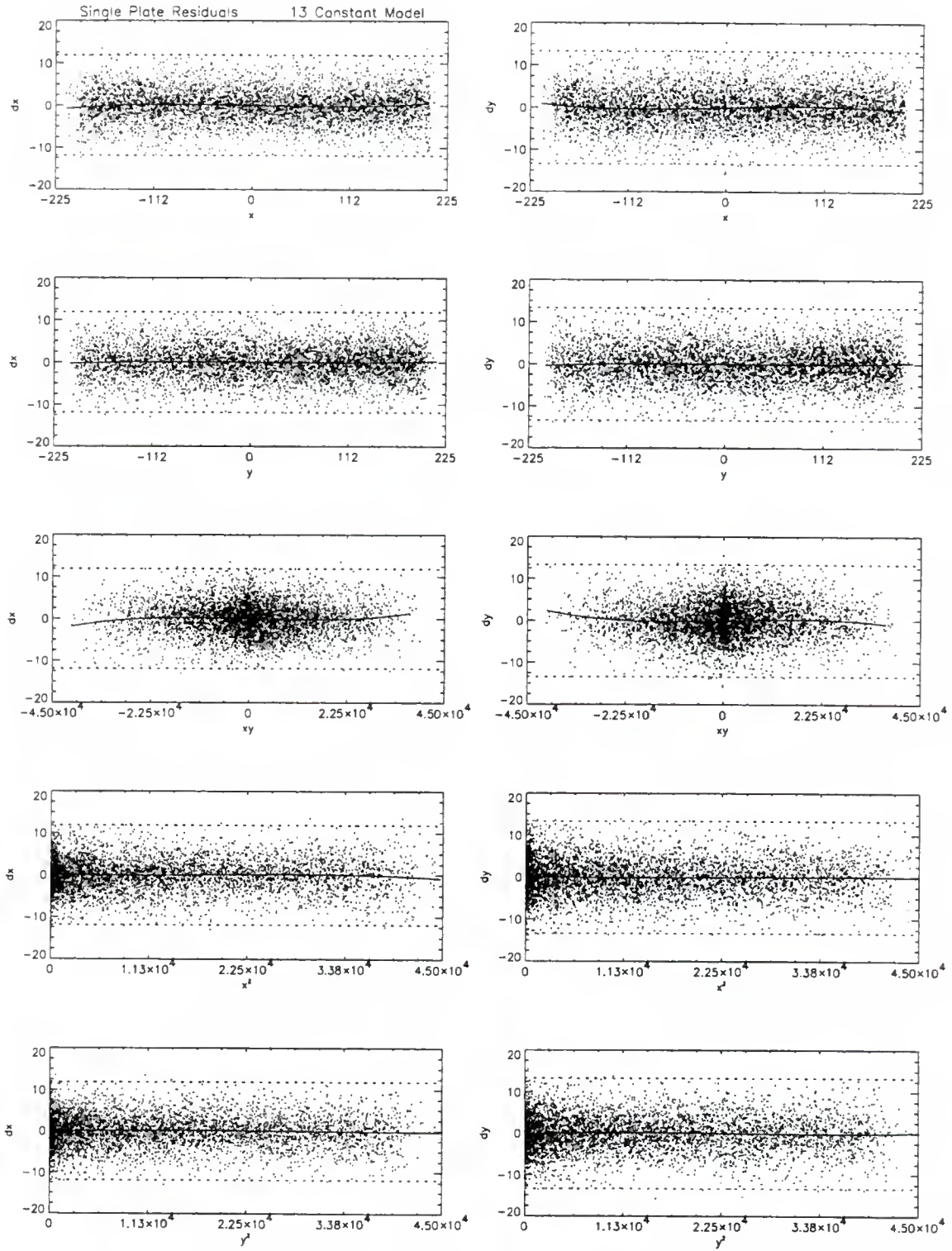


Figure 24: 13-Constant Single Plate Residuals

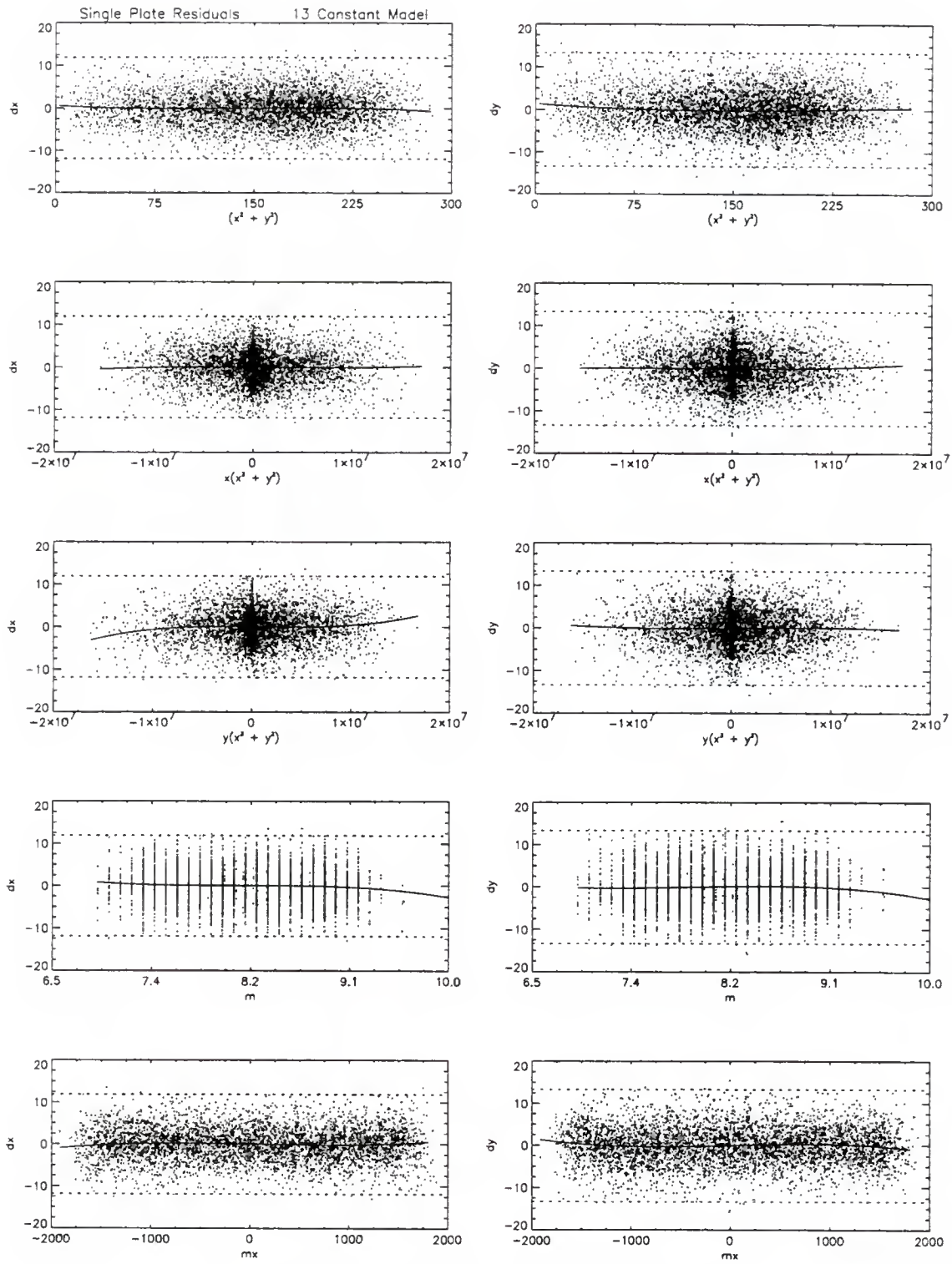


Figure 25: 13-Constant Single Plate Residuals

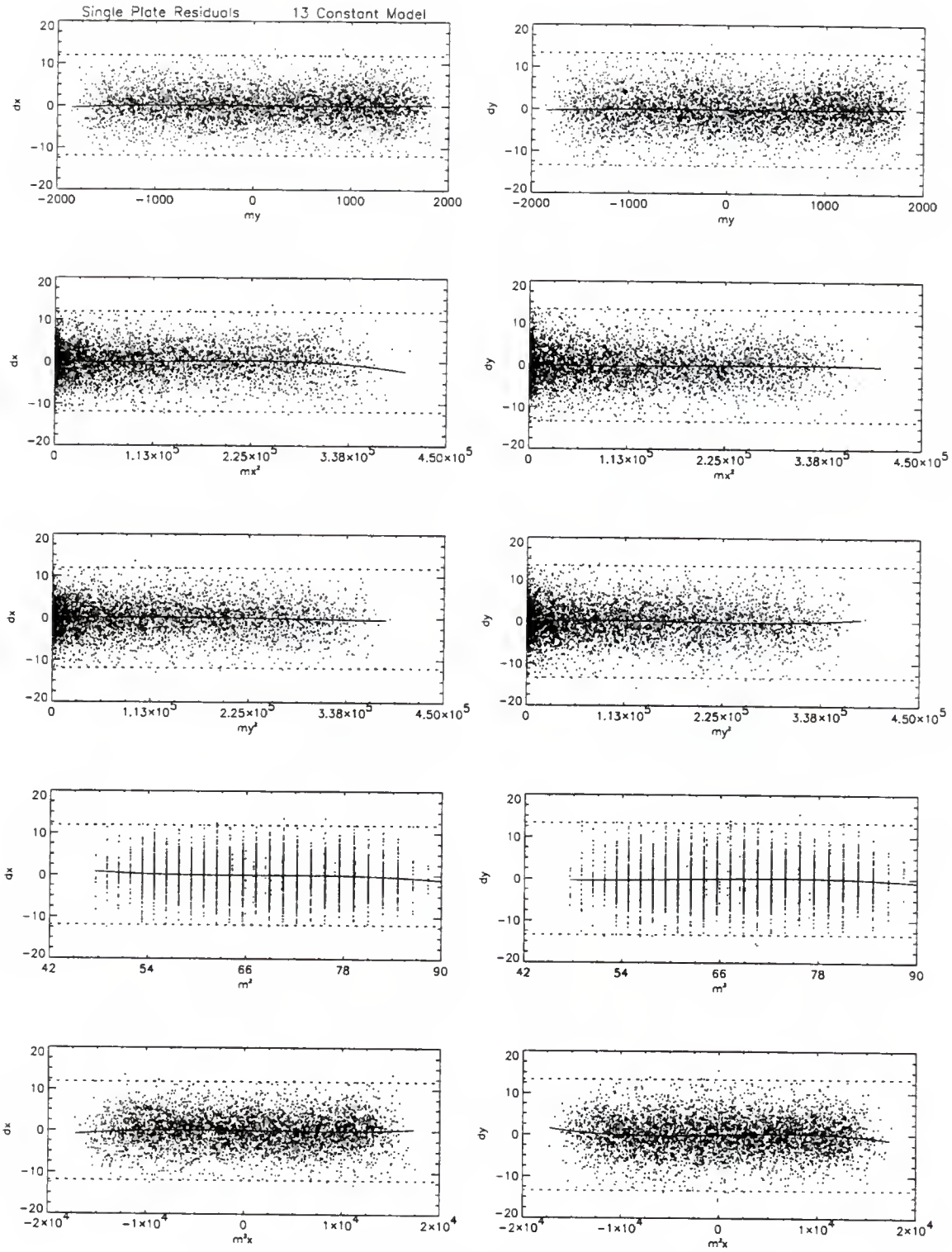


Figure 26: 13-Constant Single Plate Residuals



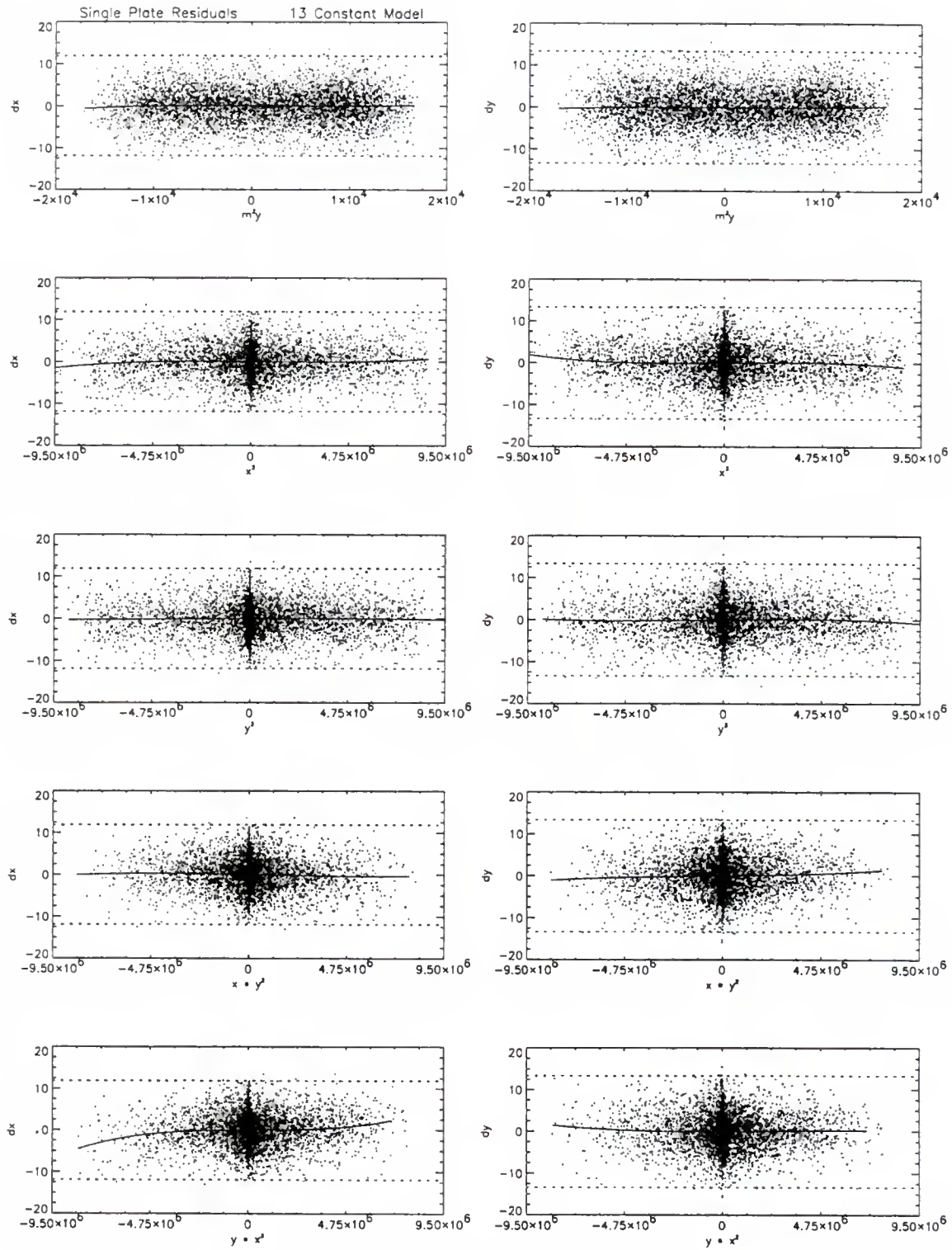


Figure 27: 13-Constant Single Plate Residuals

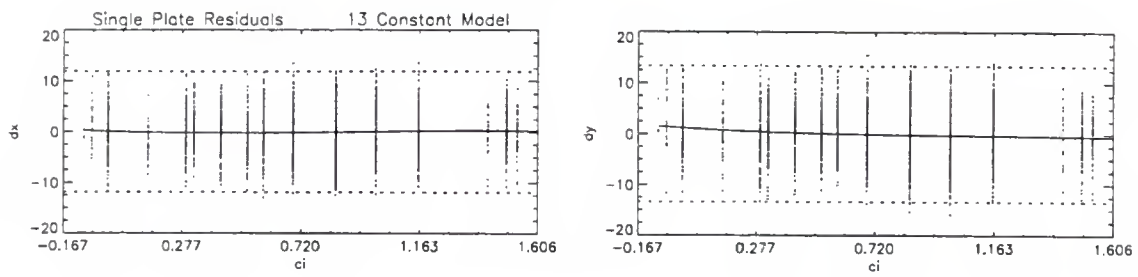


Figure 28: 13-Constant Single Plate Residuals

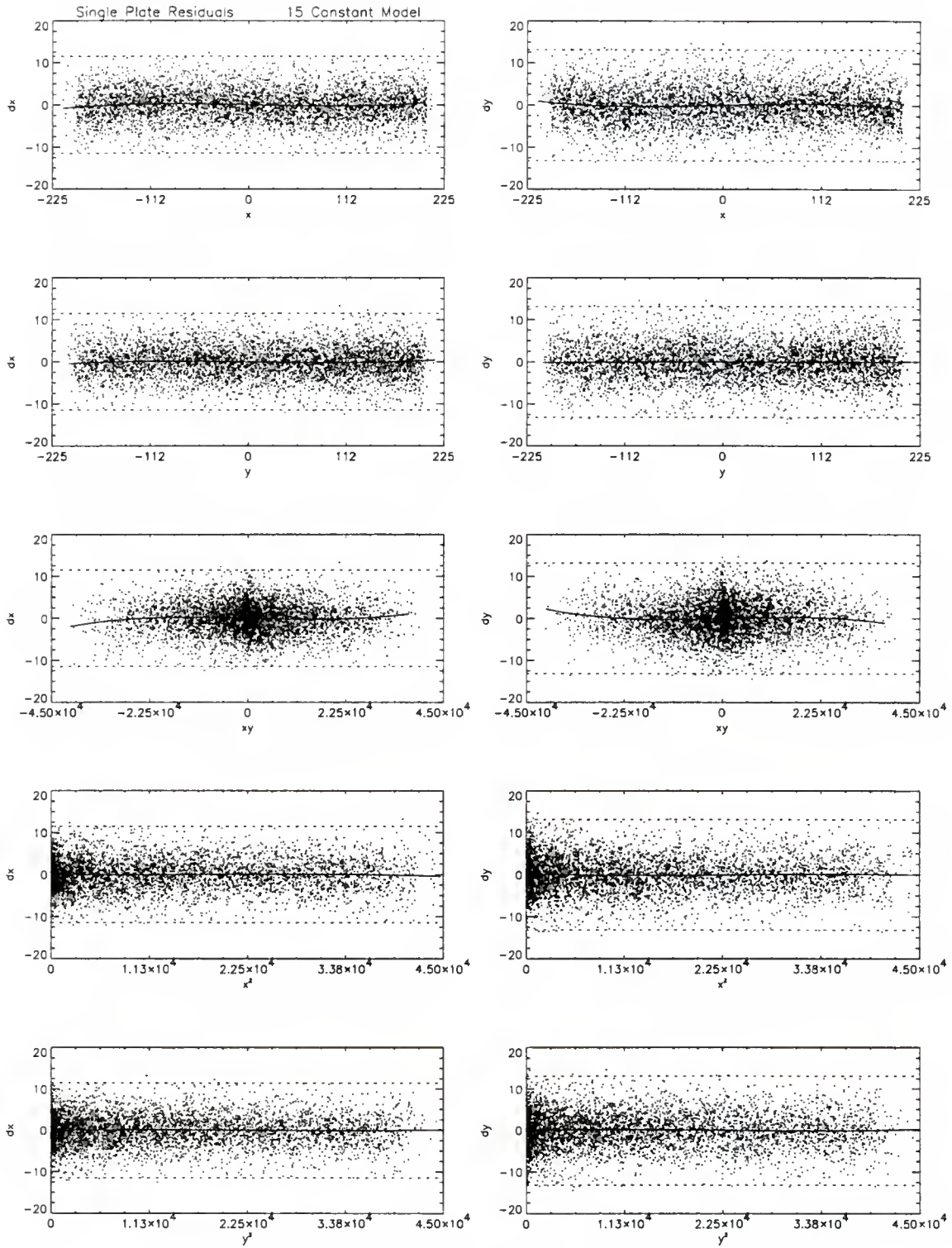


Figure 29: 15-Constant Single Plate Residuals

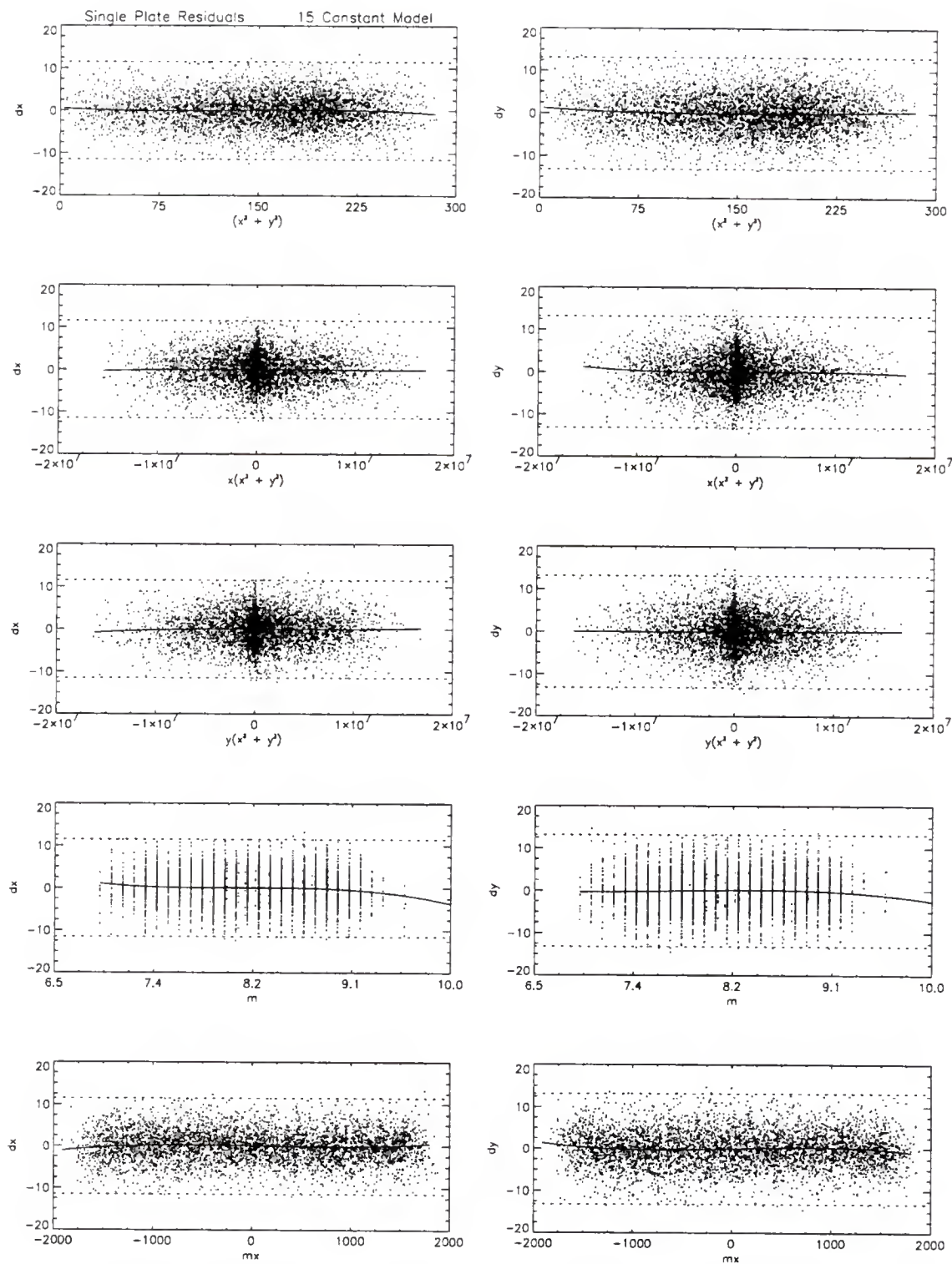


Figure 30: 15-Constant Single Plate Residuals



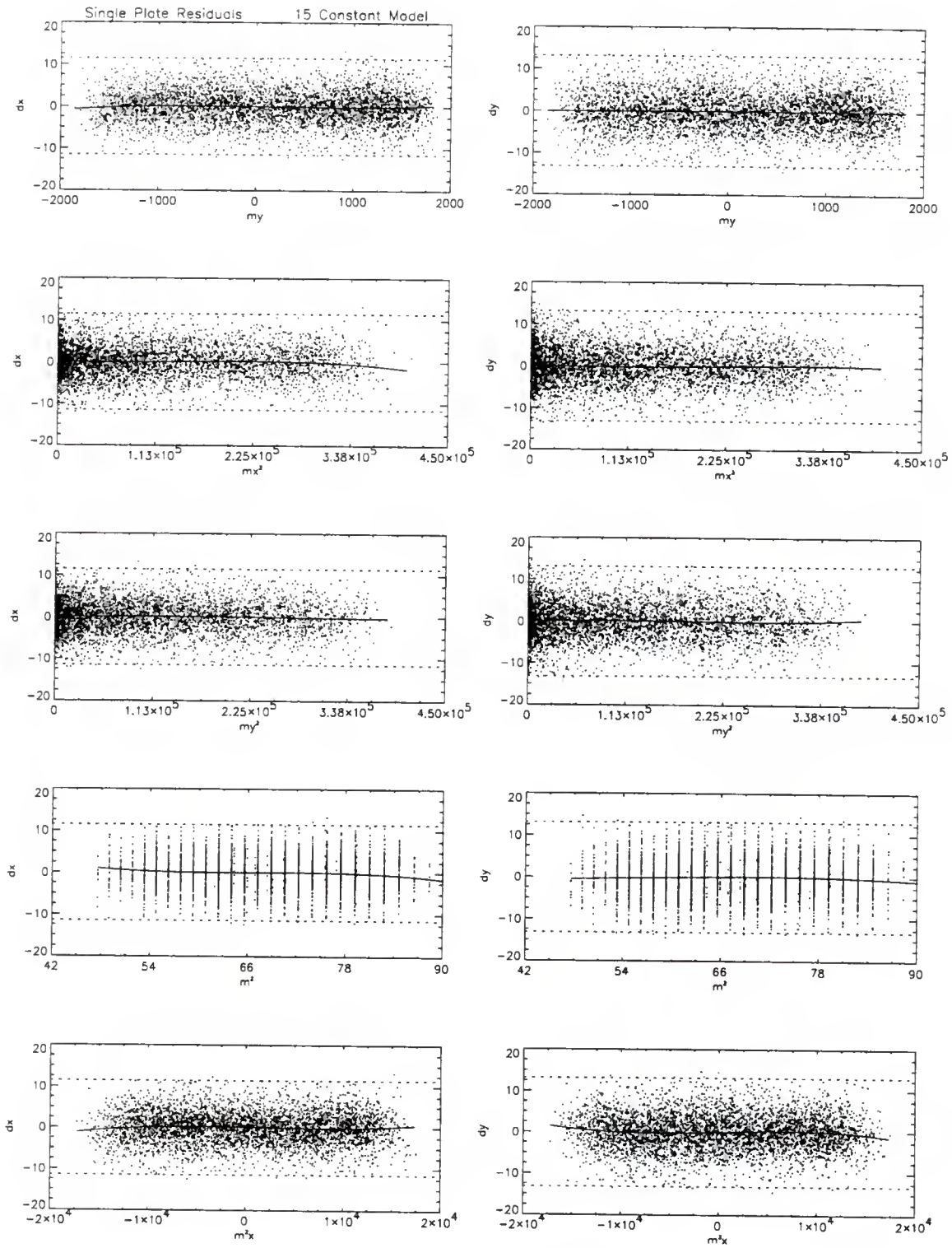


Figure 31: 15-Constant Single Plate Residuals



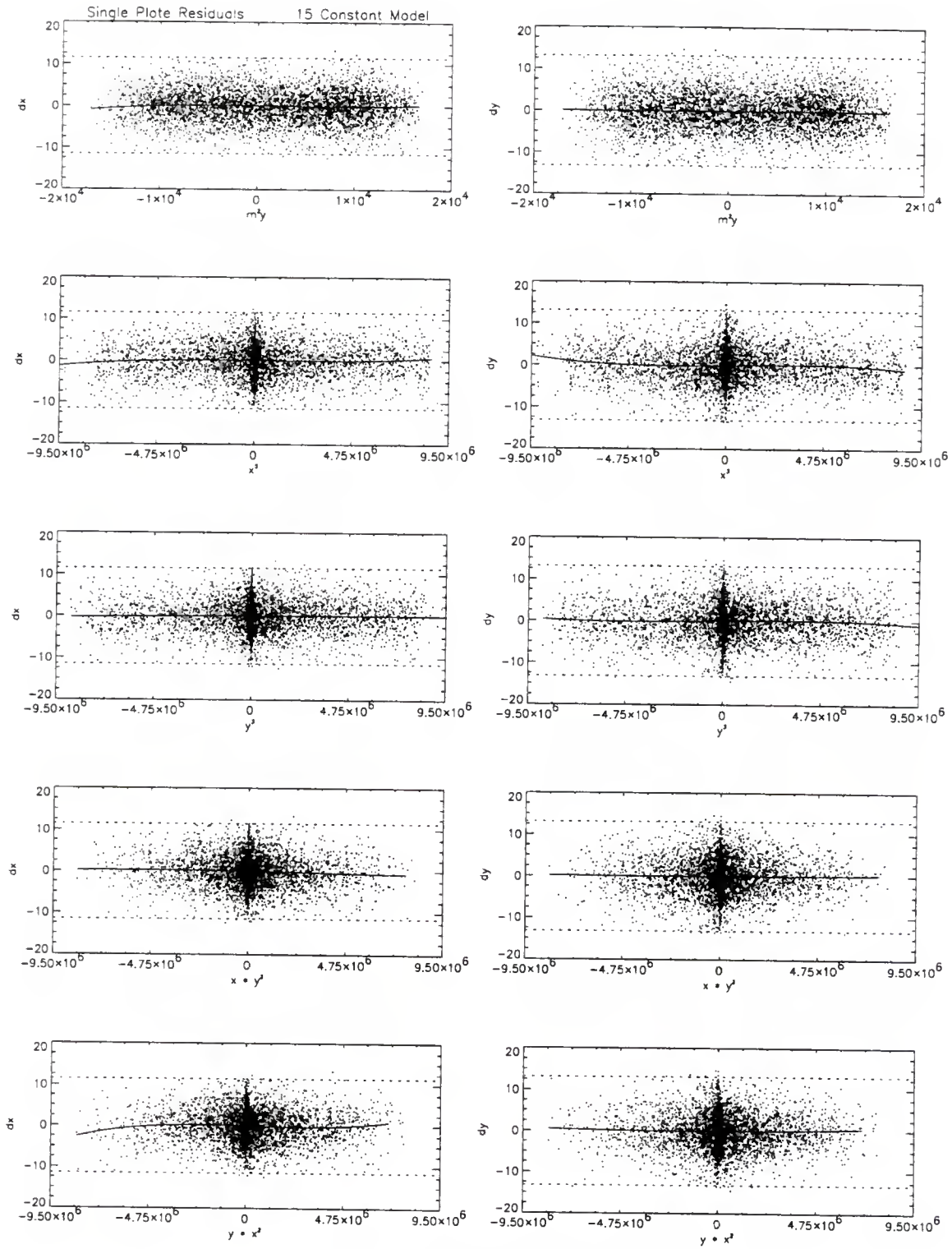


Figure 32: 15-Constant Single Plate Residuals

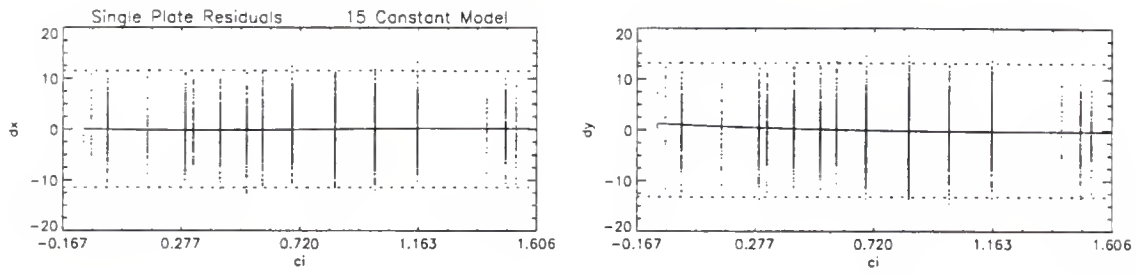


Figure 33: 15-Constant Single Plate Residuals

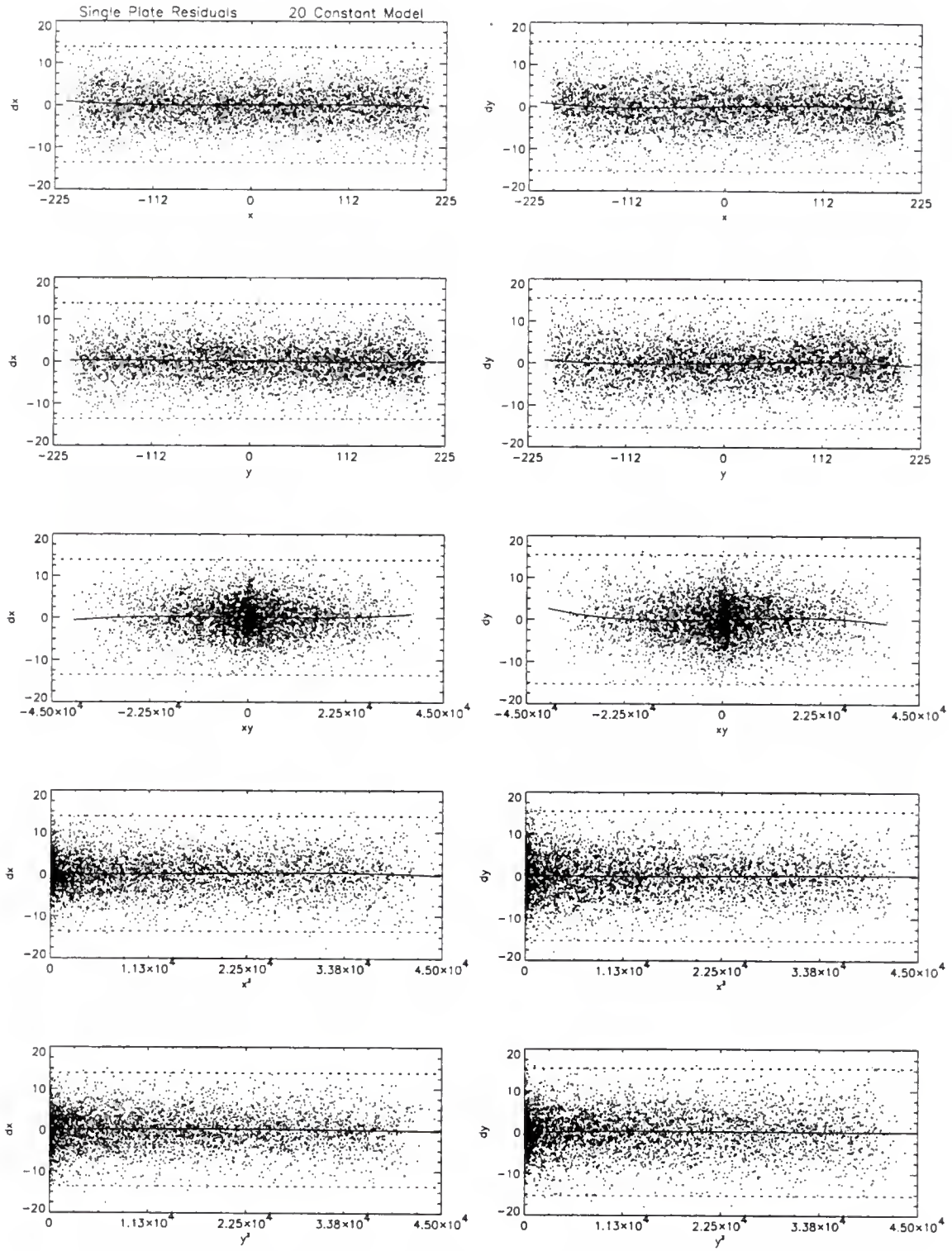


Figure 34: 20-Constant Single Plate Residuals

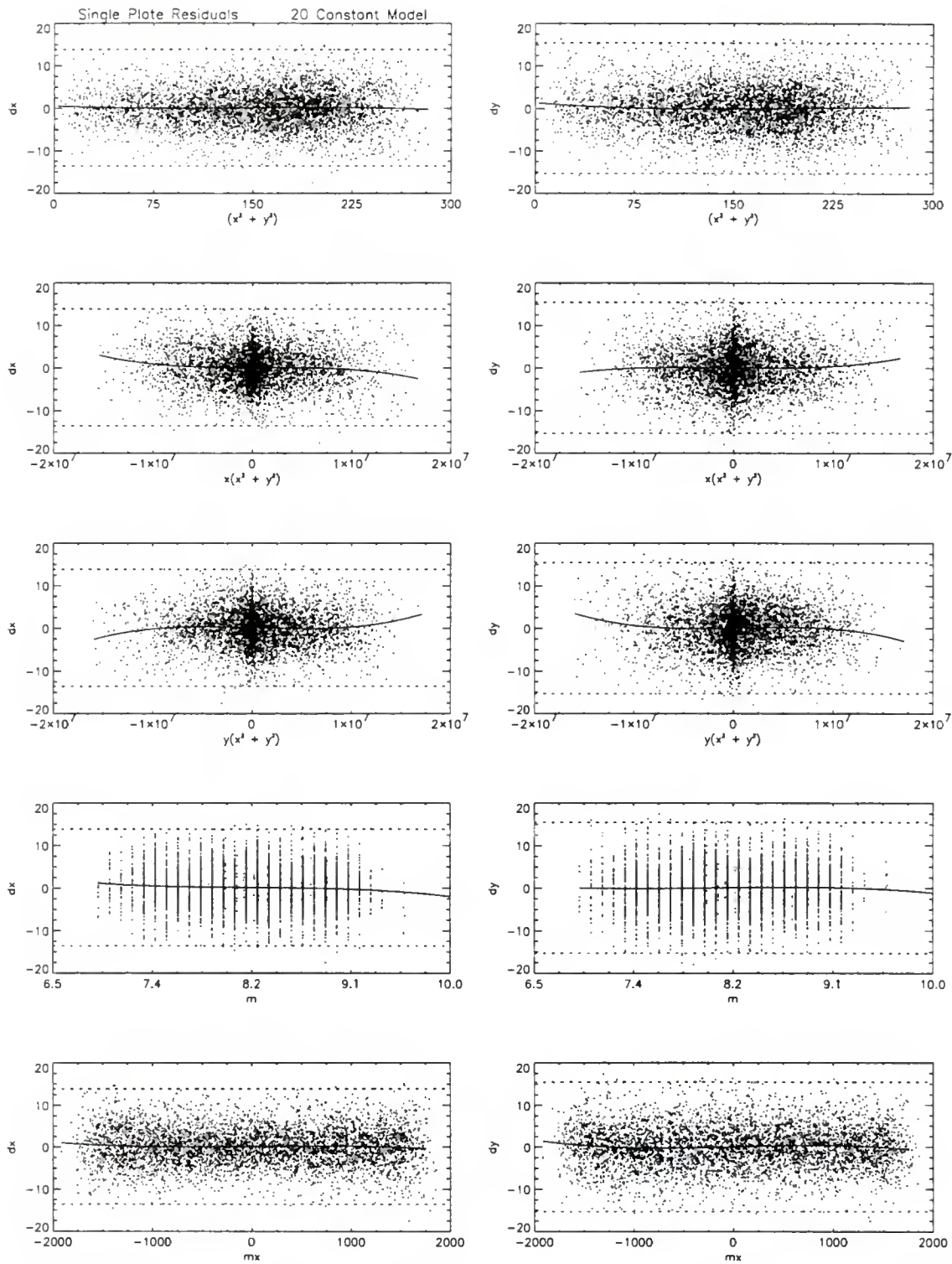


Figure 35: 20-Constant Single Plate Residuals



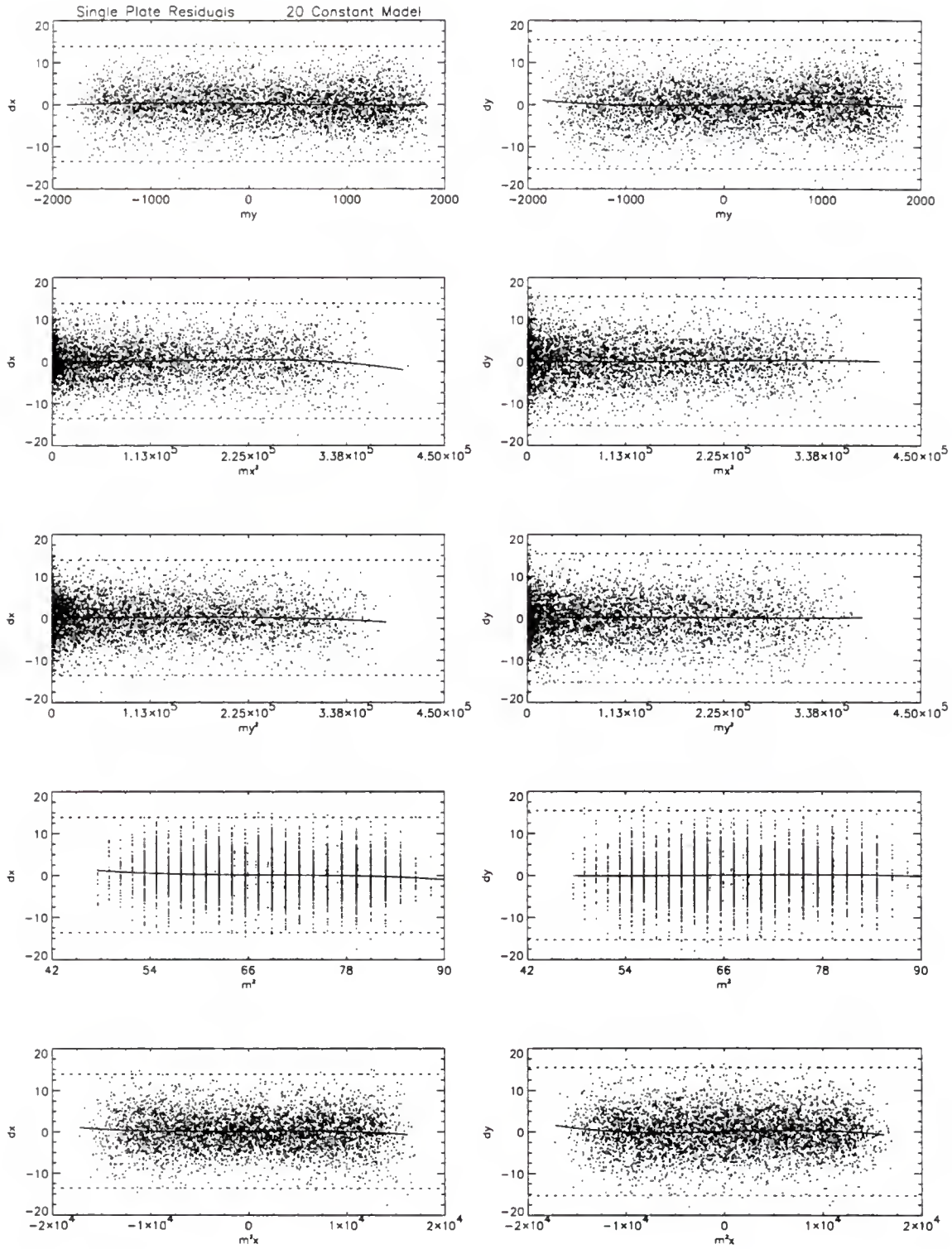


Figure 36: 20-Constant Single Plate Residuals

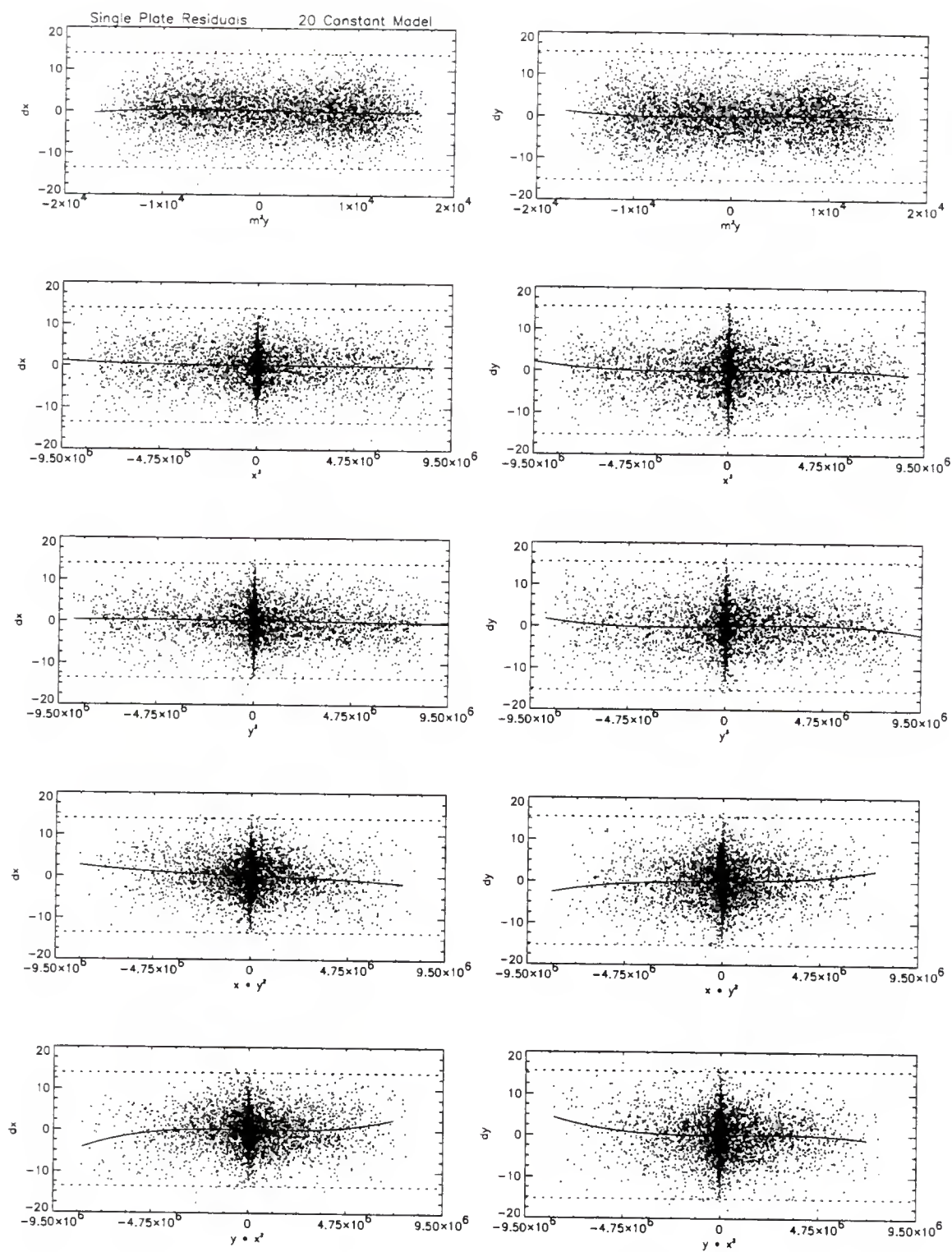


Figure 37: 20-Constant Single Plate Residuals

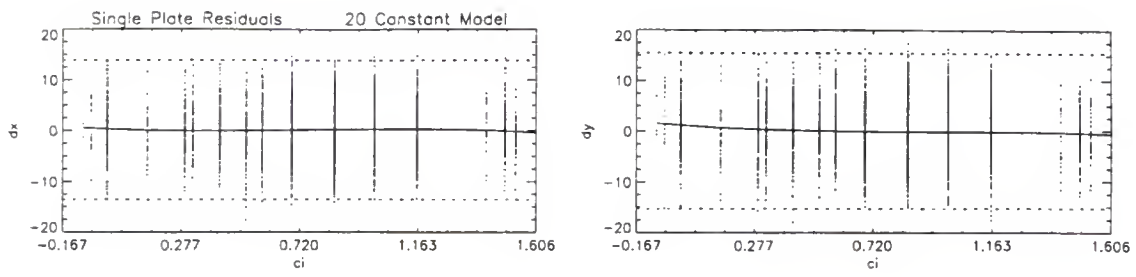


Figure 38: 20-Constant Single Plate Residuals

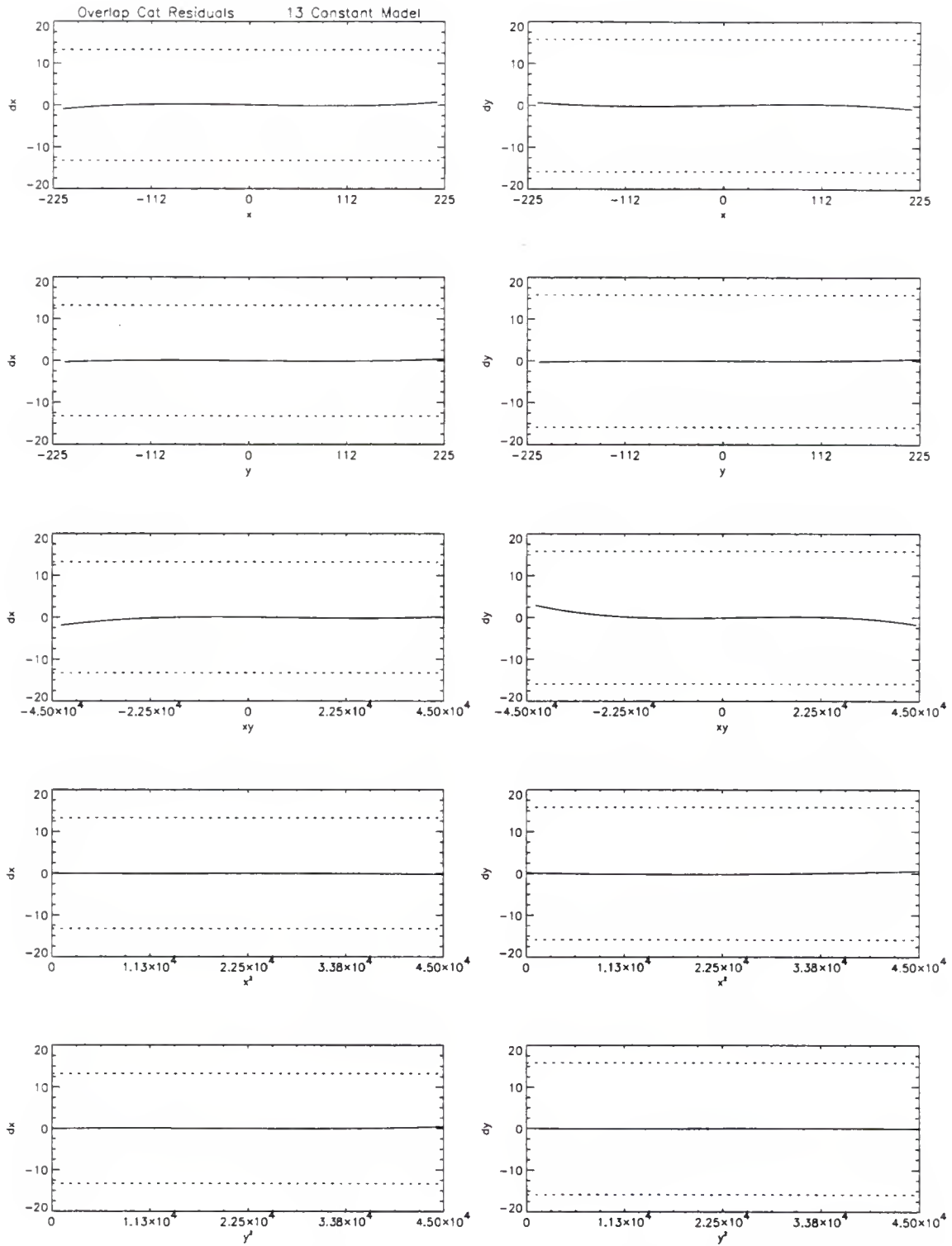


Figure 39: 13-Constant Overlap Residuals



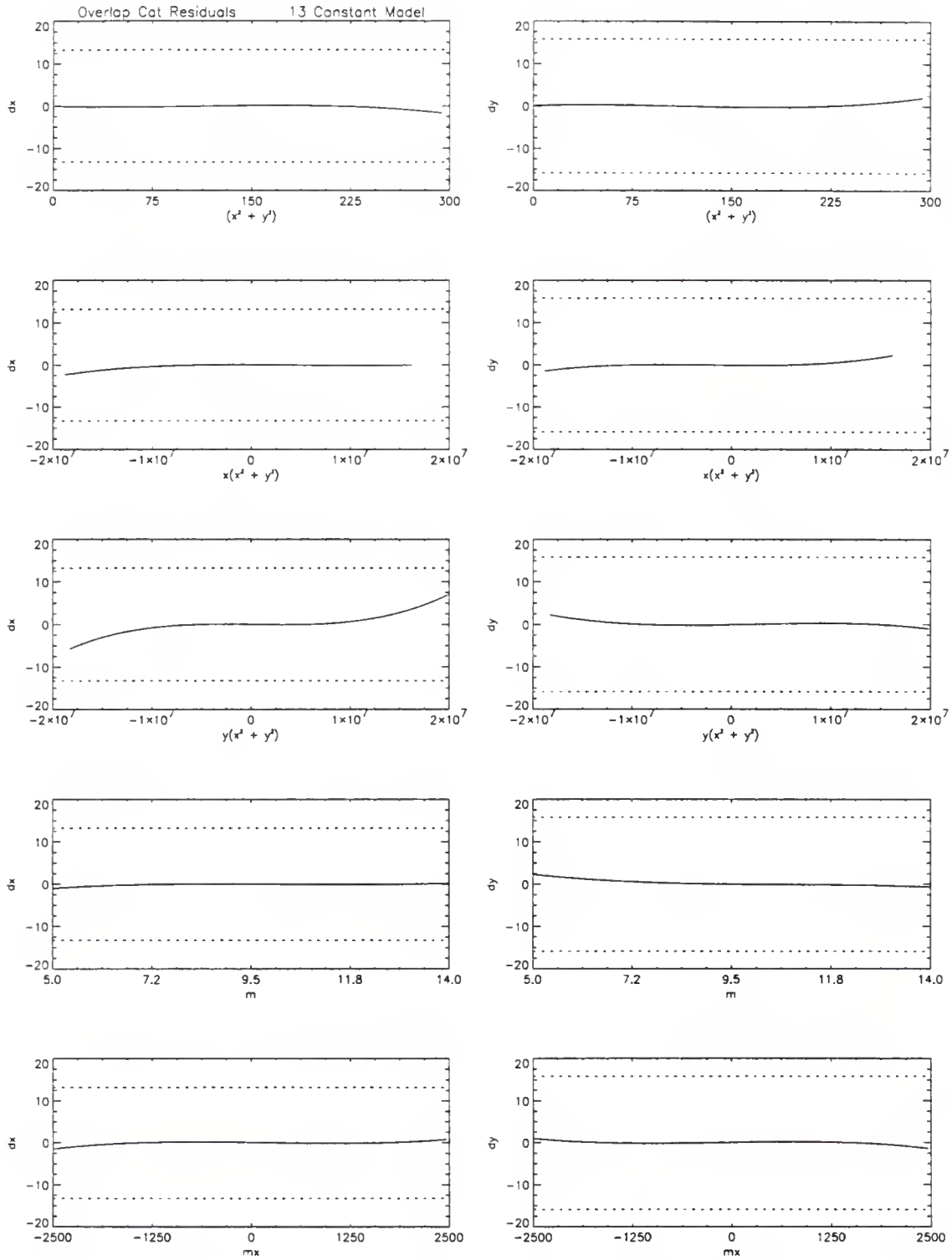


Figure 40: 13-Constant Overlap Residuals

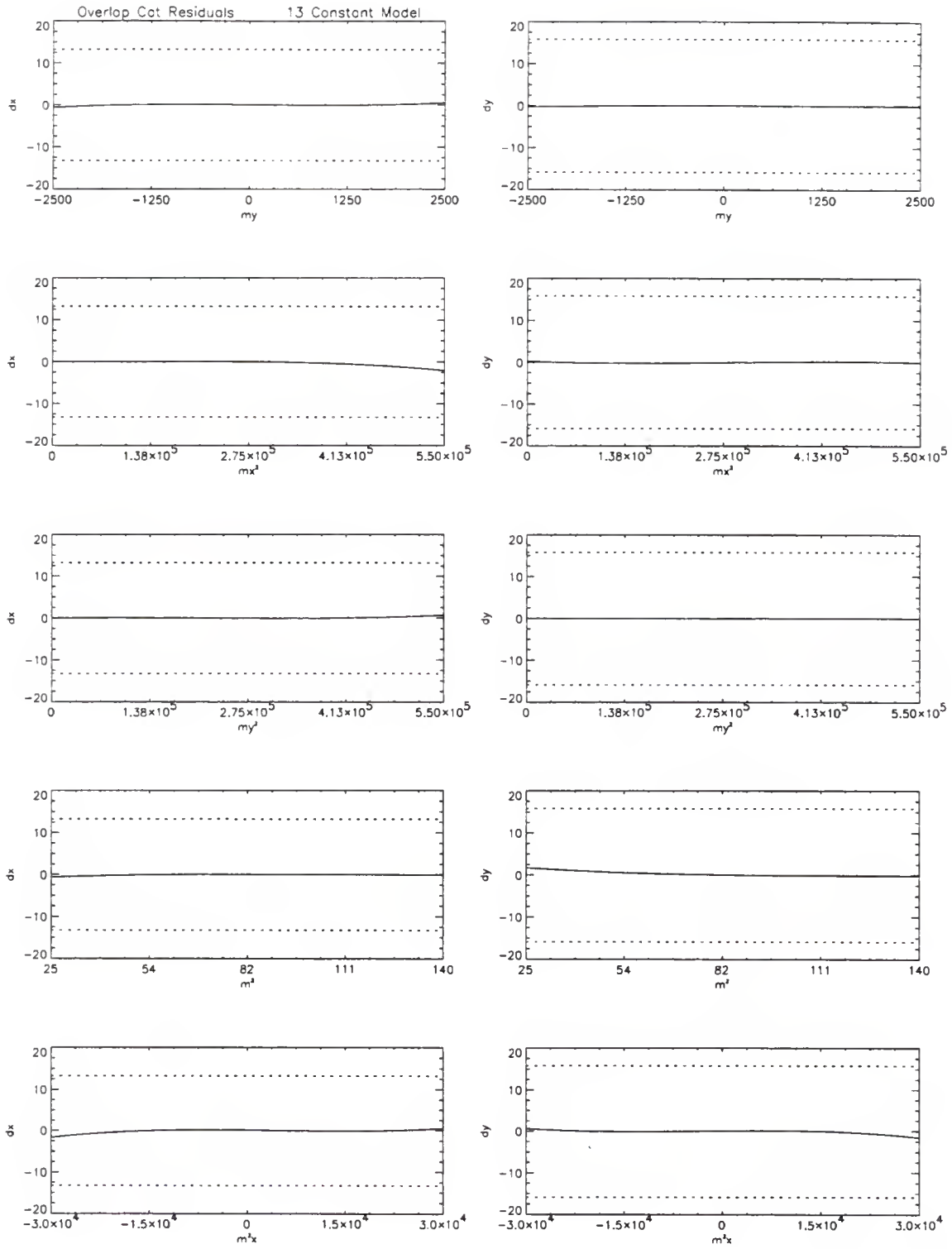


Figure 41: 13-Constant Overlap Residuals

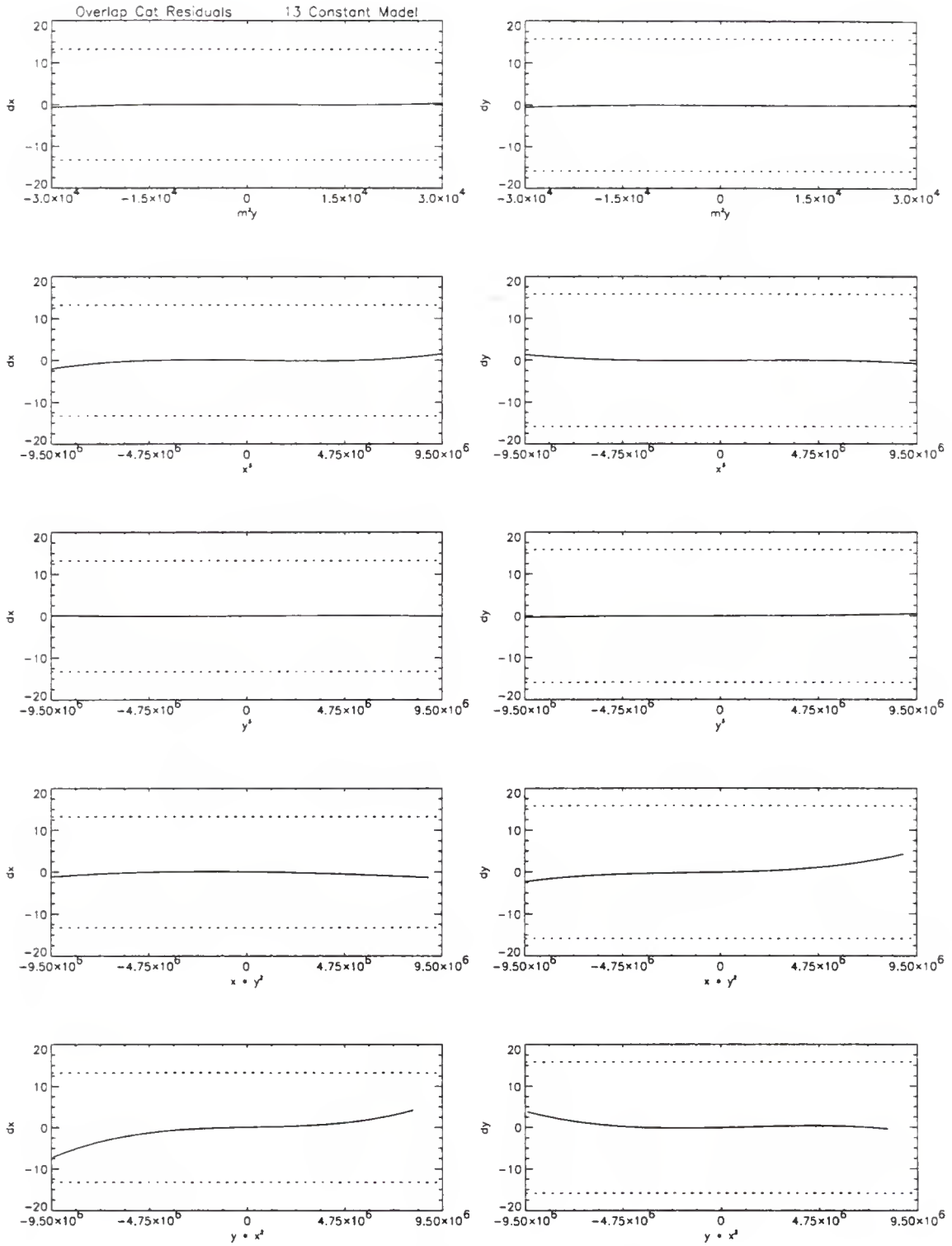


Figure 42: 13-Constant Overlap Residuals

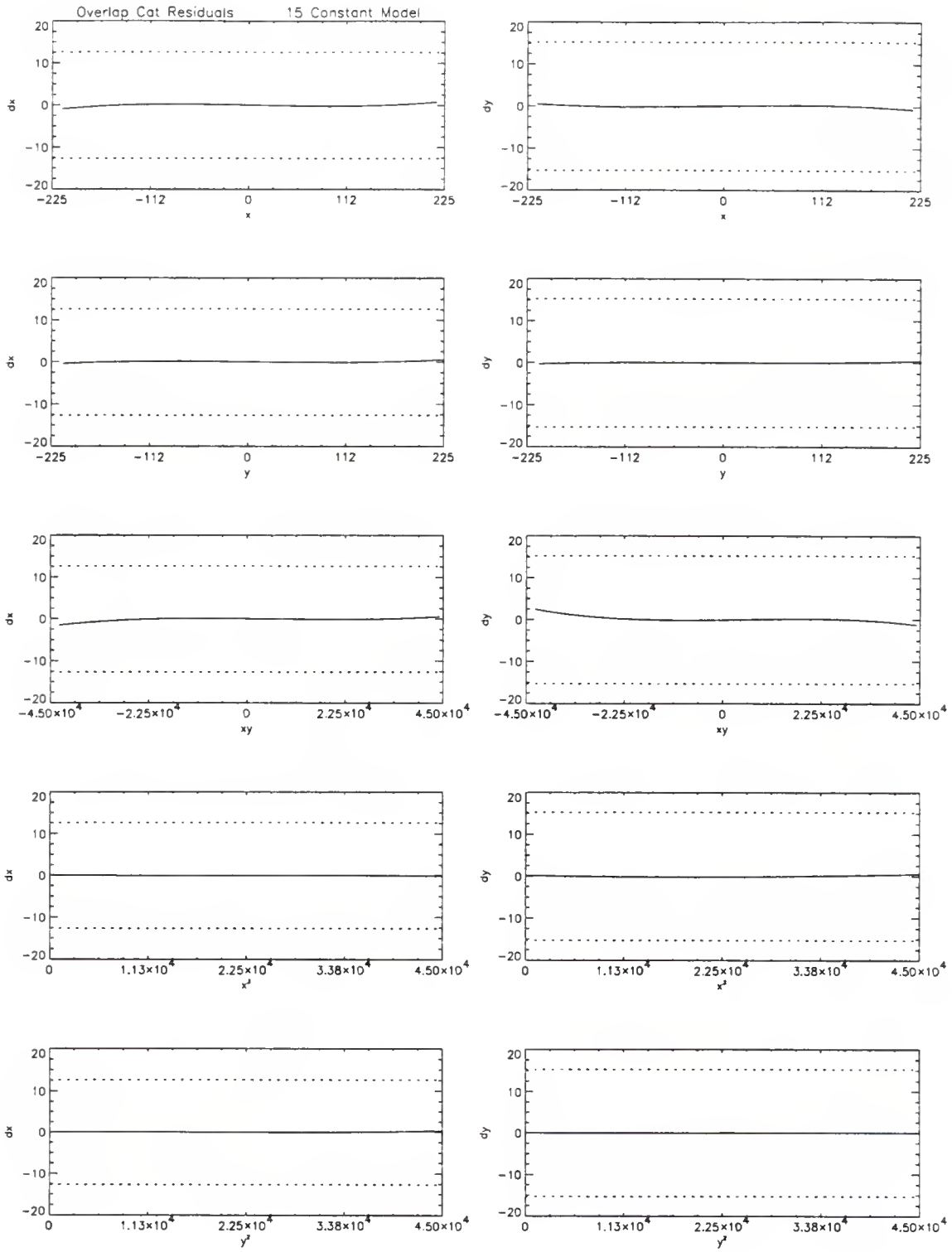


Figure 43: 15-Constant Overlap Residuals

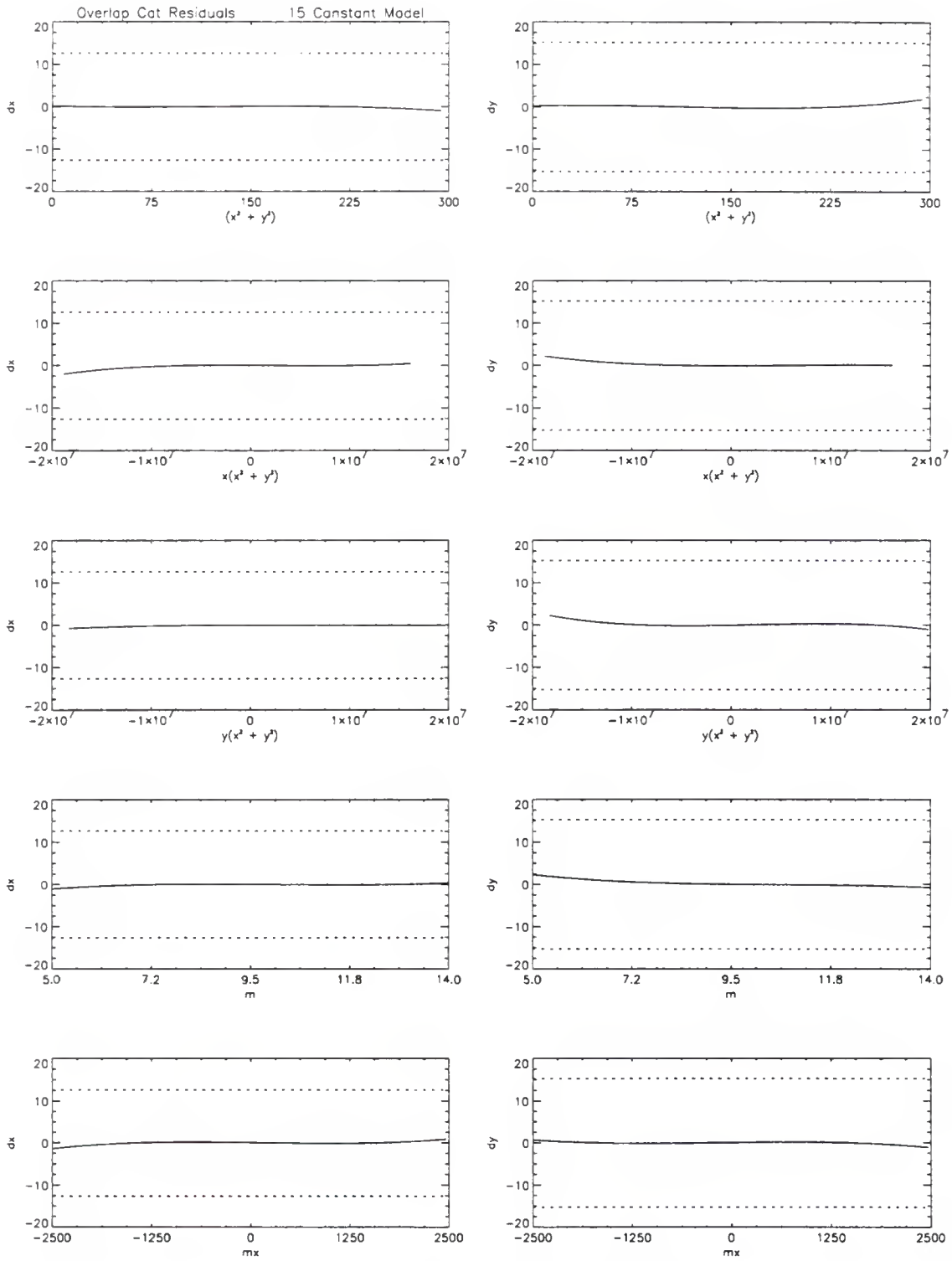


Figure 44: 15-Constant Overlap Residuals

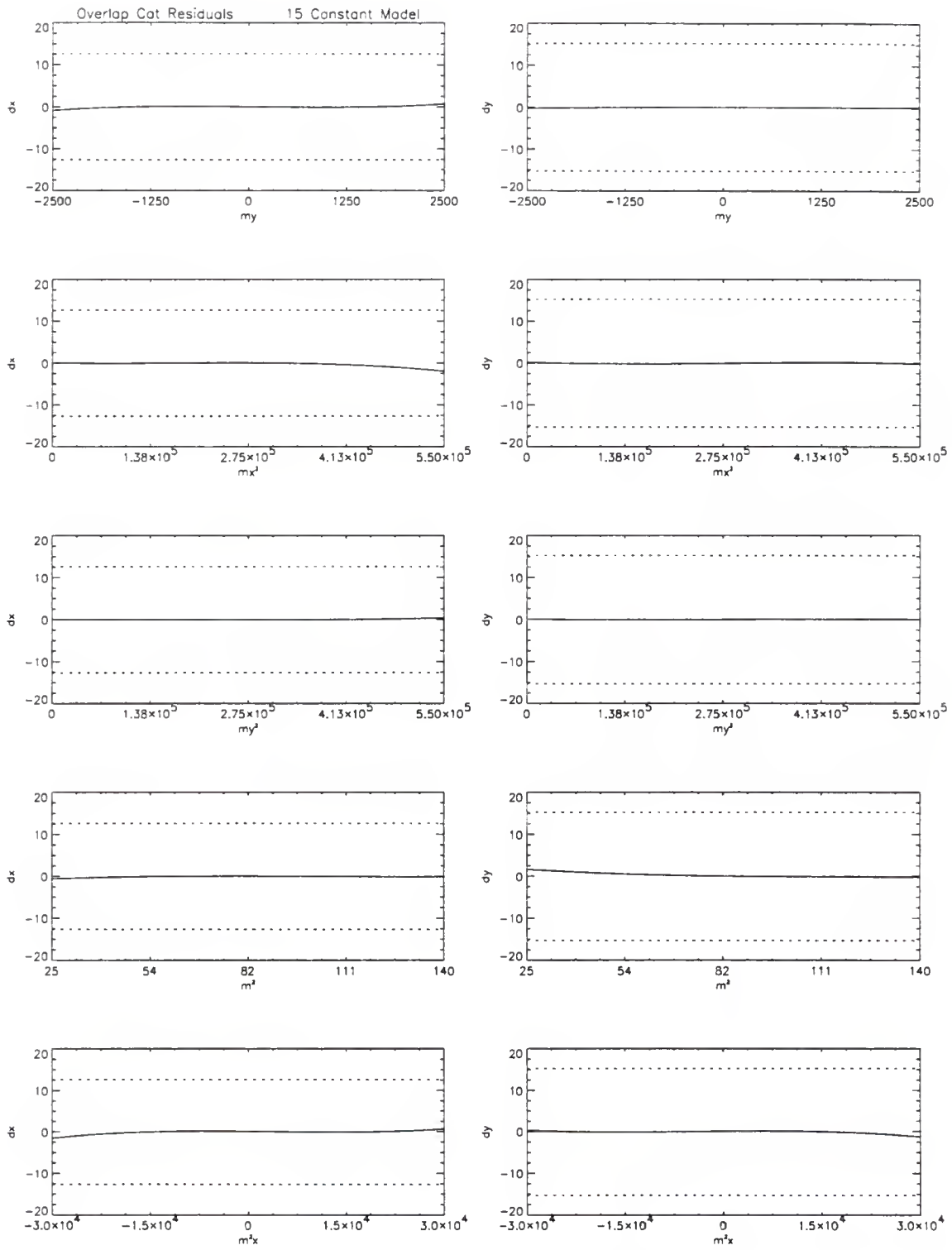


Figure 45: 15-Constant Overlap Residuals

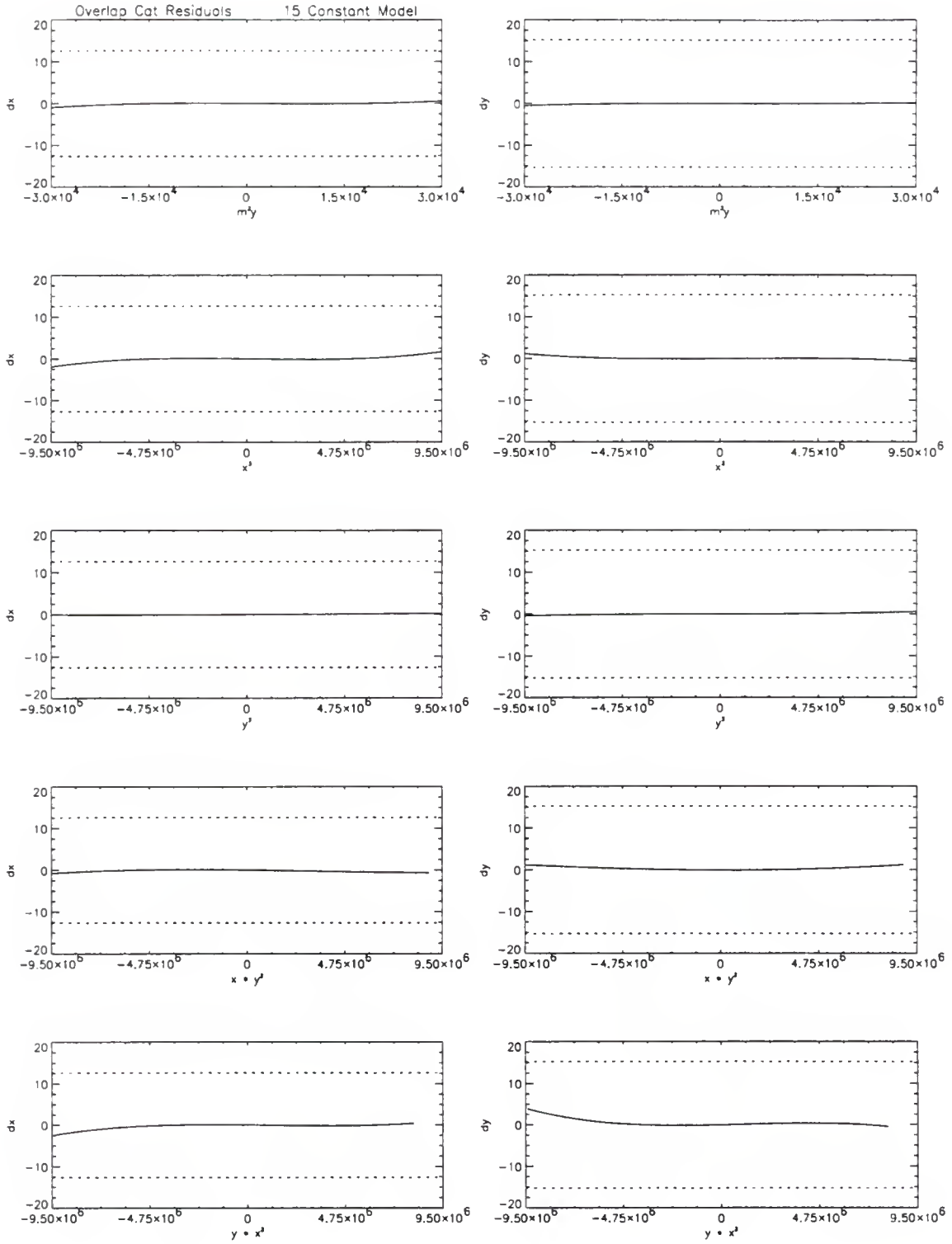


Figure 46: 15-Constant Overlap Residuals

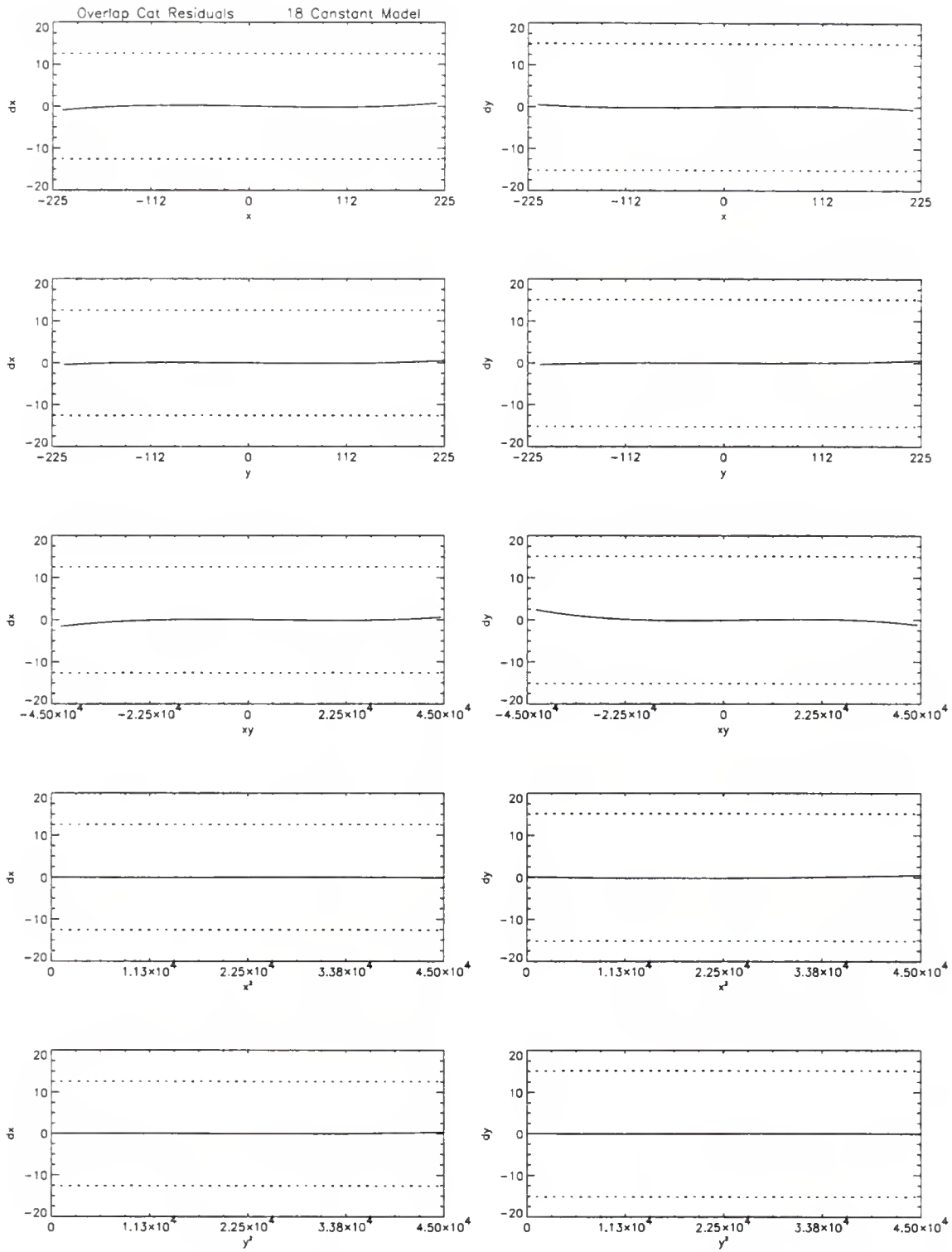


Figure 47: 18-Constant Overlap Residuals



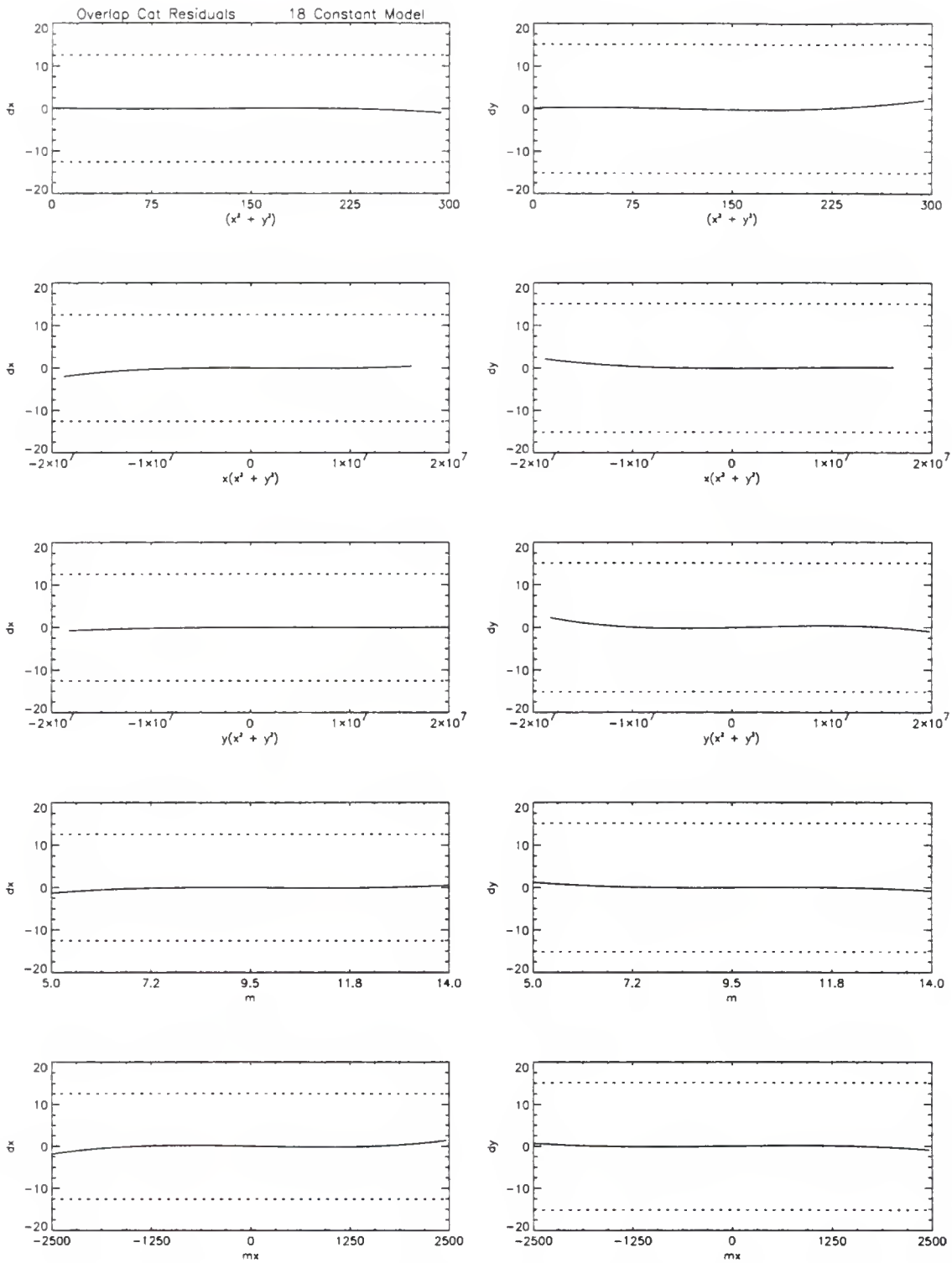


Figure 48: 18-Constant Overlap Residuals

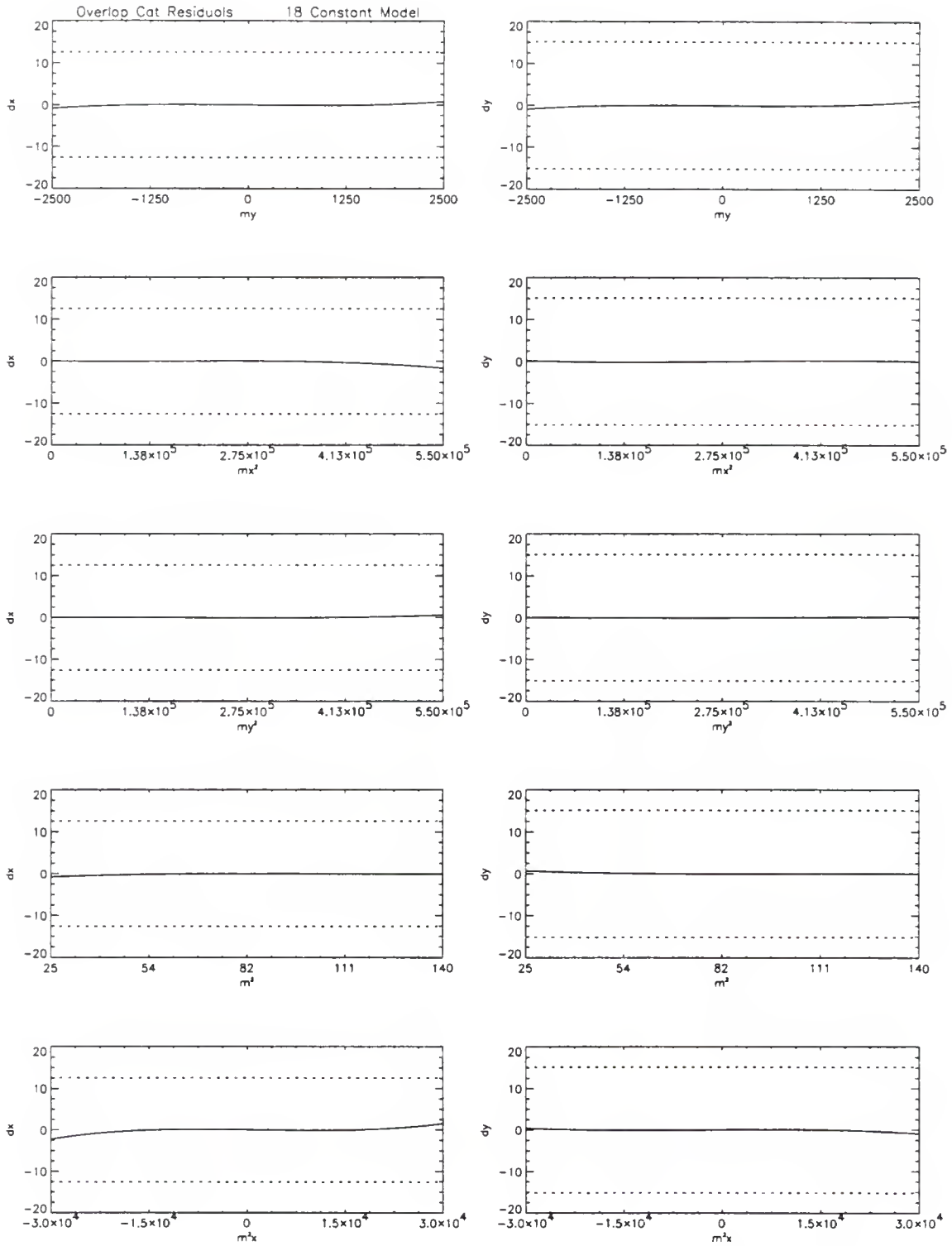


Figure 49: 18-Constant Overlap Plate Residuals

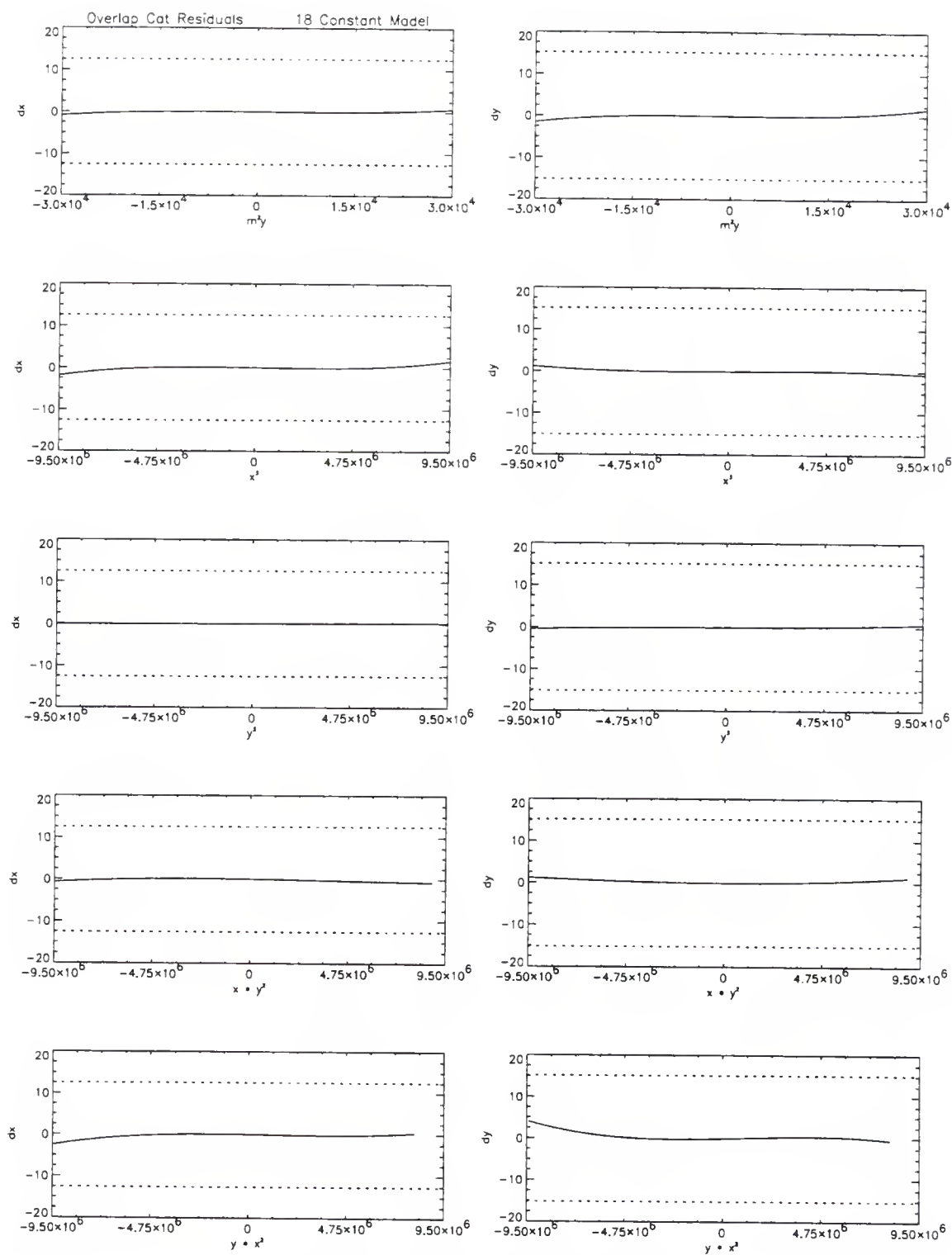


Figure 50: 18-Constant Overlap Residuals

## BIBLIOGRAPHY

Abell, G. O., Morrison, D. and Wolff, S. C., 1987. in *Exploration of the Universe*, fifth edition, Saunders College Publishing Philadelphia, Chap. 2 and Chap. 22

Astronomisches Rechen-institut. 1957 *Individuelle Verbesserungen des FK3 südlich von  $-30^\circ$  Deklination*. Veröff. des Astron. Rechen-Instituts Heidelberg, No. 7

Bastian, U., Roeser S., Yagudin, L.I., Nesterov, V. V., Polozhentsev, D. D.M Potter, K.H., Wielen, R., and Yatskiv, Y. S. ,1993 *Positions and Proper Motions: South Star Catalogue*, Astronomisches Rechen-Institut, Heidelberg

Brown, D. C., 1955, *Ballistic Research Laboratories Report No. 937*, Aberdeen Proving Grounds, MD.

Brown, D. C. 1966, *Photogrammetric Engineering*, **32**, 444.

Bystrov, N.F., Polozhentsev, D. D., Potter, Kh. I., Zalles, R. F., Zelaya, J.A. and Yagudin, L.I., 1989: *On the FOKAT catlog.. Astron. Zh.* 66, 425

Corbin, T. E. 1977, *The Proper-Motion Systems fo the AGK3R* (Ann Arbor, university Microfilms, Inc.)

Corbin, T. E. 1978, in *IAU Colloquim 48, Modern Astrometry*, ed. F. V. Prochazka & R. H. Tucker (vienna: University Obs.), 505

Corbin, T. E., 1991 *International Reference Stars Catalog*, United States Naval Observatory, Washington, DC.

- Corbin, T. E. and Urban, S. E., 1991, *Astrographic Catalogue Reference Stars*, United States Naval Observatory, Washington, DC.
- De Vegt, Chr., Ebner, H., 1972, *AA*, **17**, 276–285.
- Eichhorn, H. K., 1960, *Astron. Nach*, **285**, 233
- Eichhorn, H. K and Williams, C. A., 1963, *AJ* **68**, 221
- Eichhorn, H. K. and Gatewood G. D. 1967 *AJ* **72**, 1191
- Eichhorn, H. K., 1971, *Astron. Nachr., Bd.*, **293**, 127
- Eichhorn, H. K., 1974, *Astronomy of Star Positions*, Frederick Ungar Publishing Co., New York, Chap. 2, Chap. 5
- Eichhorn, H. K. 1985, *AA*, **150**, 251
- Fricke, W., Kopff, A. et al. 1963. *Fourth Fundamental Catalogue (Fk4)* Veröff. Astronomisches Rechen-Institut, Heidelberg. No. 10
- Fricke, W., Schwan, H. Lederle, T. , 1988, *Fifth Fundamental Catalogue (FK5). Part I The Basic Fundamental Stars*. Veröeff. Astronomisches Rechen-Institut, Heidelberg, Nr. 32.
- Gill, D. and Kapteyn, J.C., 1899. *Cape Photographic Durchmusterung Catalogue*, Annals of the Cape Observatory, **5**, Her Majesty's Stationery Office, London.
- Henderson, H. V. and Searle, S. R., 1981 *SAIM Review* **23**, 53
- Hoffleit, D., 1962, *A J* **67**, 696
- Hoffleit, D. 1967, *Transactions of the Astronomical Observatory of the Yale University*, **28**

Hoffleit, D. 1983, *Transactions of the Astronomical Observatory of the Yale University*, **32 Part II**

Jefferys, W. H, 1980, *AJ*, **85**, 177

Jefferys, W. H, 1981, *AJ*, **86**, 149

König, A, 1933, In *Handb. D. Ap.* **1.**, Springer-Verlag, Berlin, Chapter 6, Appendix 2

König, A, 1962, *Astrometry with Astrographs*. In *Astronomical Techniques (Stars and Stellar Systems vol 2*, ed. A. Hiltner), Chicago: U. of Chicago Press, Chicago, p 461

Kovalevsky, J, 1995, In *Modern Astrometry*, Springer, New York, p 191–225

Lasker, B. M. Struch, C. R., McLean, B. L., Russell, J. L., Jenkner, H., and Shara, M. M., 1990, *AJ*, **99**, 2019

Lü, P. K., 1971, *Transactions of the Astronomical Observatory of the Yale University*, **31**

McNally, D., 1975, *Positional Astronomy*, Halsted Press Book, New York

Roeser, S., Bastian, U. and Kuzmin, A., 1993, *The 90,000 Stars Supplement to the PPM Star Catalogue*, Astronomisches Rechen-Institut, Heidelberg.

Stoy, R. H, 1966. *Cape Photographic Catalogue for 1950.0, Zones  $-64^{\circ}$  to  $-80^{\circ}$* . Annals of the Cape Observatory, **21**, London: Her Majesty's Stationery Office, London

Stoy, R. H, 1968. *Cape Photographic Catalogue for 1950.0, Zones  $-80^{\circ}$  to  $-90^{\circ}$* . Annals of the Cape Observatory, **22**, London: Her Majesty's Stationery Office, London

Schlesinger, F. and Barney, I., 1933 *Transactions of the Astronomical Observatory of the Yale University*, **9**

Smith, C. A., Corbin, T. E., Huges, J. A., Jackson, E. S., Krutskaya, E. V., Polozhentsev, A. D., Polozhentsev, D. D., Yagudin, L. I., and Zverev, M. S. 1990, in *IAU Symposium No. 141, Inertial Coordinate System and the Sky*, ed. J. H. Lieske & V. K. Abalakin (dordrecht, Reidel) 457

Taff, L. G., Lattanzi, M.G., Bucciarelli, B., Gilmozzi, R., McLean B. J., Jenkner, H., Laidler V. G., Lasker, B. M., Shara, M. M., and Sturch C. R., 1990, *Ap J*, **353**, L45.

Taff, L. G., 1981, *Computational Spherical Astronomy*, Wiley-Interscience Publication, New York, Chapter 7

Zacharias, N., de Vegt, C., Nicholson, W., Penston, M. J., 1992, *AA*, **254**, 397

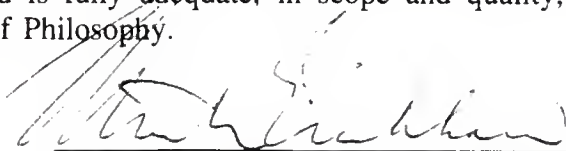
## BIOGRAPHICAL SKETCH

Jane Ellen Morrison was born in 1965 in Lafayette Indiana, the third of four children. Soon afterwards the family packed their wagon and trekked to Ohio and before the dust settled they were off again to Georgia. The time in Georgia heralded Jane's first memories of formal education. The Morrison Family Adventure was soon underway again, this time to the palm tree studded isle of Key Biscayne, Florida. Little did she realize that her kindergarten graduation here would be a premonition of her continued educational success in this state which has culminated with this dissertation. Jane took an extended hiatus from Florida, traveling with her family to the Keystone State. During these formative years in Pennsylvania the Morrison clan represented the United States as spectators in the 1972 Montreal Olympic Games. After failing to medal the dejected Morrisons soon picked up stakes and moved to Music City USA to pursue other interests. On a family excursion to the Great Smoky Mountains, downwind from the Oak Ridge National Lab, Jane was bitten by a radioactive spider which gave her temporary prescient abilities, allowing her to foresee her life long ambition in mathematics and the sciences. The Tennessee educational system offered itself as a springboard to accomplish these goals. Disguised as a mild-mannered geeky student, voted "Most Studious" in Brentwood High School, Jane graduated and went on to Middle Tennessee State University where she studied under the eminent Professor



Robert Carlton. On an unusually blustery spring day in 1987 she received her Bachelors of Science degree. Following the Sun south in the Indian summer of the fall of '88, Jane returned to the Sunshine State to fulfill her destiny. After thoroughly exhausting the possibilities in the New World, Jane now sets her sails for the Old World to seek out new adventures.

I certify that I have read this study and that in my opinion it conforms to acceptable standards of scholarly presentation and is fully adequate, in scope and quality, as a dissertation for the degree of Doctor of Philosophy.



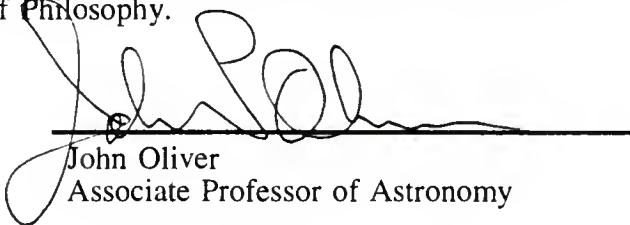
Heinrich Eichhorn, Chair  
Professor of Astronomy

I certify that I have read this study and that in my opinion it conforms to acceptable standards of scholarly presentation and is fully adequate, in scope and quality, as a dissertation for the degree of Doctor of Philosophy.



Haywood Smith  
Associate Professor of Astronomy

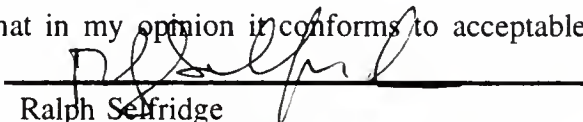
I certify that I have read this study and that in my opinion it conforms to acceptable standards of scholarly presentation and is fully adequate, in scope and quality, as a dissertation for the degree of Doctor of Philosophy.



John Oliver  
Associate Professor of Astronomy

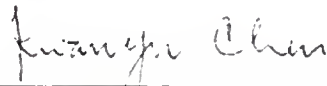
I certify that I have read this study and that in my opinion it conforms to acceptable standards of scholarly presentation and is fully adequate, in scope and quality, as a dissertation for the degree of Doctor of Philosophy.

I certify that I have read this study and that in my opinion it conforms to acceptable



Ralph Selfridge  
Professor of Computer and Information  
Science and Engineering

standards of scholarly presentation and is fully adequate, in scope and quality, as a dissertation for the degree of Doctor of Philosophy.



---

Kwan-Yu Chen  
Professor of Astronomy

This dissertation was submitted to the Graduate Faculty of the Department of Astronomy in the College of Liberal Arts and Sciences, and to the Graduate School and was accepted as partial fulfillment of the requirements for the degree of Doctor of Philosophy.

August 1995

---

Dean, Graduate School

LD  
1780  
1995  
.M879

